TECHNISCHE UNIVERSITÄT MÜNCHEN

Pflanzengenetik

Auxin signaling downstream of *RAM1* and a non-cell autonomous role of CCaMK in *Lotus japonicus* arbuscular mycorrhiza development

Fan Du

Vollständiger Abdruck der von der TUM School of Life Sciences der Technischen Universität München zur Erlangung des akademischen Grades eines

Doktors der Naturwissenschaften (Dr. rer. nat.)

genehmigten Dissertation.

Vorsitzende: Prof. Dr. Brigitte Poppenberger-Sieberer

Prüfer der Dissertation: 1. Prof. Dr. Caroline Gutjahr
2. Priv.-Doz. Dr. Ulrich Hammes

Die Dissertation wurde am 27.07.2020 bei der Technischen Universität München eingereicht und durch die TUM School of Life Sciences am 03.02.2021 angenommen.

Table of Contents

I. Abbreviation Index

ABA	Abscisic acid
ABC	adenosine triphosphate–binding cassette
ACP	Acyl-acyl Carrier Protein
AFB	AUXIN SIGNALING F-BOX
AMS	arbuscular mycorrhiza symbiosis
AMT2.2	Ammonium Transporter 2.2
AP2	APETALA2
ARF	AUXIN RESPONSIVE FACTOR
At	*Arabidopsis thaliana*
AuxRE	auxin-responsive element
Aux/IAA	AUXIN/INDOLE-3-ACETIC ACID
BCP1	Blue copper binding protein1
BiFC	bimolecular fluorescence complementation
bsh	*bushy*
CaM	calmodulin
CCaMK	calcium and calmodulin-dependent kinase
CCD8	CAROTENOID CLEAVAGE DIOXYGENASE 8
CDS	Coding sequence
COs	chitooligosaccharides
dgt	*diageotropica*
DIS	Disorganized Arbuscules
ERF1	ETHYLENE RESPONSE FACTOR 1
EV	empty vector
FatM	Fatty Acid Thioesterase M
GA	gibberellic acid
GH3.4	Gretchen Hagen 3.4
GRAS	GIBBERELLIC-ACID INSENSITIVE, REPRESSOR of GAI,

	AND SCARECROW
GUS	ß-glucuronidase
IAA	Indole-3-acetic acid
IBA	indole-3-butyric acid
LCOs	lipochitooligosaccharides
Lj	*Lotus japonicus*
MIG1	MYCORRHIZA INDUCED GERF1RAS 1
MS	Murashige and Skoog
Mt	*Medicago truncatula*
NAA	1-Naphthaleneacetic acid
PAA	phenylacetic acid
PAM	peri-arbuscular membrane
PAS	peri-arbuscular space
PBS	phosphate-buffered saline
pct	*polycotyledon*
Pi	phosphorus
PM	plasma membrane
PPA	prepenetration apparatus
PP2A	PROTEIN PHOSPHATASE 2A
PT4	Phosphate Transporter 4
RAD1	REQUIRED FOR ARBUSCULE DEVELOPMENT 1
RAM1	Reduced Arbuscular Mycorrhiza 1
RAM2	Reduced Arbuscular Mycorrhiza 2
RT-qPCR	Reverse transcriptase quantitative real time PCR
SAUR	small auxin up RNA
SCF	Skp, Cullin, F-box
SDS	sodium dodecylsulfate
SL	strigolactone
SNARE	soluble N-ethylmaleimide-sensitive factor attachment protein

	receptor
SSP	secretion signal peptide
STR	Stunted Arbuscules
SYP	SYNTAXIN OF PLANTS
TAA1	AMINOTRANSFERASE OF ARABIDOPSIS 1
TIR1	TRANSPORT INHIBITOR RESISTANT 1
Ubi	Ubiquitin
VAMP72	vesicle-associated membrane protein 72
WGA	wheat-germ-agglutinin
WRI	WRINKLED
WT	wild-type
YUC6	YUCCA6
2,4-D	2,4-Dichlorophenoxyacetic acid

II. Declaration of contribution

Most of the work in part I has been done by myself, for some of the work in part II I cooperated with Dr. Priya Pimprikar and Dr. Karen V. Hobecker. Prof. Dr. Caroline Gutjahr supported by work by discussing the experimental design. The following people or lab contributed to this study:

- The lab of Prof. Dr. Karin Ljung in Swedish University of Agricultural Sciences, carried out the mass spectrometry to measure the amount of indole acetic acid in part I Fig. 7D.
- Dr. Priya Pimprikar did all the cloning for the experiments corresponding to Fig. 14, 15, 16, 17, 19 in part II.
- Dr. Priya Pimprikar cooperated with me to set up and analyze the experiments shown in Fig. 16 and 17 in part II.
- Dr. Karen V. Hobecker did the RT-qPCR in part II Fig. 17.
- Kristina Scheitz, as student helper helped to set up and analyzed the experiments corresponding to Fig. 16 under Dr. Priya Pimprikar’s or my supervision in Part II.

III. Summary

The exchange of nutrients in arbuscular mycorrhiza symbiosis between plants and glomeromycotan fungi occurs between fungal tree-shaped structures, called arbuscules and host cortex cells, in which the arbuscules develop. *REDUCED ARBUSCULAR MYCORRHIZA1* (*RAM1*), encoding a GRAS transcription factor, was identified to be a core regulator of arbuscule development. The *ram1* mutant displays a stunted arbuscule phenotype. Arbuscule branching also requires auxin signaling. I addressed how auxin signaling is placed relative to RAM1 in a signaling network regulating arbuscule development. I found in *L. japonicus* that the auxin reporter *DR5*:*GUS* is active in arbuscule containing cells in the wild-type but not in *ram1* mutants, indicating that *RAM1* is required for induction of auxin response in these cells. Furthermore, ectopic expression of *RAM1* activated *DR5*:*GUS* and the formation of lateral roots in absence of the fungus as indication for induced auxin signaling. In addition, the AM-induced auxin response genes, *LjARF17* and *SAUR*s were not induced in the *ram1* mutants. Taken together, this indicates that activation of auxin signaling or biosynthesis in arbuscule containing cells may involve RAM1. *LjARF17* was suggested to specific to genomes of AM-competent plants by phylogenetic analysis. However, *arf17* mutants were not affected in arbuscule morphology, indicating that ARF17 is not required for arbuscule branching. Exogenous auxin treatment promoted arbuscule growth in a first experiment but this was not reproducible in the further independent experiments. Based on the result of the first auxin treatment essay, I activated auxin signaling or auxin biosynthesis in arbuscule containing cells of *ram1* by transgenically expressing *VP16-IAA17mImII* as auxin signaling activator or co-expression of two auxin biosynthesis genes *YUC6* and *TAA1*, respectively, under the control of RAM1 promoter. None of them showed effects on arbuscule growth, indicating that induction of auxin signaling in arbuscule cells of *ram1* mutants is not sufficient to trigger arbuscule growth and other RAM1-dependent mechanisms are required.

The *RAM1* gene is activated by a complex comprising the calcium and calmodulin-dependent kinase CCaMK and two transcription factors CYCLOPS and DELLA. Mutants of *CCaMK* or *CYCLOPS* exhibit severe phenotypes, and *ccamk* fails to allow formation of

intracellular hyphae and arbuscules; while *cyclops* displays severely impaired formation of intracellular hyphae and no arbuscules. We found that expression of *CCaMK* using an epidermis-specific promoter could restore intraradical colonization in *ccamk-3* mutant including intraradical hyphae and arbuscules in the cortex. When CCaMK was fused with 3xGFP there was no restoration of intraradical colonization and arbuscule development, suggesting that CCaMK is able to move from the epidermis to cortex. Epidermis expression of *CYCLOPS* could also rescue the arbuscule formation in *cyclops-4*. However, this also occurred with *CYCLOPS*-3x*GFP*, suggesting that CYCLOPS itself may not move but may be able to induce a mobile molecular signal(s).

IV. Introduction

1 Arbuscular mycorrhiza (AM) Symbiosis

The term “symbiosis” describes a relationship between two or more different organisms which live closely together. Many microorganisms form a symbiosis with plants that range from parasitism to mutualism according to different situations of beneficial association. Among them, the most widespread mutually beneficial symbiosis is arbuscular mycorrhiza symbiosis, which is formed between the majority of terrestrial plant species and fungi of the subphylum Glomeromycotina (Fitter, 2005; Bonfante and Anca, 2009; Spatafora et al., 2016). Fossil records indicate that the AM symbiosis is an ancient association that can be traced back to 400 million years ago, as early as the emergence of early land plants, suggesting a possible role in the process that plant colonizes land (Remy et al., 1994). “In agricultural field conditions plants do not, strictly speaking, have roots, they have Mycorrhizas”, said by the American plant pathologist Stephen William, suggests that the AM symbiosis dominates the situation in Agro-ecosystems.

AM symbiosis is a crucial strategy of plants to adapt to harsh environments. Via the fungal symbiont, plants acquire water, mineral nutrients, predominantly phosphorus (Pi) from soil to improve their growth (Hijikata et al., 2010; Smith and Smith, 2011). Pi is an essential micronutrient that constitutes about 0.2% plant dry weight and a significant quantity of Pi from soil is needed by plants (Schachtman et al., 1998). Due to its extremely inactive and insoluble chemical characteristics, only a small proportion of Pi exists in soil solution and can be absorbed directly by plants, and the available amount is usually limiting for plant growth and health (Holford, 1997). Fungal extraradical hyphal networks in soil enhance the ability of the plants to capture scarce and immobile nutrients like Pi. They therefore significantly improve plant development and contribute to plant biodiversity and ecosystem productivity (Smith et al., 2003; St-Arnaud et al., 1996; Van Der Heijden et al., 1998). Conversely, as obligate biotrophs, AM fungi are fueled by organic carbon supplied entirely from the host for proliferation and completion of their life cycle via spore formation (Ho and Trappe, 1973; Bago et al., 2000; Parniske, 2008; Luginbuehl et al., 2017; Jiang et al., 2017; Keymer et al., 2017; Luginbuehl and Oldroyd, 2017).

1.1 Development of AM Symbiosis

AM development remains highly similar through a long evolutionary history and a wide array of plant and fungal species is involved (MacLean et al., 2017). In short, AM fungi inhabit roots and form arbuscules in specialized host-derived membrane compartments mainly in inner cortical cells. This interaction is accompanied by significant alterations in transcriptional regulation and cellular morphology of both symbionts. AM development is initiated with an exchange of signaling molecules secreted from the two symbionts, followed by growth of the fungal hyphae towards the root, hyphopodium formation, penetration of the hyphae into the root surface, and progression through epidermal cell layer into cortex, and arbuscule development and degeneration in the inner cortical cells (Gutjahr and Parniske, 2013; Luginbuehl and Oldroyd, 2017).

1.1.1 Pre-symbiotic phase

Prior to physical contact, establishment of AM symbiosis starts with a molecular "dialogue" between both symbionts that release recognition signal compounds to trigger preparative responses in the other symbiont (Buee et al., 2000; Chabaud et al., 2011) (Fig.1).

Fungal spores can germinate and grow limitedly in absence of a host (Giovannetti et al., 1993; Giovannetti, 2000). In response to phosphate deficiency, plants secrete a group of carotenoid-derived phytohormones, strigolactones (SLs), into the roots rhizosphere (Akiyama et al., 2005; Yoneyama et al., 2007; Ruyter-Spira et al., 2013; Kretzschmar et al. 2012). The SLs, identified originally as stimulants for seed germination of parasitic weeds (Cook et al., 1966; Xie et al., 2010), are capable to trigger hyphal branching of germinating spores by activating mitochondrial energy metabolism, therefore increase the chance of physical contact with the host root to establish symbiosis (Akiyama et al., 2005; Besserer et al., 2006; Besserer et al., 2008). Thus, they were called "branching factors" prior to their identification (Buee et al., 2000).

In response to plant-derived signals, fungal signaling molecules are synthesized and released to switch on plant reprogramming. These fungal exudates, called Myc factors, are unraveled to be a mixture of chitooligosaccharides (COs) and lipochitooligosaccharides (LCOs). These short-chain oligomers elicit root responses mainly as calcium spiking in the epidermis and changes of gene expression at a cellular level, starch accumulation, and modify root architecture like promoting root branching in an organ level (Genre et al., 2013; Sun et

al., 2015; Chabaud et al., 2011; Gutjahr et al., 2009; Maillet et al., 2011; Mukherjee and Ané, 2011; Oláh et al., 2005).

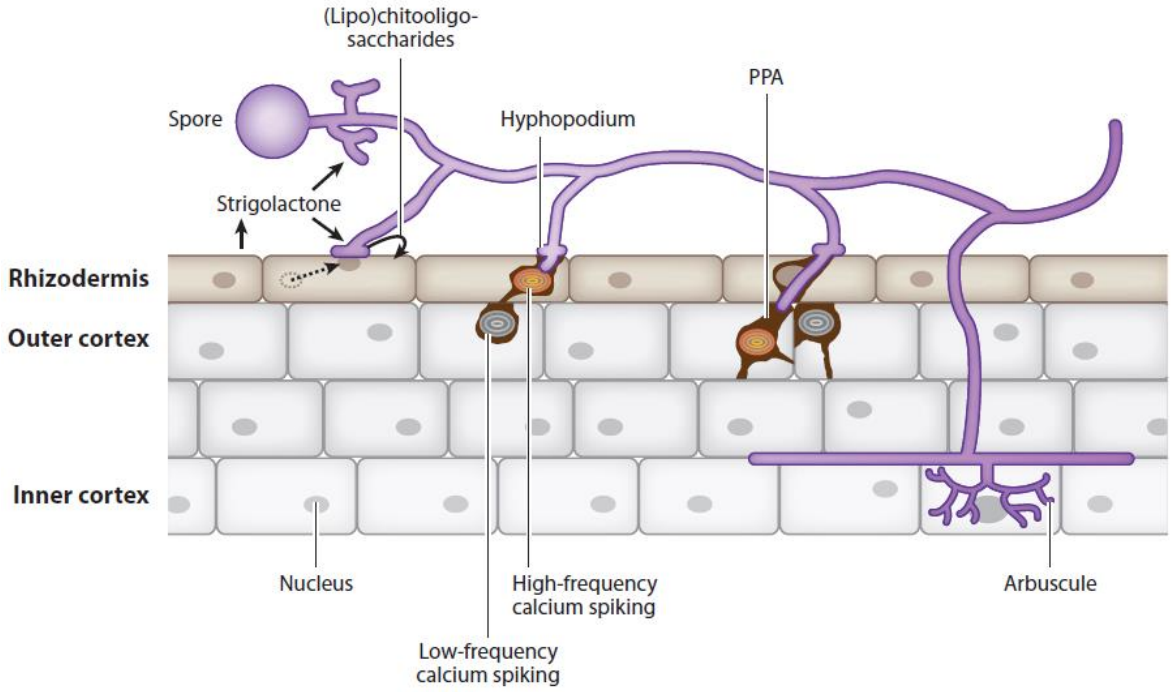

Fig. 1 Process of AM development. Plant roots exude strigolactones (Yoneyama et al., 2007; Ruyter-Spira et al., 2013; Kretzschmar et al., 2012) to stimulate fungal spore germination and hyphal branching (Akiyama et al., 2005; Besserer et al., 2006; Besserer et al., 2008). The adjacent fungus also produces signaling molecules such as (lipo) chitooligosaccharides, which trigger plant preparation for symbiosis, such as calcium spiking (Genre et al., 2013; Sun et al., 2015; Chabaud et al., 2011; Gutjahr et al., 2009; Maillet et al., 2011; Mukherjee and Ané, 2011; Oláh et al., 2005). Upon formation of a hyphopodium, migration of the nucleus towards the fungal entry on the root surface (dotted arrow) and subsequent movement of the nucleus across the cell width (not drawn) (Genre et al., 2005), prepenetration apparatus (PPA) is established and calcium spiking is induced, which guides the fungal hyphae through the root cell. The lateral PPA formation and calcium spiking in outer cortical layers continue to promote the progression of fungal hyphae (Sieberer et al., 2012). Once the hypha reaches inner cortex, arbuscule development initiates. The figure is taken from Gutjahr and Parniske, 2013.

1.1.2 Fungal penetration and growth in epidermis and cortex

Following germination, the hyphal germ tube grows through the soil and reaches the surface of the host root where the hyphal tip differentiates into a contact structure called hyphopodium (Harrison, 1998) (Fig. 1). Upon formation of the hyphopodium on the surface of an epidermal cell, the nucleus of the cell migrates to the site of hyphal attachment and subsequently moves across the cell lumen away from the hyphopodium, directing the assembly of a novel cytoskeleton (Genre et al., 2005). Accompanied by the migration of the

nucleus away from the hyphopodium, a bridge-like structure, the prepenetration apparatus (PPA) forms by assembling endoplasmic reticulum (ER), actin filaments, and microtubules. Following the path determined by the PPA, the fungal hypha enters and passes through the cell, and is enveloped by the host-derived membrane in this process (Genre et al., 2005; Novero et al., 2002). By the subsequent establishment of the PPA, the fungal hypha passes the exodermis and outer cortex intracellularly and reaches the inner cortex (Fig. 1). Furthermore, fungal penetration and intracellular elongation in the root are accompanied by rearrangement of plant cell cytoskeleton and remodeling of organelles (Genre et al., 2005).

1.1.3 Arbuscule development and degeneration in cortical cells

Once fungal hyphae arrive in the inner cortex, they stop crossing as they do in the epidermis and outer cortex, instead, they spread longitudinally in the cell apoplastic space and differentiate to tree-like structures, arbuscules, in the inner cortical cells (Luginbuehl and Oldroyd, 2017). Arbuscules together with their host cells are the key structures of the symbiosis as they are sites where AM fungi release mineral nutrients to the host (Smith and Smith, 2011). Abundance of arbuscules can vary in different plant species or varieties and under different conditions (Carbonnel and Gutjahr, 2014). Arbuscule amount and branching pattern may critically influence nutritional benefit. The strategy how fungi colonize the inner cortex varies among different fungal and plant species. Arum-type, Paris-type and an intermediate pattern comprising both types were reported (Dickson et al., 2007; Dickson, 2004; Bonfante and Genre, 2008). Among them, the Arum-type is the best studied since economic crops and major model plant species such as *Medicago truncatula and Lotus japonicus* mainly display this colonization pattern (Thangavelu and Tamilselvi, 2010). In Arum-type mycorrhization, hyphae spread longitudinally in the apoplastic space and differentiate to terminal arbuscules in the inner cortical cells (Fig. 2B). In Paris-type, hyphae spread intracellularly and form intercalary arbuscules. This type is for example found in carrot and *Brachypodium distachyon* (Bonfante and Genre, 2008; Hong et al., 2012).

Although hyphae penetrate the cell wall, the plasma membrane (PM) of the host cell does not fracture, but extends *de novo* and develops the so called peri-arbuscular membrane (PAM) surrounding the arbuscule and following the contour of hyphal branches (Pumplin and Harrison, 2009; Harrison, 2005). The plant-derived PAM is a specialized membrane separating fungal hypha from the plant cytoplasm and all the transporters known so far that facilitate exchange of nutrients localize in the PAM, thereby being the heart of this

endosymbiosis (Harrison et al., 2002; Zhang et al., 2010; Harrison, 2012) (Fig. 2B). The apoplastic compartment between the PAM and fungal cell wall is defined as peri-arbuscular space (PAS) (Gutjahr and Parniske, 2013).

Arbuscule development in the root cortex involves five major stages starting with I) formation of the PPA. II) The fungus enters the cortical cell forming a hyphal trunk. And the III) birdsfoot stage, which is the name for small arbuscules with the first-order thick branches. The birdsfoot stage is followed by IV) the development of fine arbuscule branches, leading to a fully developed, mature arbuscule. V) Collapse of the arbuscule (Fig. 2B) (Gutjahr and Parniske, 2013).

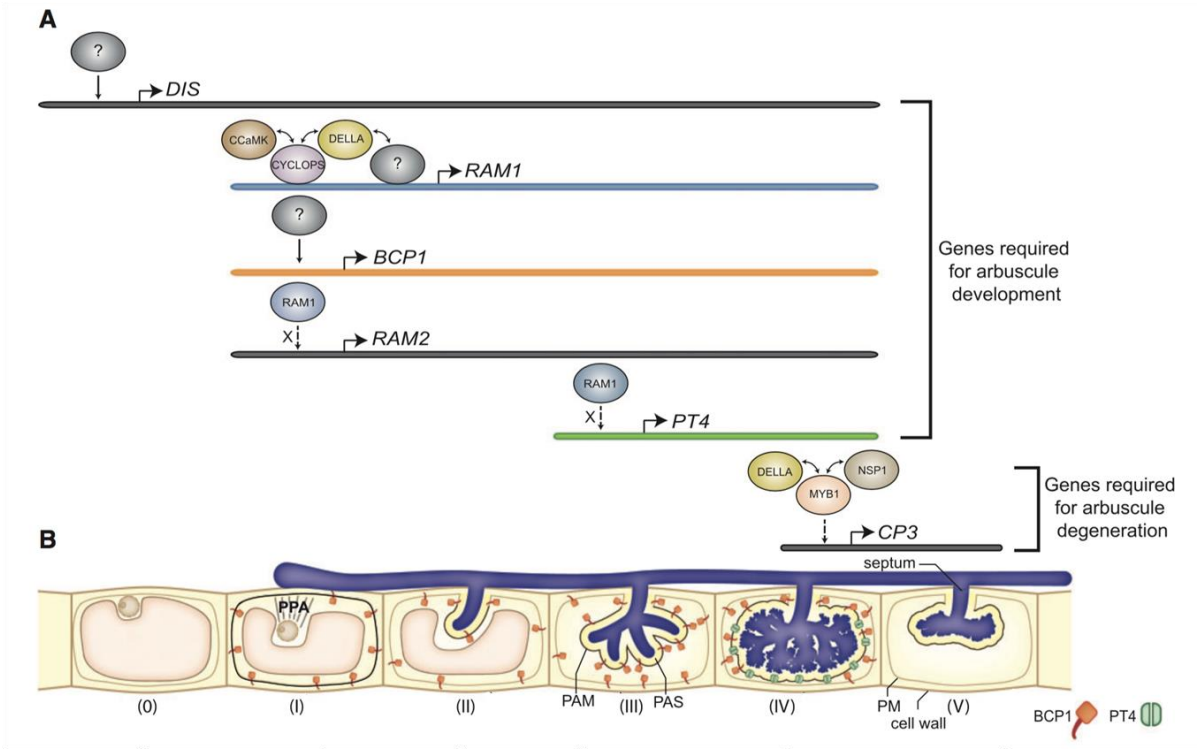

Fig. 2 Transcriptional regulation and morphological development of an arbuscule in root inner cortical cell. A, transcriptional activity corresponding to stages of arbuscule development. The question marks indicate unknown transcription factors. Two-way arrows mean binary interactions. The dotted arrows beside X represent that the dependence of *RAM2* and *PT4* induction on *RAM1* is different between *M. truncatula* and *L. japonicus*. **B**, five morphological stages of arbuscule development and polar localization of corresponding secreted proteins. PPA, pre-penetration apparatus; PAM, peri-arbuscular membrane; PAS, peri-arbuscular space; PM, plasma membrane. The figure is taken from Pimprikar and Gutjahr, 2018.

1.2 Signal transduction and transcriptional regulation of AM symbiosis

Signals generated by perception of fungi-released Myc-factors via LysM receptor-

like kinases (Girardin et al., 2019) are transmitted through the plasma membrane to the nucleus where Ca^{2+} spiking is elicited (MacLean et al., 2017). In the nucleus, the calcium signal is thought to be deciphered by a calcium- and calmodulin-dependent kinase (CCaMK), which acts as a master regulator to initiate symbiosis-associated transcriptional cascade (Lévy et al., 2004; Miller et al., 2013). The CCaMK consists of an N-terminal serine-threonine kinase domain, a middle domain and a calmodulin (CaM)-binding/autoinhibitory domain, as well as a C-terminal visinin-like domain with three EF-hands capable of binding Ca^{2+} (Routray et al., 2013). During AM symbiosis, *ccamk* mutants in *Lotus*, *Medicago* and rice (*Oryza sativa*), exhibit a severe phenotype in which only hyphopodia can be developed but not intracellular hyphae and arbuscules (Hayashi et al., 2010; Lévy et al., 2004; Gutjahr et al., 2008). Overexpression of an auto-activated *CCaMK* (*CCaMK*^{T265D}), which is Ca^{2+}- independent resulting from substitution of threonine to aspartate at the auto-phosphorylation site, is sufficient to fully complement the severe symbiotic phenotypes displayed in mutants of genes upstream in the pathway such as *dmi*/*pollux*, *castor*, and *dmi2*/*symrk*, and is required for the generation of the calcium oscillation (Hayashi et al., 2010). The restoration of symbiotic phenotypes in mutants of upstream genes reveals the significance of *CCaMK* as these upstream genes are required solely to activate *CCaMK*. In addition, overexpression of the auto-activated kinase domain alone with a nuclear localization signal, *CCaMK*$_{314}^{T265D}$*-NLS*, triggers cytoplasmic aggregation to a dense PPA-like structure in the cortical cells in the absence of AM fungi (Takeda et al., 2012). Besides, AM symbiotic genes such as a subtilase gene *SbtM1*, *Reduced Arbuscular Mycorrhiza 1* (*RAM1*) and *2* (*RAM2*), as well as *Vapyrin1* are also induced by the overexpression of *CCaMK*$_{314}^{T265D}$*-NLS* in the absence of AM fungi (Takeda et al., 2015).

Calcium binding of CCaMK leads to a conformational change of CCaMK, resulting in activation of the kinase. CCaMK further phosphorylates a transcription factor CYCLOPS (Yano et al., 2008; Singh et al., 2014). CYCLOPS carries a nuclear localization signal and a predicted DNA-banding coiled-coil domain at C-terminus (Messinese et al., 2007; Yano et al., 2008; Singh et al., 2014). It interacts with CCaMK to initiate the transcriptional cascade for AM symbiosis development (Pimprikar et al., 2016). *cyclops* mutants in *L. japonicus* and *O. sativa* fail to form arbuscules and penetration of intraradical hyphae into inner cortical cells is severely impaired (Gutjahr et al., 2008; Yano et al., 2008; Floss et al., 2013; Singh et al., 2014). However, mutants of the *CYCLOPS* ortholog *INTERACTING PROTEIN OF DOES NOT MAKE INFECTIONS 3* (*IPD3*) and a recently reported double mutant of *IPD3* and *IPD3 LIKE*

(*IPD3L*) in *M. truncatula* retained the ability to form arbuscules although colonization levels are reduced, probably resulting from undiscovered functional redundancy of *IPD3* or additional alternate route through the AM symbiosis pathway (Floss et al., 2013; Horváth et al., 2011; Lindsay et al., 2019). Induction of AM symbiotic genes such as the *SbtM1* and *PT4* (*Phosphate Transporter 4*) is dependent on *CYCLOPS* (Takeda et al., 2011).

It has been shown that CCaMK and CYCLOPS form a complex that acts in concert with GRAS (GIBBERELLIC-ACID INSENSITIVE, REPRESSOR of GAI, AND SCARECROW) transcription factors such as DELLA proteins to induce the expression of downstream cascades (Jin et al., 2016; Pimprikar et al., 2016) (Fig. 2). The DELLA proteins, inhibitors of signaling pathway of the phytohormone gibberellic acid (GA), are also required for the arbuscule development, highlighting that the arbuscule development is also under the control of phytohormone signaling pathways (Alvey and Harberd, 2005; Floss et al., 2013; Gutjahr, 2014; Müller and Harrison, 2019). GA treatment severely interferes with establishment of AM symbiosis (Floss et al., 2013; Takeda et al., 2015; Pimprikar et al., 2016). Depending on the concentration, entry of fungal hyphae into the roots and arbuscule formation is impeded (Takeda et al., 2015). AM-symbiotic genes expression is also perturbed upon GA treatment (Takeda et al., 2015; Pimprikar et al., 2016). In contrast, mutations in *DELLA*s cause strong reduction in mycorrhizal colonization and suppression of arbuscule formation (Floss et al., 2013; Yu et al., 2014). These results indicate the role of the DELLA proteins in arbuscule development. Expression of dominant versions of *DELLA*, $DELLA1^{\Delta 17}$ (in *L. japonicus*) and $DELLA1^{\Delta 18}$ (in *M. truncatula*) are not only sufficient to complement arbuscule formation in *cyclops/ipd3* and GA treated wild-type roots, but also induce several AM marker genes such as *BCP1* (*Blue copper binding protein1*), *SbtM1* and *Vapyrin* in absence of AM fungi (Floss et al., 2013, Floss et al., 2016; Pimprikar et al., 2016). The dominant *DELLA* restores arbuscule formation in absence of *CYCLOPS*/*IPD3*, raising the speculation that an additional DNA-binding protein may exist and interacts with DELLA (Pimprikar et al., 2016).

CCaMK-CYCLOPS-DELLA complex transactivates a downstream gene encoding a GRAS protein RAM1 by direct binding of the CYCLOPS to an *AMCYC* cis-element in *RAM1* promotor (Pimprikar et al., 2016). *RAM1* is strongly and specifically induced in AM colonized roots and the *RAM1* promoter activity is specifically related to colonized regions (Park et al., 2015; Rich et al., 2015; Pimprikar et al., 2016). Plants mutated in *RAM1* fail to develop mature arbuscules with elaborate branches but exhibit a stunted arbuscule phenotype with only trunks, coiling hypha, or coarse low-order branches (Park et al., 2015; Xue et al.,

2015; Rich et al., 2015; Pimprikar et al., 2016). Ectopic *RAM1* expression in *cyclops* mutants is sufficient to restore arbuscule formation and branching (Pimprikar et al., 2016). Transcript analysis by RT-qPCR and global transcriptome RNA sequencing (RNAseq) analysis of *ram1* mutants indicate that RAM1 acts as a central transcriptional regulator to induce downstream responsive genes required for multiple processes involved in the AM development (reviewed in Pimprikar and Gutjahr, 2018). For example, *RAM1* induced genes such as *PT4* and *AMT2.2* (*Ammonium Transporter 2.2*) are involved in transporting phosphate and ammonium delivered by the fungus into the plant cell (Park et al., 2015; Xue et al., 2015; Pimprikar et al., 2016). RAM1-dependent genes also participate in lipid biosynthesis and export to AM fungi, encoding such as glycerol-3-phosphate acyl transferase RAM2, fatty acyl–acyl carrier protein thioesterase FatM, DIS (encoded by *Disorganized Arbuscules*), 3-ketoacyl-acyl carrier protein (ACP) synthase III KASIII, symbiosis-induced transporters STR (encoded by *Stunted Arbuscules*) and STR2 (Jiang et al., 2017; Rich et al., 2017; Pimprikar et al., 2016; Keymer et al., 2017; Bravo et al., 2016; Luginbuehl et al., 2017). Besides, induction of a chimeric structural protein *Vapyrin* and a subunit of the exocyst complex *Exo70I*, has been proposed to function in PAM formation, are dependent on *RAM1* (Rich et al., 2015; Park et al., 2015; Pimprikar et al., 2016; Feddermann et al., 2010; Zhang et al., 2015). RNAseq analysis of *ram1* also revealed that many other transcription factors act downstream of RAM1 (Rich et al., 2017; Luginbuehl et al., 2017). Among them are three APETALA2 (AP2)-domain proteins WRINKLED (WRI) 5a, b, and c, evolutionarily conserved in AM-competent plant species (Bravo et al., 2016; Luginbuehl et al., 2017). The *MtWRI* genes are able to promote triacylglycerol production in *Nicotiana benthamiana* expression system (Luginbuehl et al., 2017). microRNA-mediated silencing of *MtWRI5b* driven by *MtPT4* promoter results in stunted arbuscule phenotype, indicating that WRI5b is required for arbuscule branching (Devers et al., 2013).

1.3 Genes required for arbuscule development

Discovery of genes required for arbuscule formation has developed into a “hot topic” in the past years. Forward genetic studies and targeted reverse genetic approaches identified a growing number of genes playing role in distinct steps of arbuscule development.

Some transcription factors are identified to be required for arbuscule development including *CYCLOPS*, *DELLA*, *RAM1*, *RAD1* (*REQUIRED FOR ARBUSCULE DEVELOPMENT 1*) and *MIG1* (*MYCORRHIZA INDUCED GERF1RAS 1*), and AP2-type

WRI5b/*ERF1* (*ETHYLENE RESPONSE FACTOR 1*) homologs (Yano et al., 2008; Gobbato et al., 2013; Rich et al., 2015; Park et al., 2015; Xue et al., 2015; Heck et al., 2016; Devers et al., 2013). CYCLOPS and DELLA are dispensable for penetration of hyphae into the inner cortical cell at the initiation stage of arbuscule development (Gutjahr et al., 2008; Yano et al., 2008; Floss et al., 2013; Singh et al., 2014; Yu et al., 2014; Pimprikar et al., 2016). RAM1 and its homolog RAD1 are essential for arbuscule branching in *L. japonicus* since *rad1* also displays stunted arbuscules (Pimprikar et al., 2016; Xue et al., 2015). RAD1 interacts with RAM1 and DELLA respectively *in vivo* (Xue et al., 2015; Floss et al., 2016). RNAi-based down-regulation of *MIG1* in *M. truncatula* causes reduced abundance of fine-branching arbuscules and increased stunted arbuscules despite the colonization amount is unchanged. Overexpression of a dominant *DELLA* (*DELLA1*$^{\Delta 18}$) in the *MIG1* RNAi background rescues the impaired arbuscule development, revealing that stabilized DELLA could compensate for the reduced *MIG1* expression (Heck et al., 2016). MIG1 interacts with DELLA in *N. benthamiana* leaves in bimolecular fluorescence complementation (BiFC) assays. Overexpression of *DELLA1*$^{\Delta 18}$ in the *MIG1* RNAi background leads to increased width of arbuscule-containing cells and number of cortex layers, suggesting that MIG1 may interact with DELLA1 to regulate cortical cell architecture during mycorrhizal colonization (Heck et al., 2016). Given that constitutive expression of *DELLA1*$^{\Delta 18}$ restores the malformed arbuscule phenotype and results in radial expansion of smaller cells harboring arbuscules in *MIG1* RNAi background, indicating that radial cell expansion may be related to arbuscule development (Heck et al., 2016). These studies suggest that GRAS proteins may assemble transcription-factor complexes to regulate genes involved in arbuscule development. The AP2 transcription factor WRI5b/ERF1 is downstream of RAM1 and required for arbuscule branching as RNAi silencing of the *WRI5b* causes stunted arbuscules (Luginbuehl et al., 2017; Devers et al., 2013).

RAM1 acts as a central regulator for transcriptional modulation of arbuscule development and many genes downstream of *RAM1* are essential for arbuscule formation. *RAM1* induced AM symbiotic genes have been described in the transcriptional regulation part. Among those genes, *Vapyrin* is required for intracellular penetration of hyphae into inner cortical cells, and *PT4*, *RAM2*, *FatM*, *DIS*, *STR*, *Exo70I* are indispensable for arbuscule branching according to their mutants phenotype (Pumplin et al., 2010; Zhang et al., 2010; Bravo et al., 2016; Javot et al., 2007a; Keymer et al., 2017; Zhang et al., 2015).

Upon arbuscule development, some proteins, such as BCP1 and PT4, have to be secreted and incorporated into the PAM. *BCP1* is induced from the early stage of arbuscule

development and the protein is secreted to plasma membrane, trunk and fine branching domain of the PAM. While *PT4* is induced from bird's foot stage and localized solely in the fine branching domain of the PAM (Pimprikar and Gutjahr, 2018) (Fig. 2). The promoter region of *PT4* has been used in molecular studies to drive gene expression specifically in cortical cells hosting developing arbuscules (Devers et al., 2013; Heck et al., 2016; Keymer et al., 2017). Multiple exocytotic events that traffick cellular membrane components to the expanding PAM, have been proposed to participate in the *de novo*-synthesis of PAM, and some of them are required for arbuscule development (Genre et al., 2012; Ivanov et al., 2012; Lota et al., 2013; Pan et al., 2016). Members in exocytotic vesicle-associated membrane protein 72 (VAMP72) family, MtVAMP721d and MtVAMP721e, are required for formation of the symbiotic membrane interface PAM. Silencing of both genes resulted in rare formation of mature arbuscules and marked increase of stunted arbuscules (Ivanov et al., 2012). Vesicle-associated and soluble N-ethylmaleimide-sensitive factor attachment protein receptor (SNARE) proteins have been known to mediate the exocytosis pathway (Ungar and Hughson, 2003). Two mycorrhizae induced genes encoding SNARE proteins, LjVTI12, MtSYP132A (SYNTAXIN OF PLANTS 132A) and SYP13IIα, are required for arbuscule development according to the distorted arbuscule phenotype caused by RNAi silencing (Lota et al., 2013; Pan et al., 2016; Huisman et al., 2016). In addition, EXO70I, a subunit of the exocyst complex, is essential for arbuscule development as *exo70i* showed reduced arbuscule branching and aberrant hyphal branches in *M. truncatula* (Zhang et al., 2015). It was also reported that absence of EXO70I limited the incorporation of two PAM-resident adenosine triphosphate–binding cassette (ABC) transporters STR and STR2. EXO70I accumulates adjacent to the PAM around hyphal tips of arbuscules and it interacts with Vapyrin (Zhang et al., 2015). Vapyrin functions in intracellular penetration of hyphae. Mutation and RNAi down-regulation of *Vapyrin* impaired hyphal penetration into epidermal cells and inner cortical cells. Hyphae that occasionally penetrated cortical cells mostly failed to develop arbuscules (Reddy D. M. R et al., 2007; Pumplin et al., 2010; Feddermann et al., 2010).

2 Phytohormones in AM symbiosis

Plant hormones are well known to control plant physiology in terms of architecture, nutrition, and stress response (Vanstraelen and Benková, 2012; Pozo et al., 2015). Plant hormones also regulate AM symbiosis (Gutjahr, 2014; Liao et al., 2018). Almost all phytohormones change in amount during establishment of AM symbiosis (Shaul-Keinan et al.,

2002; López-Ráez et al., 2010; Liao et al., 2018). AM development is largely controlled by the plant. As an emerging area of research, several phytohormones, such as SLs, GAs (as described above) and auxin, have been found to regulate AM development from early recognition between symbionts to arbuscule formation (Fig. 3). In the following paragraphs, I will focus on the role of auxin and abscisic acid (ABA) in AM formation.

2.1 The role of auxin in AM development

Plant endogenous auxins, including indole-3-acetic acid (IAA, the main type), indole-3-butyric acid (IBA), phenylacetic acid (PAA), etc., affect almost every aspect of plant development from early embryogenesis to fruit ripening. In cell-based processes, auxin plays a key role in promoting cell division, expansion and differentiation, and it is the principal regulator of lateral root formation (Paque and Weijers, 2016; Vanneste and Friml, 2009; Fukaki and Tasaka, 2009).

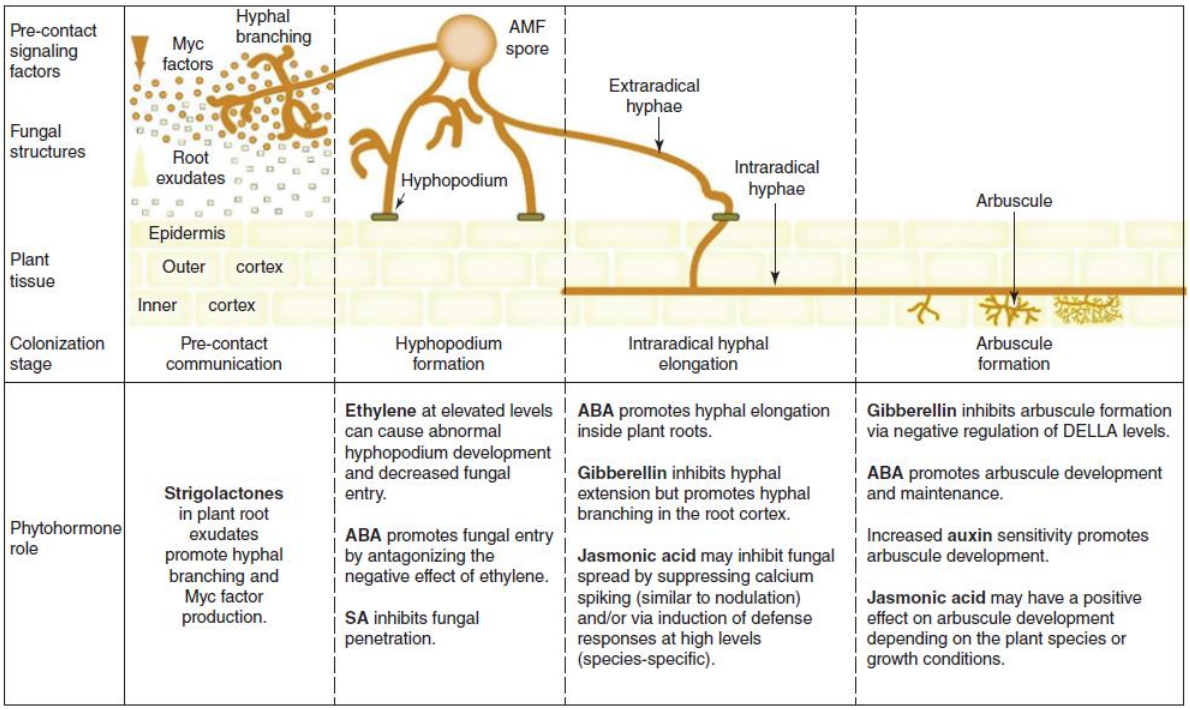

Fig. 3 Role of phytohormones in different stages of AM development. The figure is taken from Das and Gutjahr, 2019.

A growing amount of studies have shown that auxin plays a role in AM development. Increased free auxin and auxin conjugates are detected in mycorrhizal roots compared with

non-mycorrhizal roots in different plant species. However, colonization stages at which auxin is induced and induced auxin type may differ among species (Fitze et al., 2005; Jentschel et al., 2007; Campanella et al., 2007). Consistent with this, an auxin-responsive gene *Gretchen Hagen 3.4* (*GH3.4*) in *Solanum lycopersicum*, which encodes an IAA amido synthetase, is strongly induced in AM fungal-colonized roots and its promoter activity is observed predominantly in arbuscule-containing cells (Liao et al., 2015). These data imply a complicated regulatory system to balance free and conjugated auxin in mycorrhizal plants to modulate the AM development. Except for one auxin-responsive element (AuxRE), two motifs MYCRS1 and MYCRS2 have been also identified in the promotor of *SlGH3.4* by promoter deletion assay. The motifs of MYCRS1 and MYCRS2 can drive expression of *ß-glucuronidase* (*GUS*) reporter gene specifically in arbuscule-resident cells of rice, soybean and tobacco. These data suggest an evolutionarily conserved cross-talk between the auxin and mycorrhizal regulatory mechanism on the *GH3* expression (Chen et al., 2017).

Exogenous treatment of auxin analogs, 1-Naphthaleneacetic acid (NAA) and 2,4-Dichlorophenoxyacetic acid (2,4-D), increase arbuscule abundance in tomato, *Medicago*, and rice (Etemadi et al., 2014). Consistent with this, another study reports that in roots of a low auxin pea mutant *bushy* (*bsh*), arbuscule abundance and colonization level are decreased (Foo, 2013). This study also links auxin to SL in the regulation of AM symbiosis since *bsh* mutant exhibits reduced SL exudation and reduced expression of a key SL biosynthesis gene *CAROTENOID CLEAVAGE DIOXYGENASE 8* (*CCD8*). Reduced arbuscule abundance and colonization level in *bsh* can be partially complemented by the treatment of synthetic SL, GR24, suggesting SL is at least partially responsible for the phenotype of *bsh* (Foo, 2013). In addition, colonization is affected by auxin transport events, as a *polycotyledon* (*pct*) mutant of tomato with hyperactive polar auxin transport causes poor colonization, in accordance with the application of auxin transport inhibitor promotes the colonization level in pea (Hanlon and Coenen, 2011; Muller, 1999).

Auxin is perceived via direct binding to the nuclear-localized TRANSPORT INHIBITOR RESISTANT 1/AUXIN SIGNALING F-BOX (TIR1/AFB) F-box proteins, which is a subunit of an SCF (Skp, Cullin, F-box) ubiquitin ligase complex. Further, auxin serves as molecular glue to promote the interaction of the $SCF^{TIR1/AFB}$ with AUXIN/INDOLE-3-ACETIC ACID (Aux/IAA) transcriptional repressors, resulting in ubiquitination and degradation of Aux/IAA proteins by proteasome. Therefore, AUXIN RESPONSIVE FACTOR (ARF) is released from the Aux/IAA and activated to regulate auxin-responsive

gene expression (Peer, 2013; Weijers and Wagner, 2016).

DR5:*GUS* is a widely-used auxin-responsive reporter. It shows activity in arbuscule-harbouring cells in colonized roots of tomato, *Medicago* and rice, indicating that auxin response is activated in arbuscule-containing cells (Etemadi et al., 2014). Overexpression of *miR393*, which targets mRNA encoding auxin receptors TIR1/AFBs, leads to significantly reduced colonization and stunted arbuscules. This demonstrates that auxin perception is required for arbuscule formation (Etemadi et al., 2014). This may provide a hint why high phosphate may inhibit AM colonization, since high phosphate impedes the expression of *TIR1* therefore reducing auxin sensitivity (Pérez-Torres et al., 2008). Furthermore, an auxin-resistant tomato mutant *dgt* displays reduced colonization rate and may indicate a role of auxin signalling in AM development. Yet the failure of root branching in *dgt* mutants may also affect colonization level and the correct reason for the reduction of root colonization of this mutant needs to be confirmed (Hanlon and Coenen, 2011).

2.2 The role of abscisic acid in AM symbiosis

Abscisic acid (ABA) controls many plant developmental processes including seed maturation and germination, leaf abscission and inhibition of fruit ripening (Leung and Giraudat, 1998; Zhang, 2014). ABA is well known for its essential role in plant survival under a variety of abiotic environmental stresses, such as drought, salinity, temperature, heavy metal, and radiation stress (Leung and Giraudat, 1998; Vishwakarma et al., 2017). Genome-wide profiling indicates that genes involved in ABA biosynthesis are up-regulated in leaves of mycorrhizal *M. truncatula* (Adolfsson et al., 2017). In line with this, ABA level is also increased in those plants (Adolfsson et al., 2017). This may explain improved tolerance of drought stress in AM associated plants (Subramanian et al., 1995; Khalvati et al., 2005; Fester and Hause, 2007; Augé et al., 2015). The ABA level is also changed in mycorrhizal roots. For example, AM colonization results in a strong increase of ABA content in roots of soybean, tomato and maize (Meixner et al., 2005; Rodriguez et al., 2010; Danneberg et al., 1993). The effect of exogenous ABA treatment on root colonization seems to be dose dependent. Colonization level is promoted at low concentrations of ABA in tomato and *Medicago*, while suppressed at high concentrations (Herrera-Medina et al., 2007; Charpentier et al., 2014). In addition, mutant studies provide genetic evidence for involvement of ABA in AM development. *sitiens*, an ABA biosynthesis-defective tomato mutant, exhibits strongly decreased amounts of colonization (Herrera-Medina et al., 2007; Rodriguez et al., 2010). The

low colonization phenotype can be partially restored by exogenous ABA treatment (Herrera-Medina et al., 2007; Rodriguez et al., 2010). Arbuscule development in *sitiens* is impaired as proportion of stunted arbuscules increased significantly compared to wild-type (Herrera-Medina et al., 2007). These results suggest that ABA may positively affect mycorrhizal intensity and arbuscule branching. Because of increased accumulation of ethylene in *sitiens*, it has been proposed that ethylene signaling possibly acts downstream of ABA to regulate AM development (Rodriguez et al., 2010). The molecular regulatory mechanism of ABA in AM development is not understood. It has been shown that the promotion of AM colonization via ABA is dependent on a PROTEIN PHOSPHATASE 2A (PP2A) holoenzyme subunit, PP2AB'1 (Charpentier et al., 2014). PP2AB'1 is proposed to be involved in ABA signaling and induced upon AM fungal infection (Charpentier et al., 2014). Mutations in *PP2AB'1* cause a reduction in AM colonization, which cannot be restored with application of ABA (Charpentier et al., 2014). Thus, it is reasonable to speculate a molecular regulatory mechanism that ABA may modulate AM colonization via PP2AB'1.

V. Materals and Methods

a) Plant materials

For all experiments, *L. japonicus* ecotype Gifu wild-type or mutant lines were used. The mutants *ram1-3*, *ram1-4*, *ram2-1*, *ram2-2*, *ccamk-3* and *cyclops-4* have been previously described (Pimprikar et al., 2016; Keymer et al., 2017; Tirichine et al., 2006; Yano et al., 2008). The *Ljarf17* mutants are LORE1 retrotransposon insertion lines. *Ljarf17-1* (30152074) and *Ljarf17-2* (30083262) carry LORE1 insertions in the fifth and eighth exons, respectively, in the genomic sequence of *ARF17*. Seeds for LORE1 insertion lines were obtained from the Lotus Base (https://lotus.au.dk/).

b) Seed germination and growth conditions

L. japonicus seeds were manually scarified with sand-paper, surface sterilized with solution containing 10% DanKlorix hygiene cleaner (https://www.danklorix.de/products/hygiene-cleaner-original) and 0.1% sodium dodecylsulfate (SDS), washed thoroughly and incubated for at least 2 hours to overnight in sterile water for seed swelling. Imbibed seeds were germinated on Petri dishes with half-strength Murashige and Skoog (MS) medium containing 0.8% agar at 24˚C for 3 days in dark. Subsequently, plates were shifted to a long-day condition of 16 h light / 8 h dark cycles with 60% humidity for 10-14 days (not for seedlings used for hairy root transformation).

c) Plasmid generation

Genes and promoter regions were amplified using Phusion PCR according to standard protocols and using primers indicated in Table 1. Plasmids were constructed by Golden Gate cloning (Binder et al., 2014) as indicated in Table 2.

Table 1 List of oligonucleotide primers used for cloning.

Purpose	**Primers**	
RD29b cloning	FD01	TACGGGTCTCAGCGGCTCAAGTT
	FD02	GGTCTCACAGACCTTCAAGTGAATCA
GUS cloning	GUS_F	ATGGTCTCATCTGATGTTACGTCCTGTAGAAACCCCAAC

	GUS_R	TAGGTCTCAGATTTCATTGTTTGCCTCCCTGCTG
RAM1 fragment A cloning	PP05	ATGAAGACTTTACGGGTCTCACACCATGATCAATTCAATGTGTGGAAG
	PP06	TAGAAGACAAAACCTTGTTTGATGAATTTGAATACC
RAM1 fragment B cloning	PP07	ATGAAGACTTGGTTTCTTCTGATATTGGAAGCTC
	PP08	TAGAAGACAATCCCTGCTTAAGCTATGCAA
RAM1 fragment C cloning	PP09	ATGAAGACTTGGGACTCTGGTTGATCCTACC
	PP10	TAGAAGACAACCTTATCATGGACAACAAATTCC
RAM1 fragment D cloning	PP11	TAGAAGACAAAAGGGACCAAGCACCTAACA
	PP12	ATGAAGACTTCAGAGGTCTCACCTTGCATCTCCATGCAGAGGC
p*RAM1* fragment 1 cloning	PP02	ATGAAGACTTTACGGGTCTCAGCGGGTAAGAGATAATGCGCGTTTGG
	PP132	TAGAAGACAAGATCAAATATCATTGTAATGCCTACATC
p*RAM1* fragment 1 cloning	PP133	ATGAAGACTTGATCTGTATTCAAAATTATGAATAAATTAC
	PP03	ATGAAGACTTCAGAGGTCTCACAGAGTTTTGTCTTTTTGGTAGAACAGAAA
VP16 cloning	JAVA76	ATGAAGACTTTACGGGTCTCATCTGATGGCGCAT
	JAVA77	TAGAAGACAATCATATGCCCACCGTACTCG
IAA17mImII cloning	JAVA78	TAGAAGACAAATGATGGGCAGTGTCGAGCT
	JAVA114	ATGAAGACTTCAGAGGTCTCTCCTTAGCTCTGCTCTTGCACTTCT
TAA1 genomic cloning	FD44	AAGAAGACAATACGGGTCTCACACCATGGTGGTCGCCAAGGCTGCTT
	FD45	ATGAAGACAACAGAGGTCTCTCCTTATATTTAGCATTTGACAACCTC
YUC6 genomic cloning	FD40	AAGGTCTCAGCGGACGTCTCACACCATGGACTATTACCTGAGAGAAATTGAAGG
	FD41	AAGGTCTCTGACATCGTCTCACCTTTGAATTTGATTGTGGCAAAATTGATCG
p*SbtM1* fragment 1 cloning	JAVA23	ATGAAGACTTTACGGGTCTCAGCGGAACATTGAGGACAGATTAAGG

	JAVA24	TAGAAGACAATTGCCTTCATTTGTGCCAAA
p*SbtM1* fragment 2 cloning	JAVA25	TAGAAGACAAGCAAATAAACCGTCCAAGGC
	JAVA26	ATGAAGACTTCAGAGGTCTCTCAGAGCTCCATCTTTAATTGGAATTTGATG
SbtM1 secretion signal peptide cloning	SC278	TATGGTCTCATCTGATGGAGCAAACCAAGTATAGGA
	SC279	TATGGTCTCAGGTGTCATGCTCTTGGCCTTCCT
CCaMK genomic fragment A cloning	PP204	ATGAAGACTTTACGGGTCTCACACCATGGGATATGATCAAACCAG
	PP207	TAGAAGACAATGATTAATTGTACTTTTGTATGTTTG
CCaMK genomic fragment B cloning	PP208	ATGAAGACTTATCATCAAACACTAAGAACAAAG
	PP209	TAGAAGACAAAGTCTTTTCATAGAAACTGAAATTC
CCaMK genomic fragment C cloning	PP210	ATGAAGACTTGACTTGGAAGGGCATTACCCAATC
	PP211	TAGAAGACAATGTTCATGGATATGTTTGAGTAAATAGGTTAACTAAG
C-terminal tag 3x*GFP* fragment A cloning	SC216	ATGAAGACTTTACGGGTCTCAAAGGGAGGTGGAGGAGGTTCTGG
	SC217	TTGAAGACTACACCCTTGTACAGCTCGTCCATGCC
C-terminal tag 3x*GFP* fragment B cloning	SC218	TTGAAGACTAGGTGGAGGAGGTTCTGGAGGCGG
	SC219	TTGAAGACTAACCCTTGTACAGCTCGTCCATGCC
C-terminal tag 3x*GFP* fragment C cloning	SC220	TTGAAGACTAGGGTGGAGGAGGTTCTGGAGGCGGT
	SC221	ATGAAGACTTCAGAGGTCTCAGATTTTACTTGTACAGCTCGTCCATG
CCaMK genomic fragment D cloning	PP212	TAGAAGACAAAACACATGCACATAGACAAGAATGCACACACATATAG
	PP213	ATGAAGACTTCAGAGGTCTCACCTTTGATGGACGAAGAGAAGAGAGGAGCATG
C-terminal $Citrine_N$	PP398	ATGAAGACTTTACGGGTCTCAAAGGATGGCGGCAGCGGCGGATCCATGGTGAGCAAGGGCGAGG
	PP399	ATGAAGACTTCAGAGGTCTCAGATTTTAGTCCTCGATGTTGTGGCGGAT
N-terminal $Citrine_C$ fragment A	PP394	ATGAAGACTTTACGGGTCTCATCTGATGGGCAGCGTGCAGCTCGC

	PP395	ATGAAGACTTGCTTGGACTGGTAGCTCAGGTAGTGGT
N-terminal *Citrine$_C$* fragment B	PP396	TAGAAGACAAAAGCTGAGCAAAGACCCCAAC
	PP397	ATGAAGACTTCAGAGGTCTCAGGTGATGGATCCGCCGCTGCCGCC
CCaMK$_{314}$ fragment 1 cloning	PP82	ATGAAGACTTTACGGGTCTCACACCATGGGATATGATCAAACCAGAAAG
	PP83	TAGAAGACAATGACCACATGTCACTCTTGGCAG
CCaMK$_{314}$ fragment 2 cloning	PP84	ATGAAGACTTGTCACTGGGAGTGATTCTATATATC
	PP85	TAGAAGACAATTTCTCATAGAAACTGAAATTCCCA
CCaMK$_{314}$ fragment 3 cloning	PP86	TAGAAGACAAGAAAACTTGGAAGGGCATTAC
	PP87	ATGAAGACTTCAGAGGTCTCACCTTAATCTCAGGGTCCATTTGCTC
CYCLOPS genomic fragment A cloning	PP168	ATGAAGACTTTACGGGTCTCACACCATGGAAGGGAGGGGGTTTTCTG
	PP169	TAGAAGACAATTTCAGGAACAATTCTTCACTTGAGTTTC
CYCLOPS genomic fragment B cloning	PP170	ATGAAGACTTGAAAACAGTGATGGAGAGC
	PP171	TAGAAGACAACTGATTGGAAAATTGAAATC
CYCLOPS genomic fragment C cloning	PP172	ATGAAGACTTTCAGGTAATTGCTCTATTCTTC
	PP173	TAGAAGACAACATTTACTGGCGTTTGATTAC
CYCLOPS genomic fragment D cloning	PP174	ATGAAGACTTAATGTTCAAGTAGACTCTAT
	PP175	TAGAAGACAAATAGATCCATATCTTTCTAG
CYCLOPS genomic fragment E cloning	PP176	ATGAAGACTTCTATAACATCAGCTGTTTCAG
	PP177	TAGAAGACAAATCTTCTATCTGCTTTGTTTG
CYCLOPS genomic fragment F cloning	PP178	TAGAAGACAAAGATCTTCAGAAGCAGAATG
	PP179	ATGAAGACTTCAGAGGTCTCACCTTCATTTTTTCAGTTTCTGATAG
N-terminal tag 3xGFP fragment A cloning	PP372	ATGAAGACTTTACGGGTCTCATCTGATGGTGAGCAAGGGCGAGGAG
	PP373	TAGAAGACAATCACGCTACCTCCGCCACCACT
N-terminal tag 3xGFP fragment B cloning	PP374	ATGAAGACTTGTGAGCAAGGGCGAGGAGCTG
	PP375	TAGAAGACAATTGCTCACGCTACCTCCGCCACCACTTC

N-terminal tag 3xGFP fragment C cloning	PP376	TAGAAGACAAGCAAGGGCGAGGAGCTGTTCACCGGGGT
	PP377	ATGAAGACTTCAGAGGTCTCAGGTGCCTCCGCCACCACTTCCACCG
BCP1 promoter cloning	CG342	TTTGGTCTCTCACCAGGTTGGGATGTACCATGTGAG
	CG343	AAAGGTCTCTTGTCCCAGCCATGGCAACTGAGGAAAC
TIP1 fragment A cloning	AK28	ATGAAGACATTACGGGTCTCACACCATGCCGATCAGAAAC
	AK29	TTGAAGACTACTACTAGACCAGAAGGAGTGGTGGCTCCG
TIP1 fragment B cloning	AK30	ATGAAGACATGTAGCTGCTGCAGTGGCTCATGCCTTTGG
	AK31	ATGAAGACATCAGATAGACCAAAAGCCGGCACAGCCAAGCC
TIP1 fragment C cloning	AK32	GCGAAGACGCTCTGCTGGAGTAGGAGTGTTGAACGC
	AK33	GCGAAGACATCAGAGGTCTCACCTTGTAGTCTGTGGTTGGGAGC

Table 2 List of plasmids used for experiments in this study. c, cloning vector; β, expression vector; F, forward; R, reverse; dy, dummy; GOI, replaceable gene of interest; POI, replaceable promoter of interest; -T, -terminator; ins, insulator; fin, final.

Name	**Description**
Golden Gate Level 0	
L0 $_{A\text{-}B}$ *RD29b*	PCR amplification with primers FD1 + FD2. Assembly by StuI cut ligation into L0-pUC57 (BB02)
L0 $_{B\text{-}E}$ *GUS*	PCR amplification with primers GUS_F + GUS_R. Assembly by SmaI cut ligation into backbone L0-pUC57 (BB02)
L0 $_{D\text{-}E}$ *Citrine$_N$*	PCR amplification with primers PP398 + PP399. Assembly by StuI cut ligation into L0-pUC57 (BB02)
L0 $_{A\text{-}B}$ p*BCP1*	PCR amplification with primers CG342 + CG343 from genomic DNA. Assembly by StuI cut ligation into backbone L0-pUC57 (BB02)
Golden Gate Level I	
LI $_{A\text{-}B}$ *DR5*	from Dr. David Chiasson

LI $_{C-D}$ *RAM1*	(Pimprikar et al., 2016)
LI $_{A-B}$ p*RAM1*	(Pimprikar et al., 2016)
LI $_{C-D}$ *VP16-IAA17mImII*	PCR amplification of VP16 with primers Java76 + Java77 and IAA17mImII with Java78 + Java114. Assembly by BpiI cut ligation into backbone LI (BB03)
LI $_{C-D}$ *TAA1*	PCR amplification with primers FD44 + FD45 from genomic DNA. Assembly by BpiI cut ligation into backbone LIIIβ $_{fin}$ (BB52)
LI $_{C-D}$ *YUC6*	PCR amplification with primers FD40 + FD41 from genomic DNA. Assembly by BsaI cut ligation into backbone LIIc F $_{3-4}$ (BB33)
LI $_{A-B}$ pSbtm1	(Keymer et al, 2017)
LI $_{B-C}$ SSP (SbtM1 secretion signal peptide)	(Keymer et al, 2017)
LI $_{A-B}$ *pEpi*	from Dr. David Chiasson
LI $_{C-D}$ *CCaMK*	PCR amplification of fragment A with primers PP204 + PP207, fragment B with PP208 + PP209, fragment C with PP210 + PP211 and fragment D with PP212 + PP213 from genomic DNA. Assembly by BpiI cut ligation into backbone LI (BB3).
LI $_{D-E}$ 3x*GFP*	PCR amplification of fragment A with primers SC216 + SC217, fragment B with SC218 + SC219 and fragment C with SC220 + SC221. Assembly by BpiI cut ligation into backbone LI (BB3).
LI $_{C-D}$ *CCaMK$_{314}$*	(Pimprikar et al., 2016)
LI $_{B-C}$ *Citrine$_{C}$*	PCR amplification of fragment 1 with primers PP394 + PP395 and fragment 2 with PP396 + PP397. Assembly by BpiI cut ligation into backbone LI (BB3).
LI *CYCLOPS*	PCR amplification of fragment A with primers PP168 + PP169, fragment B with PP170 + PP171, fragment C with PP172 + PP173, fragment D with PP174 + PP175, fragment E with PP176 + PP177 and fragment F with PP178 + PP179 from genomic DNA. Assembly by BpiI cut ligation into backbone LIIIβ A-B (BB53)
LI $_{B-C}$ 3x*GFP*	PCR amplification of fragment A with primers PP372 + PP373, fragment B with PP374 + PP375 and fragment C with PP376 + PP377. Assembly by BpiI cut ligation into backbone LI (BB3).
LI $_{C-D}$ *TIP1*	PCR amplification of fragment A with primers AK28 + AK29, fragment B with AK30 + AK31 and fragment C with AK32 +AK33. Assembly by BpiI cut ligation into backbone LI (BB3).

Golden Gate Level II	
LII $_{3-4}$ *RD29b*:*GUS*	Assembly by BsaI cut ligation from: L0 *RD29b* + LI $_{B-E}$ *GUS* + LI $_{E-F}$ nos-T (G06) +LI $_{F-G}$ dy (BB09) + LIIβ F $_{3-4}$ (BB24)
LII $_{3-4}$ *DR5*:*GUS*	Assembly by BsaI cut ligation from: LI $_{A-B}$ *DR5* + LI $_{B-E}$ *GUS* + LI $_{E-F}$ nos-T (G06) +LI $_{F-G}$ dy (BB09) + LIIc F $_{3-4}$ (BB33)
LII $_{5-6}$ *DR5*:*GUS*	Assembly by BsaI cut ligation from: LI $_{A-B}$ *DR5* + LI $_{B-E}$ *GUS* + LI $_{E-F}$ HSP-T (G45) +LI $_{F-G}$ dy (BB09) + LIIc F $_{5-6}$ (BB36)
LII $_{5-6}$ p*Ubi*:*RAM1*	Assembly by BsaI cut ligation from: LI $_{A-B}$ p*Ubi* (G07) + LI $_{B-C}$ dy + LI $_{C-D}$ *RAM1* + LI $_{D-E}$ dy (BB08) + LI $_{E-F}$ HSP-T (G45) +LI $_{F-G}$ dy (BB09) + LIIc F $_{5-6}$ (BB37)
LII $_{3-4}$ p*RAM1*:*VP16-IAA17mImII*	Assembly by BsaI cut ligation from: LI $_{A-B}$ p*RAM1* + LI $_{B-C}$ dy + LI $_{C-D}$ *VP16-IAA17mImII* + LI $_{D-E}$ dy (BB08) + LI $_{E-F}$ nos-T (G06) +LI $_{F-G}$ dy (BB09) + LIIc F $_{3-4}$ (BB33)
LII $_{1-2}$ p*SbtM1*:*SSP-mCherry*	Assembly by BsaI cut ligation from: LI $_{A-B}$ p*SbtM1* + LI $_{B-C}$ *SSP* + LI $_{C-D}$ dy (BB7) + LI $_{D-E}$ *mCherry* (G25) + LI $_{E-F}$ nos-T (G06) +LI $_{F-G}$ dy (BB09) + LIIβ F $_{1-2}$ (BB20)
LII $_{5-6}$ p*RAM1*:*TAA1*	Assembly by BsaI cut ligation from: LI $_{A-B}$ p*RAM1* + LI $_{B-C}$ dy + LI $_{C-D}$ *TAA1* + LI $_{D-E}$ dy (BB08) + LI $_{E-F}$ 35s-T (G59) +LI $_{F-G}$ dy (BB09) + LIIc F $_{5-6}$ (BB36)
LII $_{3-4}$ p*RAM1*:GOI	Assembly by BsaI cut ligation from: LI $_{A-B}$ p*RAM1* + LI $_{B-C}$ dy + LI $_{C-D}$ GOI+ LI $_{D-E}$ dy (BB08) + LI $_{E-F}$ nos-T (G06) +LI $_{F-G}$ dy (BB09) + LIIc F $_{3-4}$ (BB33)
LII $_{1-2}$ p*Ubi*:*mCherry*	Assembly by BsaI cut ligation from: LI $_{A-B}$ p*AtUbi* + LI $_{B-C}$ dy (BB06) + LI $_{C-D}$ *mCherry* (G23) + LI $_{D-E}$ dy (BB08) + LI $_{E-F}$ 35s-T (G59) +LI $_{F-G}$ dy (BB09) + LIIβ F $_{1-2}$ (BB20)
LII $_{5-6}$ p*Ubi*:*mCherry*	Assembly by BsaI cut ligation from: LI $_{A-B}$ p*Ubi* (G07) + LI $_{B-C}$ dy (BB06) + LI $_{C-D}$ *mCherry* (G23) + LI $_{D-E}$ dy (BB08) + LI $_{E-F}$ 35s-T (G59) +LI $_{F-G}$ dy (BB09) + LIIβ F $_{5-6}$ (BB28)
LII $_{3-4}$ p*Ubi*:*CCaMK*	Assembly by BsaI cut ligation from: LI $_{A-B}$ p*Ubi* (G07)+ LI $_{B-C}$ dy + LI $_{C-D}$ *CCaMK* + LI $_{D-E}$ dy (BB08) + LI $_{E-F}$ HSP-T (G45) +LI $_{F-G}$ dy (BB09) + LIIc F $_{3-4}$ (BB33)
LII $_{3-4}$ p*Epi*:*CCaMK*	Assembly by BsaI cut ligation from: LI $_{A-B}$ p*Epi* + LI $_{B-C}$ dy + LI $_{C-D}$ *CCaMK* + LI $_{D-E}$ dy (BB08) + LI $_{E-F}$ HSP-T (G45) +LI $_{F-G}$ dy (BB09) + LIIc F $_{3-4}$ (BB33)
LII $_{3-4}$ p*Ubi*:*CCaMK-GFP*	Assembly by BsaI cut ligation from: LI $_{A-B}$ p*Ubi* (G07)+ LI $_{B-C}$ dy + LI $_{C-D}$ *CCaMK* + LI $_{D-E}$ GFP (G11) + LI $_{E-F}$ HSP-T (G45) +LI $_{F-G}$ dy (BB09) + LIIc F $_{3-4}$ (BB33)
LII $_{3-4}$ p*Epi*:*CCaMK-GFP*	Assembly by BsaI cut ligation from: LI $_{A-B}$ p*Epi* + LI $_{B-C}$ dy + LI $_{C-D}$ *CCaMK* + LI $_{D-E}$ GFP (G11) + LI $_{E-F}$ HSP-T (G45) +LI $_{F-G}$ dy (BB09) + LIIc F $_{3-4}$ (BB33)

LII $_{3-4}$ p*Ubi*:*CCaMK*-3x*GFP*	Assembly by BsaI cut ligation from: LI $_{A-B}$ p*Ubi* (G07)+ LI $_{B-C}$ dy + LI $_{C-D}$ *CCaMK* + LI $_{D-E}$ 3x*GFP* + LI $_{E-F}$ HSP-T (G45) +LI $_{F-G}$ dy (BB09) + LIIc F $_{3-4}$ (BB33)
LII $_{3-4}$ p*Epi*:*CCaMK*-3x*GFP*	Assembly by BsaI cut ligation from: LI $_{A-B}$ p*Epi* + LI $_{B-C}$ dy + LI $_{C-D}$ *CCaMK* + LI $_{D-E}$ 3x*GFP* + LI $_{E-F}$ HSP-T (G45) +LI $_{F-G}$ dy (BB09) + LIIc F $_{3-4}$ (BB33)
LII $_{3-4}$ p*Ubi*:*CcaMK*$_{314}$	Assembly by BsaI cut ligation from: LI $_{A-B}$ p*Ubi* (G07)+ LI $_{B-C}$ dy + LI $_{C-D}$ *CCaMK*$_{314}$ + LI $_{D-E}$ dy (BB08) + LI $_{E-F}$ HSP-T (G45) +LI $_{F-G}$ dy (BB09) + LIIc F $_{3-4}$ (BB33)
LII $_{3-4}$ p*Epi*:*CcaMK*$_{314}$	Assembly by BsaI cut ligation from: LI $_{A-B}$ p*Epi* + LI $_{B-C}$ dy + LI $_{C-D}$ *CCaMK*$_{314}$ + LI $_{D-E}$ dy (BB08) + LI $_{E-F}$ HSP-T (G45) +LI $_{F-G}$ dy (BB09) + LIIc F $_{3-4}$ (BB33)
LII $_{3-4}$ p*Ubi*:*CCaMK*-*Citrine*$_N$	Assembly by BsaI cut ligation from: LI $_{A-B}$ p*Ubi* (G07) + LI $_{B-C}$ dy + LI $_{C-D}$ *CCaMK* + LI $_{D-E}$ *Citrine*$_N$ + LI $_{E-F}$ nos-T (G06) +LI $_{F-G}$ dy (BB09) + LIIc F $_{3-4}$ (BB33)
LII $_{5-6}$ p*Ubi*:*Citrine*$_C$-*CYCLOPS*	Assembly by BsaI cut ligation from: LI $_{A-B}$ p*Ubi* (G07) + LI $_{B-C}$ *Citrine*$_C$ + LI $_{C-D}$ *CYCLOPS* + LI $_{D-E}$ dy (BB08) + LI $_{E-F}$ 35s-T (G59) +LI $_{F-G}$ dy (BB09) + LIIc F $_{5-6}$ (BB36)
LII $_{3-4}$ p*Ubi*:*CYCLOPS*	Assembly by BsaI cut ligation from: LI $_{A-B}$ p*Ubi* (G07)+ LI $_{B-C}$ dy + LI $_{C-D}$ *CYCLOPS* + LI $_{D-E}$ dy (BB08) + LI $_{E-F}$ HSP-T (G45) +LI $_{F-G}$ dy (BB09) + LIIc F $_{3-4}$ (BB33)
LII $_{3-4}$ p*Epi*:*CYCLOPS*	Assembly by BsaI cut ligation from: LI $_{A-B}$ p*Epi* + LI $_{B-C}$ dy + LI $_{C-D}$ *CYCLOPS* + LI $_{D-E}$ dy (BB08) + LI $_{E-F}$ HSP-T (G45) +LI $_{F-G}$ dy (BB09) + LIIc F $_{3-4}$ (BB33)
LII $_{3-4}$ p*Ubi*:*GFP*-*CYCLOPS*	Assembly by BsaI cut ligation from: LI $_{A-B}$ p*Ubi* (G07)+ LI $_{B-C}$ *GFP* (G28) + LI $_{C-D}$ *CYCLOPS* + LI $_{D-E}$ dy (BB08) + LI $_{E-F}$ HSP-T (G45) +LI $_{F-G}$ dy (BB09) + LIIc F $_{3-4}$ (BB33)
LII $_{3-4}$ p*Epi*:*GFP*-*CYCLOPS*	Assembly by BsaI cut ligation from: LI $_{A-B}$ p*Epi* + LI $_{B-C}$ *GFP* (G28) + LI $_{C-D}$ *CYCLOPS* + LI $_{D-E}$ dy (BB08) + LI $_{E-F}$ HSP-T (G45) +LI $_{F-G}$ dy (BB09) + LIIc F $_{3-4}$ (BB33)
LII p*Ubi*:3x*GFP*-*CYCLOPS*	Assembly by BsaI cut ligation from: LI $_{A-B}$ p*Ubi* (G07)+ LI $_{B-C}$ 3x*GFP* + LI $_{C-D}$ *CYCLOPS* + LI $_{D-E}$ dy (BB08) + LI $_{E-F}$ HSP-T (G45) +LI $_{F-G}$ dy (BB09) + LIIc F $_{3-4}$ (BB33)
LII p*Epi*:3x*GFP*-*CYCLOPS*	Assembly by BsaI cut ligation from: LI $_{A-B}$ p*Epi* + LI $_{B-C}$ 3x*GFP* + LI $_{C-D}$ *CYCLOPS* + LI $_{D-E}$ dy (BB08) + LI $_{E-F}$ HSP-T (G45) +LI $_{F-G}$ dy (BB09) + LIIc F $_{3-4}$ (BB33)
LII $_{3-4}$ POI:*YFP-TIP1*	Assembly by BsaI cut ligation from: LI $_{A-B}$ POI (G82) + LI $_{B-C}$ *YFP* (G29) + LI $_{C-D}$ *TIP1*+ LI $_{D-E}$ dy (BB08) + LI $_{E-F}$ nos-T (G06) +LI $_{F-G}$ dy (BB09) + LIIc F $_{3-4}$ (BB33)

LII $_{3-4}$ p*BCP1*:*YFP-TIP1*	Assembly by BsaI cut ligation from: LI $_{A-B}$ p*BCP1* + LI $_{B-C}$ *YFP* (G29) + LI $_{C-D}$ *TIP1*+ LI $_{D-E}$ dy (BB08) + LI $_{E-F}$ nos-T (G06) +LI $_{F-G}$ dy (BB09) + LIIc F $_{3-4}$ (BB33)
Golden Gate Level III	
LIII *RD29b*:*GUS*	Assembly by BpiI cut ligation from: LIIc F $_{1-2}$ *pUbi*:*mCherry* + LII $_{2-3}$ ins (BB43) + LIIβ F $_{3-4}$ *RD29b*:*GUS* +LII $_{4-6}$ dy (BB41) + LIIIβ $_{fin}$ (BB52)
LIII *DR5*:*GUS*	Assembly by BpiI cut ligation from: LIIc F $_{1-2}$ p*Ubi*:*mCherry* + LII $_{2-3}$ ins (BB43) + LIIβ F $_{3-4}$ *DR5*:*GUS* +LII $_{4-6}$ dy (BB41) + LIIIβ $_{fin}$ (BB52)
LIII p*Ubi*:*RAM1*	Assembly by BpiI cut ligation from: LIIc F $_{1-2}$ p*Ubi*:*mCherry* + LII $_{2-3}$ ins (BB43) + LIIβ F $_{3-4}$ *DR5*:*GUS* +LII $_{4-5}$ dy (BB40) + LIIc F $_{5-6}$ p*Ubi*:*RAM1* + LIIIβ $_{fin}$ (BB52)
LIII p*RAM1*:*VP16-IAA17mImII*	Assembly by BpiI cut ligation from: LIIc F $_{1-2}$ p*Ubi*:*mCherry* + LII $_{2-3}$ ins (BB43) + LIIc F $_{3-4}$ p*RAM1*:*VP16-IAA17mImII* +LII $_{4-5}$ dy (BB40) + LIIc F $_{5-6}$ *DR5*:*GUS* + LIIIβ $_{fin}$ (BB52)
LIII p*RAM1*:GOI-p*RAM1*:*TAA1*	Assembly by BpiI cut ligation from: LIIc F $_{1-2}$ p*Ubi*:*mCherry* + LII $_{2-3}$ ins (BB43) + LIIc F $_{3-4}$ p*RAM1*:GOI +LII $_{4-5}$ dy (BB40) + LIIc F $_{5-6}$ *pRAM1*:*TAA1* + LIIIβ $_{fin}$ (BB52)
LIII p*RAM1*:*YUC6*-p*RAM1*:*TAA1*	Assembly by Esp3I cut ligation from: LIII β $_{fin}$ p*RAM1*:GOI-p*RAM1*:*TAA1* + L0 Esp3I *YUC6*
LIII p*Ubi*:*CCaMK*	Assembly by BpiI cut ligation from: LIIβ F $_{1-2}$ p*Ubi*:*mCherry* + LII $_{2-3}$ ins (BB43) + LIIc F $_{3-4}$ p*Ubi*:*CCaMK* +LII $_{4-6}$ dy (BB41) + LIIIβ F $_{A-B}$ (BB53)
LIII p*Epi*:*CCaMK*	Assembly by BpiI cut ligation from: LIIβ F $_{1-2}$ p*Ubi*:*mCherry* + LII $_{2-3}$ ins (BB43) + LIIc F $_{3-4}$ p*Epi*:*CCaMK* +LII $_{4-6}$ dy (BB41) + LIIIβ F $_{A-B}$ (BB53)
LIII p*Ubi*:*CCaMK-GFP*	Assembly by BpiI cut ligation from: LIIβ F $_{1-2}$ p*Ubi*:*mCherry* + LII $_{2-3}$ ins (BB43) + LIIc F $_{3-4}$ p*Ubi*:*CcaMK-GFP* +LII $_{4-6}$ dy (BB41) + LIIIβ F $_{A-B}$ (BB53)
LIII p*Epi*:*CCaMK-GFP*	Assembly by BpiI cut ligation from: LIIβ F $_{1-2}$ p*Ubi*:*mCherry* + LII $_{2-3}$ ins (BB43) + LIIc F $_{3-4}$ p*Epi*:*CCaMK* +LII $_{4-6}$ dy (BB41) + LIIIβ F $_{A-B}$ (BB53)
LIII p*Ubi*:*CCaMK*-3x*GFP*	Assembly by BpiI cut ligation from: LIIβ F $_{1-2}$ p*Ubi*:*mCherry* + LII $_{2-3}$ ins (BB43) + LIIc F $_{3-4}$ p*Ubi*:*CCaMK*-3x*GFP* +LII $_{4-6}$ dy (BB41) + LIIIβ F $_{A-B}$ (BB53)
LIII p*Epi*:*CCaMK*-3x*GFP*	Assembly by BpiI cut ligation from: LIIβ F $_{1-2}$ p*Ubi*:*mCherry* + LII $_{2-3}$ ins (BB43) + LIIc F $_{3-4}$ p*Epi*:*CCaMK*-3x*GFP* +LII $_{4-6}$ dy (BB41) + LIIIβ F $_{A-B}$ (BB53)
LIII p*Ubi*:$CCaMK_{314}$	Assembly by BpiI cut ligation from: LII $_{1-2}$ dy (BB63)+ LII $_{2-3}$ ins (BB43) + LIIc F $_{3-4}$ p*Ubi*:$CcaMK_{314}$ +LII $_{4-5}$ ins (BB44) + LII F $_{5-6}$ p*AtUbi*:*mCherry* + LIIIβ F $_{A-B}$ (BB53)

LIII p*Epi*:*CCaMK*$_{314}$	Assembly by BpiI cut ligation from: LII $_{1-2}$ dy (BB63)+ LII $_{2-3}$ ins (BB43) + LIIc F $_{3-4}$ p*Epi*:*CcaMK*$_{314}$ +LII $_{4-5}$ ins (BB44) + LII F $_{5-6}$ p*AtUbi*:*mCherry* + LIIIβ F $_{A-B}$ (BB53)
LIII p*Ubi*:*CCaMK-Citrine*$_N$- p*Ubi*:*Citrine*$_C$-*CYCLOPS*	Assembly by BpiI cut ligation from: LIIβ F $_{1-2}$ p*SbtM1*:*SSP-mCherry* + LII $_{2-3}$ ins (BB43) + LIIc F $_{3-4}$ p*Ubi*:*CcaMK-Citrine*$_N$ +LII $_{4-5}$ dy (BB40) + LIIc F $_{5-6}$ p*Ubi*:*Citrine*$_C$*-CYCLOPS* + LIIIβ $_{fin}$ (BB52)
LIII p*Ubi*:*CYCLOPS*	Assembly by BpiI cut ligation from: LIIβ F $_{1-2}$ p*SbtM1*:*SSP-mCherry* + LII $_{2-3}$ ins (BB43) + LIIc F $_{3-4}$ p*Ubi*:*CYCLOPS* +LII $_{4-6}$ dy (BB41) + LIIIβ F $_{A-B}$ (BB53)
LIII p*Epi*:*CYCLOPS*	Assembly by BpiI cut ligation from: LIIβ F $_{1-2}$ p*SbtM1*:*SSP-mCherry* + LII $_{2-3}$ ins (BB43) + LIIc F $_{3-4}$ p*Epi*:*CYCLOPS* +LII $_{4-6}$ dy (BB41) + LIIIβ F $_{A-B}$ (BB53)
LIII p*Ubi*:*GFP-CYCLOPS*	Assembly by BpiI cut ligation from: LIIβ F $_{1-2}$ p*SbtM1*:*SSP-mCherry* + LII $_{2-3}$ ins (BB43) + LIIc F $_{3-4}$ p*Ubi*:*GFP-CYCLOPS* +LII $_{4-6}$ dy (BB41) + LIIIβ F $_{A-B}$ (BB53)
LIII p*Epi*:*GFP-CYCLOPS*	Assembly by BpiI cut ligation from: LIIβ F $_{1-2}$ p*SbtM1*:*SSP-mCherry* + LII $_{2-3}$ ins (BB43) + LIIc F $_{3-4}$ p*Epi*:*GFP-CYCLOPS* +LII $_{4-6}$ dy (BB41) + LIIIβ F $_{A-B}$ (BB53)
LIII p*Ubi*:3x*GFP-CYCLOPS*	Assembly by BpiI cut ligation from: LIIβ F $_{1-2}$ p*SbtM1*:*SSP-mCherry* + LII $_{2-3}$ ins (BB43) + LIIc F $_{3-4}$ p*Ubi*:3x*GFP-CYCLOPS* +LII $_{4-6}$ dy (BB41) + LIIIβ F $_{A-B}$ (BB53)
LIII p*Epi*:3x*GFP-CYCLOPS*	Assembly by BpiI cut ligation from: LIIβ F $_{1-2}$ p*SbtM1*:*SSP-mCherry* + LII $_{2-3}$ ins (BB43) + LIIc F $_{3-4}$ p*Epi*:3x*GFP-CYCLOPS* +LII $_{4-6}$ dy (BB41) + LIIIβ F $_{A-B}$ (BB53)
LIII p*Epi*:*NLS*-2X*YFP*	Assembly by BpiI cut ligation from: LIIβ F $_{1-2}$ p*SbtM1*:*SSP-mCherry* + LII $_{2-3}$ ins (BB43) + LII $_{3-4}$ dy (BB64) +LII $_{4-5}$ ins (BB40) + LIIc F $_{5-6}$ p*Epi*:*Citrine*$_C$*-CYCLOPS* + LIIIβ $_{fin}$ (BB52)
LIII p*CCaMK*:*NLS*-2X*YFP*	Assembly by BpiI cut ligation from: LIIβ F $_{1-2}$ p*SbtM1*:*SSP-mCherry* + LII $_{2-3}$ ins (BB43) + LII $_{3-4}$ dy (BB64) +LII $_{4-5}$ ins (BB40) + LIIc F $_{5-6}$ p*Ubi*:*Citrine*$_C$*-CYCLOPS* + LIIIβ $_{fin}$ (BB52)
LIII p*BCP1*:*YFP-TIP1*	Assembly by BpiI cut ligation from: LIIβ F $_{1-2}$ pSbtM1:SSP-*mCherry* + LII $_{2-3}$ ins (BB43) + LIIc F $_{3-4}$ p*BCP1*:*YFP-TIP1* +LII $_{4-5}$ ins (BB40) + LIIc F $_{5-6}$ p*Ubi*:*NLS-Cerulean* + LIIIβ F $_{A-B}$ (BB53)

d) Hairy root transformation

Three days post germination in 16 h-light / 8 h-dark cycles, seedlings were cut at the base of the hypocotyl and dipped into a fresh and concentrated solution of *Agrobacterium rhizogenes* AR1193 before being placed on B5 medium in the dark for 3 days. Seedlings were

transferred successively on new plates containing B5 medium supplied with 1% sugar and 300 µg / ml cefotaxime, at 24˚C, 60% humidity, with 16 h-light / 8 h-dark cycles. After 3 weeks, transformed roots were screened with the *mCherry* transformation marker on a stereomicroscope (Leica M165 FC or Zeiss Stereo discovery.V8).

e) Inoculation with fungal spores

After being washed and sterilized with 70% ethanol, pots were filled with autoclaved sand-vermiculite mix (2:1) or pure sand containing 500 *Rhizophagus irregularis* DAOM197198 (Agronutrition) spores per plant positioned in the middle layer of the substrate. Plantlets were then transferred from plates to pots (4-6 per pot) and grown at 24˚C with 16 h-light-8 h-dark cycles at 60% humidity. Plants were fertilized three times a week with 15-30 ml half-strength Hoagland's solution containing 5 µM phosphate. After 5 weeks post-inoculation, plants were harvested for further analysis.

f) Histochemical GUS staining

Prior to harvesting, in the case of hairy-root transformation, transformed roots expressing the *mCherry* transformation marker were screened and separated from non-transformed roots by fluorescence microscopy (Leica M165 FC or Zeiss Stereo discovery.V8). *L. japonicus* hairy roots transformed with plasmids containing a promoter:*GUS* reporter cassette were harvested five weeks post-inoculation with *R. irregularis*. Collected roots were vacuum infiltrated with GUS staining solution (0.1 M NaPO4 pH 7.0, 10 mM EDTA, 1 mM K3[Fe(CN)6], 1 mM K4[Fe(CN)6], 10% Triton-X100; 1 mM X-Gluc) and incubated at 37˚C in the dark (2 hours for roots with *RD29b*:*GUS*, overnight for *DR5*:*GUS*. The enzymatic reaction was stopped by removal of GUS staining solution. Roots were cleared and stored in pure ethanol at 4˚C.

g) Wheat-germ-agglutinin (WGA) staining

Collected roots were placed in 10% KOH for 2-3 days at room temperature or 5 min at 95˚C. After 3 times washing with water, roots were acidified in a 0.1 M HCl solution for 1-2 hours. Then, roots were gently washed with PBS (phosphate-buffered saline) and incubated in the dark for a minimum of 6 hours in a PBS solution containing 1 µg / mL wheat-germ-agglutinin-AlexaFluor488 (Molecular Probes, http://www.lifetechnologies.com/). Stained

roots were stored in PBS solution at 4˚C. Imaging was performed with a GFP filter on a fluorescent microscope (Leica DMI6000 B and DM6 B) and confocal microscope (Leica SP5).

h) Ink-acetic acid staining

Collected roots were placed in 10% KOH and heated for 5 min at 95˚C for 15 min. After 3 times washing with water, roots were acidified in 10% acetic acid and then incubated in 10% ink containing 5% acetic acid for 95˚C 5 min. After 3 times washing with water, roots were de-stained in 5% acetic acid for 15 min at room temperature and then analyzed or stored in 5% acetic acid in 4˚C. Roots were observed on a Leica microscope (020-518.500 DM/LS) and imaging was performed on a Leica microscope (DMI6000 B or DM6 B).

i) AM quantification

Fungal structures in colonized roots were stained either with WGA-AlexaFluor488 (method 7) or ink-acetic acid method (method 8). Root length colonization was quantified using the gridline intersect method (McGonigle et al., 1990) on a light microscope (Leica, type 020-518500 DM/LS) with 10 to 20 randomly picked root pieces per plant.

j) Gene expression analysis

Plant root tissue was harvested and rapidly shock-frozen in liquid nitrogen. Tissue was ground manually to fine powder and RNA was extracted using the Spectrum Plant Total RNA Kit (https://www.sigmaaldrich.com). RNA integrity was tested by 2% Agarose gel electrophoresis. Residual DNA was removed by DNase I treatment (https://www.sigmaaldrich.com). RNA purity was tested to avoid genomic DNA contamination by PCR using the pair of primers: CG344, TTTGGTCTCGAATACTGATCATATTGTGGGTGATGAC; CG345, AAAGGTCTCACCTTTCATGCAAAGAAAGCTGTGATGAC. cDNA synthesis on equal quantity of RNA from each sample, as determined by Nanodrop, was performed using the Superscript III kit (https://www.thermofisher.com). Reverse transcriptase quantitative real time PCR (RT-qPCR) reactions were carried out with a master-mix EvaGreen (http://www.metabion.com/). RT-qPCR reactions were run either on an iCycler (Biorad, https://www.bio-rad.com/) or QuantStudio5 (applied biosystems, https://www.bio-rad.com/). Thermal cycler conditions were: 95˚C 2 min, 40 cycles of 95˚C 30 sec, 60˚C 30 sec, 72˚C 20

sec, followed by a dissociation curve analysis. Expression values were calculated by the $2^{-\Delta Ct}$ method (Czechowski et al., 2004). Expression values were normalized to the expression level of the housekeeping gene *Ubiquitin10*. For each condition 2 to 4 technical and biological replicates were performed. Primers are indicated in Table 3.

Table 3 Primers for RT-qPCR.

Gene	**Primers**	
Ubiquitin	Ubi F	ATGCAGATCTTCGTCAAGACCTTG
	Ubi R	ACCTCCCCTCAGACGAAG
ARF17	FD06	AGCTTCCCTTTCTCATGCAA
	FD07	TTCCAGGTAGGCTGAAAGGA
SAURs	FD10	GTGTTGGCACAAATGAGGA
	FD11	CCTACCTAGAAGCTCGCAGA
PT4	PT4 F	GAATAAAGGGGCCAAAATCG
	PT4 R	GCTGTATCCTATCCCCATGC
AMT2.2	AMT2.2 F	TGGTTCAACTTTTCGTTCCA
	AMT2.2 R	CTTATCACCCTGACCCCAGA
IAA17mImII	FD12	CGGTAACCGGAAACAAGAGA
	FD13	GCAGGAAACCATCACGTTCT
GH3	FD24	TGCCGGTGATGAACCAATAC
	FD25	GGGTCAAATGGTCTTTTCTT
YUC6	FD14	GCAAGATGGATTCCCAAAGA
	FD15	TCCTTTGCCTCATCACCTTC
TAA1	FD16	ATCCCAAACTCGAGCTGCTA
	FD17	AAAGCAGGGAGTGCTTCAAA
RAM1	PP99	TGCATTGAATCATGCTACGTT
	PP100	CCTTGTGGAGACCATCCATT
SbtM1	SbtM1 F	CACGTTGTTAGGACCCCAAT
	SbtM1 R	TTGAGCAGCACCCTCTCTATC
Vapyrin B	Vapyrin B F	CCATCAATGGAAGGGATCAG

	Vapyrin B R	TCGATCCCTTTCTCCACAAG

k) Genomic DNA extraction

L. japonicus leaves were collected in tubes containing 2 metal beads and frozen in liquid nitrogen. Tissues were lysed using a TissueLyser (https://www.qiagen.com) at 30 Hz for 1 min. 300 µl of 65˚C pre-warmed extraction buffer pH7.4 (200 mM Tris pH7.5, 250 mM NaCl, 25 mM EDTA and 0.5% SDS) was added and quickly vortexed. Samples were incubated at 65˚C for 30 min and followed by chilling on ice for 5 min. 140 µl of 3 M potassium acetate was added and mixed by repeated inversion. Following incubation on ice for 15 min, samples were centrifuged for 15 min at 13000 rpm. 100 ml supernatants were transferred to new tubes in which 80 µl of isopropanol were added for DNA precipitation. After mixing by inversion, samples were incubated at -20˚C for 2 hours minimum and then centrifuged at 4˚C for 15 min at 13000 rpm. Supernatants were discarded and pellets were washed one time in 70% ethanol, and samples centrifuged 5 min at 13000 rpm. Supernatants were discarded, and ethanol evaporated at room temperature. Dried DNA pellets were suspended in TE buffer.

l) Plant genotyping

Following genomic DNA extraction, homozygous mutants generated by a LORE1 insertion were identified by PCR using genomic DNA extracted from each plant as template and two primer pairs: one forward and reverse flanking the insertion site, and the second using the forward and a specific primer to the *LORE1* sequence (CCATGGCGGTTCCGTGAATCTTAGG). Primers are indicated in Table 4.

Table 4 Primers used for LORE1 insertion mutant genotyping.

allele	**Primers**	
arf17-1	FD36-forward	CCCCATCATGCCAACATTCTTCTGC
	FD37-reverse	TCCAAACAAATCGAGAAACACGATGC
arf17-2	FD32-forward	TGTGTCATTGCAGTGGGGACAATGG
	FD33-reverse	CAGACATCTCCATTCTGAACCAGGCCA

m) Phylogenetic tree

Coding sequences (CDS) were retrieved using BLASTn with *LjARF17* as a query against a database of 19 species (Table 6). Hits of CDS were kept using the standard e-value < 1e-10 and sequence coverage > 30%. The multiple alignment of the protein sequences derived from CDS was used to generate a Neighbor-Joining phylogenetic tree with 1000 bootstrap replicates in MEGA X version 10.1.8 (https://www.megasoftware.net/).

n) Auxin treatment assay

Plants were watered three times a week with half-strength Hoagland medium supplemented with indicated doses of NAA and 2,4-D or with solvent starting in the second week after *R. irregularis* inoculation (Table 5).

Table 5 Compounds used in this study.

compound	Supplier	Solvent	Stock
NAA	Sigma	pure Ethanol	1 mg / ml
2,4-D	Sigma	pure Ethanol	1 mg / ml

o) Root length measurement

Each plant was harvested and transferred to a petri dish. Initiation and apices of primary root were immediately and directly marked on the petri dish and the length was measured by a ruler manually.

p) Lateral root assay

Plants with hairy roots transformed with p*Ubi*:*RAM1* or an empty vector control were grown in Petri dishes containing B5 medium supplied with 1% sugar and 300 µg/ml cefotaxime for 2 weeks. 1 cm of transformed root fragments from the tip of each plant was randomly chosen and cut into MSR liquid medium containing 10% sucrose (Declerck et al., 1998) to support the growth of shoot-less root pieces in dark. 10 days later, lateral roots were counted on a microscope (Leica M165 FC).

q) IAA measurement by MS

Transformed hairy roots were harvested by screening for the mCherry marker, weighed and frozen immediately in liquid nitrogen. Roots exhibiting an explosion of lateral roots due to *RAM1* over-expression were harvested separately. Materials were sent to be analyzed for indole acetic acid using mass spectrometry (MS) by the lab of Dr. Karin Ljung in Swedish University of Agricultural Sciences according to Edlund et al., 1995.

r) Arbuscule size measurement

Images of colonized root fragments from 5 independent plants were taken with Leica DM6 B microscope equipped with Leica DFC9000 GT and DMC2900 cameras. Arbuscules were indicated either by WGA-AlexaFluor488 staining or ink-acetic acid staining. Fiji (http://fiji.sc/) was used for analyzing the size of arbuscules. Six to ten arbuscules for Fig. S2B and ten arbuscules for Fig. 11B from each of five plants were randomly chosen and manually outlined by “freehand selections” tool, the area was measured with the “measure” tool.

s) Longitudinal root section

For the promoter activity assay of p*Epi* and p*CCaMK*, seedlings were harvested and roots were screened on a stereomicroscope (Zeiss discovery.V8) to detect root regions expressing the *mCherry* arbuscule marker. Root fragments of approximately 1 cm were cut from the same root system and embedded in 6% low-melt agarose. Sections of 40-50 μm were prepared with a Vibratome VT1100S (Leica). Live visualization and imaging were performed with the Leica DM6 B microscope equipped with a Leica DFC9000 GT and DMC2900 cameras. Processing of the images was performed with Fiji.

t) Bimolecular fluorescence complementation (BiFC) assay

The interaction between CCaMK and CYCLOPS was determined using the split-*Citrine* plasmid listed in Table 2. Live imaging was performed on confocal laser scanning microscopy Leica SP8.

u) Statistical analysis

Statistical analyses were performed using GraphPad Prism 8.0 (https://www.graphpad.com/scientific-software/prism/). For equal variance, gene expression data were log transformed prior to analysis.

VI. Results

1. Is auxin signaling part of the RAM1-regulated developmental program of arbuscule-containing cells?

a) ABA response is activated in arbuscule-containing cells but does not depend on *RAM1*

It has been shown that ABA affects AM colonization in tomato and *M. truncatula* (Charpentier et al., 2014; Herrera-Medina et al., 2007). To examine the stage of mycorrhizal colonization at which ABA signaling intervenes, I visualized the activity of *RD29b*, a classical synthetic ABA-inducible promoter (Yamaguchi-Shinozaki and Shinozaki, 1994), fused to the *GUS* reporter gene in Gifu wild-type of *L. japonicus*. Strong GUS staining was observed in big patches localized in the inner cortex and seemed to correspond with fungal colonization. To examine this more precisely, I stained the AM fungus with the dye-coupled chitin-binding lectin, fluorescein-conjugated wheat germ agglutinin (WGA) coupled to AlexaFluor488 and visualized it by fluorescence microscopy. This confirmed that the GUS staining was highly specific to the cells, which harbored arbuscules, suggesting that arbuscule development is accompanied by an ABA response (Fig. 4). To investigate whether this induction of an ABA response is downstream of *RAM1*, the *ram1-3* mutant was also tested. GUS activity was observed in the arbuscule-containing cells of *ram1-3*, indicating that the ABA response in the arbuscule-containing cells is not dependent on *RAM1* (Fig. 4).

b) Induction of auxin response in arbuscule-containing cells is dependent on *RAM1*

It has also been shown that auxin response is activated in the arbuscule-containing cells in tomato, *M. truncatula* and rice (Etemadi et. al., 2014). To investigate whether this specific pattern is also conserved in *L. japonicus* and whether it is downstream of *RAM1*, detection of auxin response and visualization of fungal structures were performed on hairy roots of a transgenic *DR5*:*GUS* line in the background of wild-type or two allelic of *ram1* mutants. *DR5* is a canonical synthetic promoter consisting of nine tandem repeats of an auxin response cis-elements (AuxREs, TGTCTC) (Ulmasov et al., 1997). I characterized the *DR5*:*GUS* expression pattern in non-colonized and colonized roots. GUS staining was detected in the root tips (data not shown) and lateral root primordia in both wild-type and *ram1*

(Fig. 5), which is a known pattern of *DR5* activity in roots (Sabatini et al., 1999; Dubrovsky et al., 2008). In mycorrhizal roots, strong additional GUS staining was present in wild-type but not in two allelic *ram1* mutants, indicating that during AM symbiosis, auxin response is activated in the arbuscule-containing cells and acts downstream of *RAM1*.

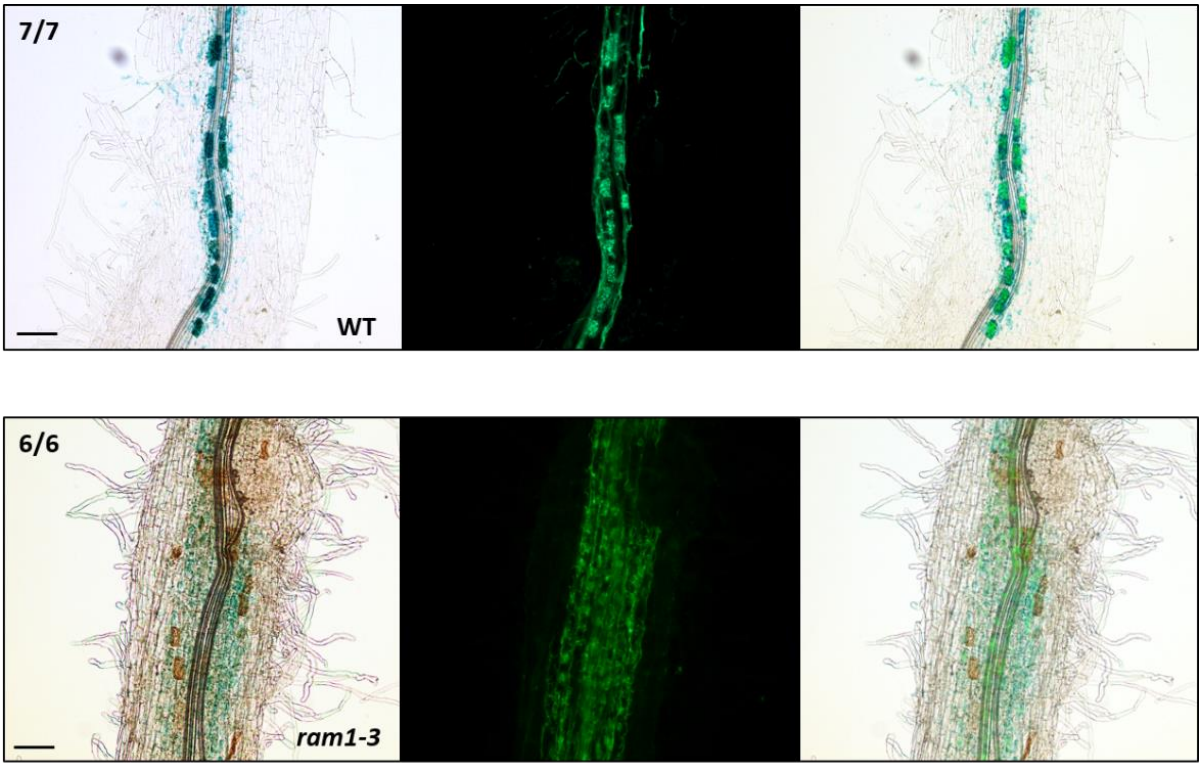

Fig. 4 *RD29b*:*GUS* expression in arbuscule-containing cells in both Gifu wild-type and *ram1-3* mutant at 5 weeks post inoculation (wpi) by *R. irregularis*. GUS staining was visualized in bright field of microscope (left column), fungal structures of the same root segment were indicated by green fluorescent WGA-AlexaFluor488 staining (intermediate column) and overlay of bright field and fluorescent images are shown in the right column. Numbers indicate root systems with the displayed phenotype per total number of analyzed transgenic root systems. Scale bars represent 100 μm.

We also included *ram2* as a control to make sure the absence of GUS activity did not relate to the defect in arbuscule branching in *ram1* mutants. *ram2* mutant has a similar arbuscule-branching phenotype to *ram1* mutants, with stunted arbuscules. However, the gene has a very different function from *RAM1*. *RAM1* encodes a GRAS transcription factor, while *RAM2* encodes a lipid biosynthesis enzyme (Keymer et al. 2017). In *ram2-2*, I observed that *DR5*:*GUS* was still induced in the arbuscule-containing cells. This means *DR5*:*GUS* is dependent on *RAM1*, not on the arbuscule branching itself.

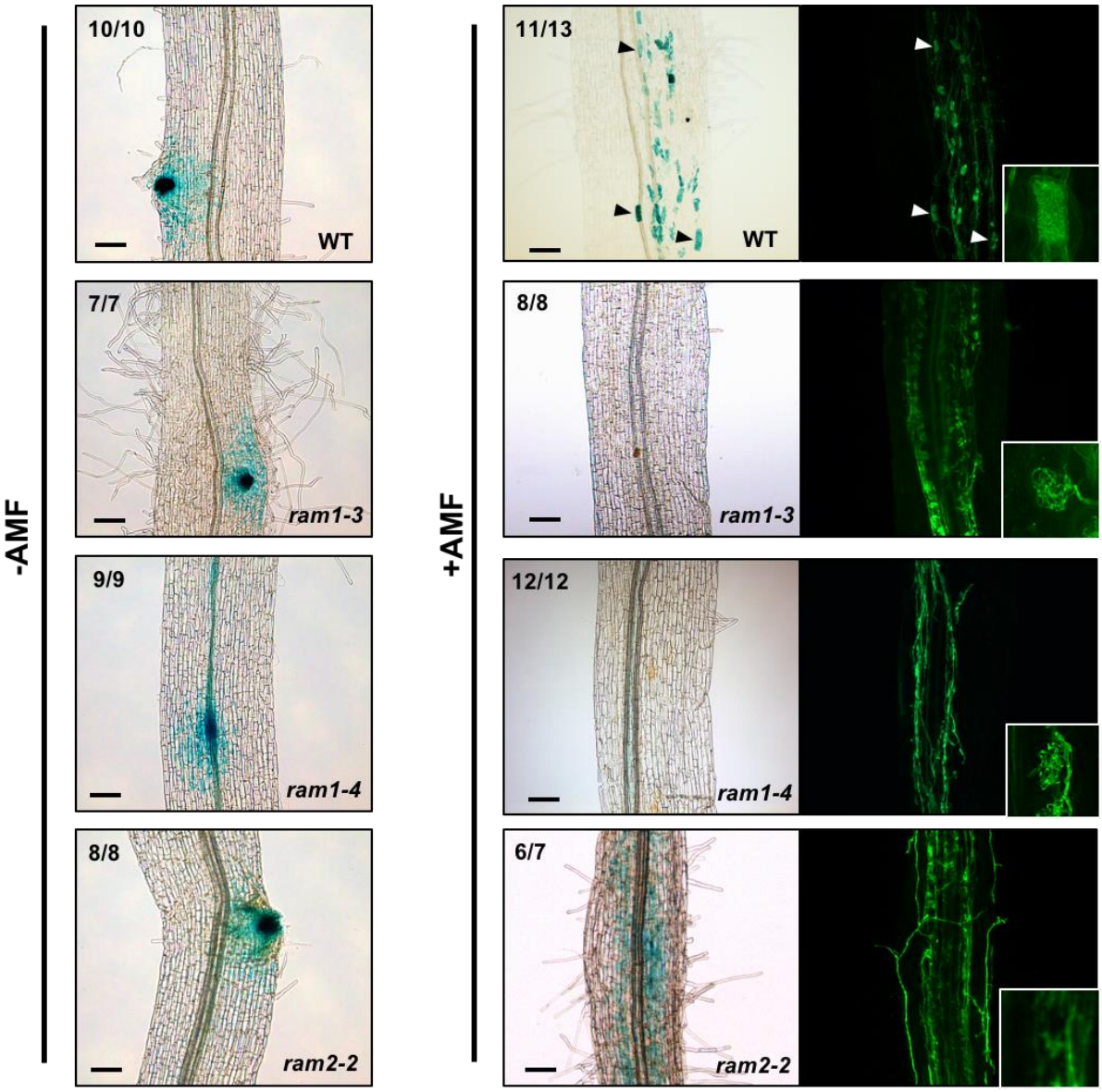

Fig. 5 *DR5*:*GUS* expression in the Gifu wild-type, two allelic *ram1* mutants and the *ram2-2* mutant at 5 wpi inoculated without (-AMF) and with *R. irregularis* (+AMF). GUS staining is visible in blue and fungal structures of the same root segment are indicated by green fluorescent WGA-AlexaFluor488 staining. Insets show close-up of arbuscules. Numbers indicate root systems with the displayed phenotype per total number of analyzed transgenic root systems. Arrowheads indicate mature arbuscules in wild-type. Scale bars represent 100 μm.

c) **The activation of AM-induced auxin response genes depends on *RAM1***

According to published RNA-seq data, few auxin-related genes were induced by AM fungi in *L. japonicus* (Takeda et al., 2015). They were annotated as *ARF* (Lj1g3v4764520.2) and 4 very conserved *SAUR*s (*small auxin up RNA*s) (CM0416.490.r2, CM0416.500.r2, CM0416.510.r2, CM0416.520.r2). The *ARF* is homologous to a *M. truncatula ARF17*

(Medtr8g446900), which is the first hit that appeared by blasting the coding sequence (CDS) of this *LjARF* in a database of *M. truncatula* (data not shown), so we named it *LjARF17*. To get an indication whether these genes are authentic auxin response genes, I first searched for cis-elements related to auxin responsiveness in the promoter region of these genes. All five genes contain one or more auxin response elements AuxREs (TGTCTC) in their promoters. Furthermore, another auxin-responsive element TGA element (AACGAC) (Huang et al., 2018) was found to be located in the promoter of *LjARF17* and of one *SAUR*, suggesting they could be induced by auxin response signaling (Fig. 6A). In the promoter of *LjARF17*, we also found a putative Myc2 element (TGAGCTTAACTCA), which has been found to be enriched in the promoters of AM-induced genes (Fig. 6A) (Favre et al., 2014). We then analyzed the transcript levels of *LjARF17* and the four *SAUR*s as one single target since their CDS are highly conserved, in wild-type and *ram1* with (+AMF) and without (mock) inoculation with *R. irregularis*. In wild-type, the *ARF* and *SAURs* expression was indeed induced by fungal colonization, consistent with the RNA-seq data (Takeda et al., 2015). However, the induction was abolished in two allelic *ram1* mutants (Fig. 6B). This observation indicated that *RAM1* plays an important role in the induction of AM-induced auxin response genes. The expression of these genes was also examined in *ram2*. As expected, the genes were induced in two allelic *ram2* mutants (Fig. 6C), which is consistent with the *DR5*:*GUS* induction in *ram2* (Fig. 5). Two colonization maker genes *PT4* and *ATM2.2* were also checked as indications that the roots were colonized and had arbuscules. *PT4* is also induced in the *ram1* mutants, whereas *AMT2.2* induction is dependent on *RAM1* (Pimprikar et al., 2016) (Fig. 6B and 6C).

d) *RAM1* overexpression induces *DR5*:*GUS* and lateral roots as indication for induced auxin signaling

To examine whether *RAM1* spontaneously induces auxin signaling, I ectopically expressed *RAM1* by driving it with a constitutive *Ubiquitin* promoter (p*Ubi*:*RAM1*). Another cassette *DR5*:*GUS* was combined with p*Ubi*:*RAM1* in one golden gate plasmid or was used alone as an empty vector control as an indicator of induction of auxin signaling. *RAM1* overexpression in non-colonized wild-type hairy roots induced more *DR5*:*GUS* activity in some root systems compared with empty vector, suggesting *RAM1* might be able to trigger auxin signaling (Fig. 7A). Surprisingly, overexpression of *RAM1* was accompanied by a drastic increase in number of lateral roots in some root systems (Fig. 7A). This finding supported that *RAM1* induces auxin signaling because it is well known that auxin induces

lateral root formation (Dubrovsky et al., 2008). I further cultivated the transformed root pieces with *RAM1* overexpression *in vitro* and counted the number of lateral roots. Eight out of 25 of the *RAM1* overexpressing roots showed a massive increase in lateral roots in comparison with the empty vector control (Fig. 7B-C). Root materials were also collected to detect endogenous IAA content by mass spectrometry (MS) in collaboration with Prof. Dr. Karin Ljung from University of Uppsala (Sweden). Five out of 13 root systems with *RAM1* overexpression contained more IAA than those controls with empty vector, consistent with the increased lateral root phenotype and increases the evidence that *RAM1* promotes IAA biosynthesis (Fig. 7D).

e) *LjARF17* is a putative AM specific *ARF* in *L. japonicus*

To investigate if this AM induced and *RAM1*-dependently expressed *LjARF17* is unique to genomes of AM-competent plants, we used *LjARF17* as a query to blast against CDS of a diverse set of 19 plant species including eleven AMS hosts and eight non-hosts. They are involved in different taxonomic groups of dicot, monocot and bryophyte (Table 6). This diversity is essential to reduce the possibility of false positives of *LjARF17*. Amino acid sequences of these blast hits were used to construct an unrooted phylogenetic tree (Fig. 8A). By manual analysis of tree topology, *LjARF17* clustered with those ARFs from the AMS host species except the non-host *Lupinus album* (Fig. 8B). The presence of *L. album* is tolerant since this legume species still maintains some symbiosis specific genes in its transcriptome despite the loss of AM symbiosis (Delaux et al., 2014). These data indicated that *LjARF17* has an AMS-conserved phylogenetic pattern.

f) *LjARF17* deficiency does not affect arbuscule morphology

To investigate whether *LjARF17* regulates arbuscule morphology, we ordered two *LORE1* retrotransposon insertion mutants from Lotus base (https://lotus.au.dk/) and named them *Ljarf17-1* (30152074) and *Ljarf17-2* (30083262), which carried insertions in exon 5 and 8, respectively (Fig. 9A). Neither of the allelic *arf* mutants displayed a phenotype of impaired arbuscule branching compared with wild-type, suggesting that the absence of *LjARF17* is not sufficient to disturb arbuscule growth (Fig. 9B).

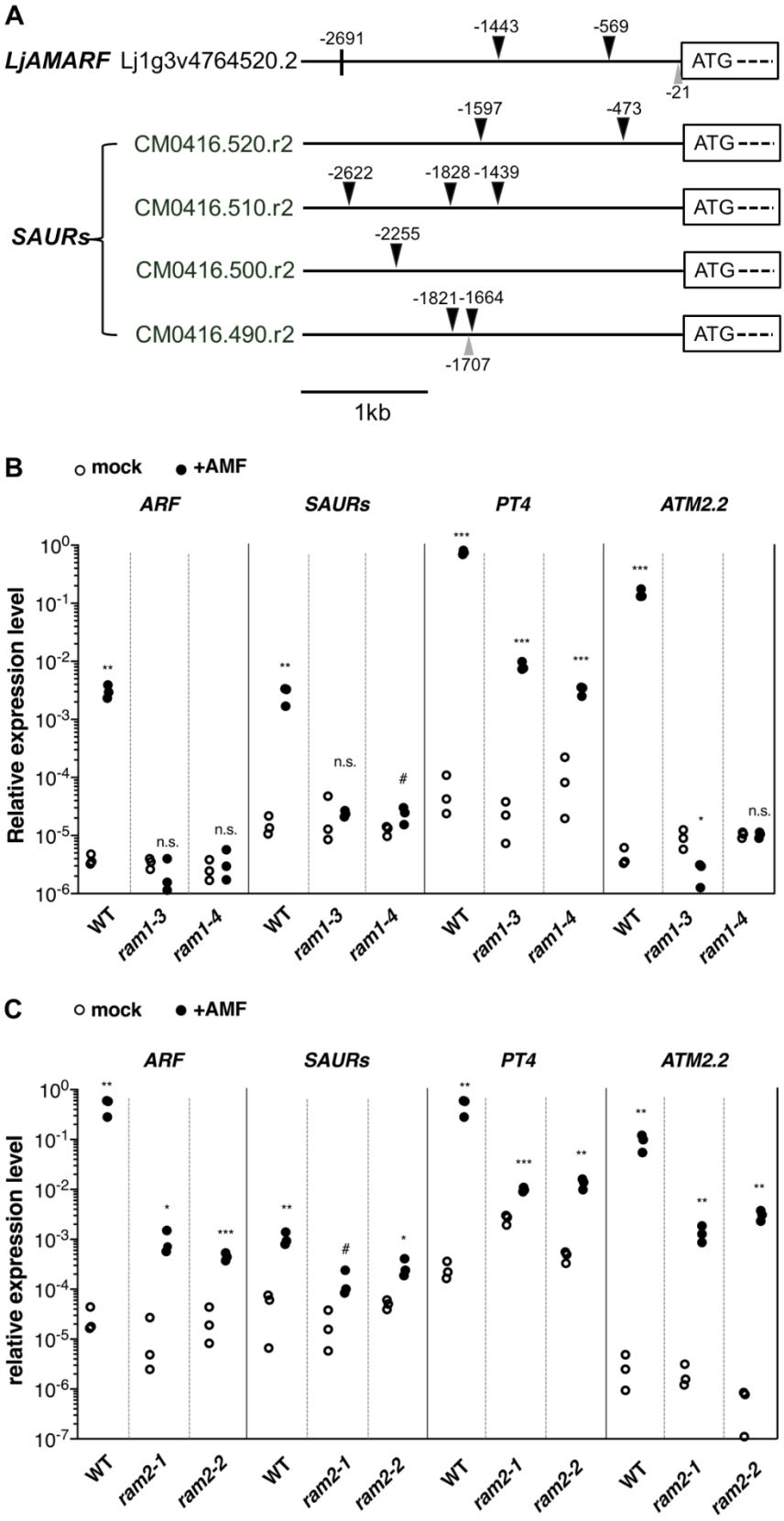

Fig. 6 Induction of AM-induced auxin response genes depends on *RAM1*. (**A**) Schematic representation of cis-elements in the promoters of *ARF17* and four *SAURs*. The numbers next to triangles or vertical lines indicate the starting nucleotide positions of the AuxREs (black triangle), TGA element (gray triangle) and putative Myc2

element (vertical line) (Huang et al., 2018; Favre et al., 2014). Nucleotide positions are numbered relative to the ATG start codon (+1). Black boxes indicate the genomic sequence starting from ATG of each gene. (**B**) and (**C**), transcript accumulation of auxin response genes and mycorrhiza marker genes in root materials from *ram1* (**B**) and *ram2* (**C**), both compared to wild-type in the absence (mock, hollow dots) or presence (+AMF, solid dots) of AM fungus. Transcript accumulation was determined by RT-qPCR, and the housekeeping gene *Ubiquitin10* was used for normalization. Asterisks indicate significant difference compared with mock according to the student's t-test. n.s., not significant; # < 0.1; *, p < 0.05; **, p < 0.01; ***, p < 0.001.

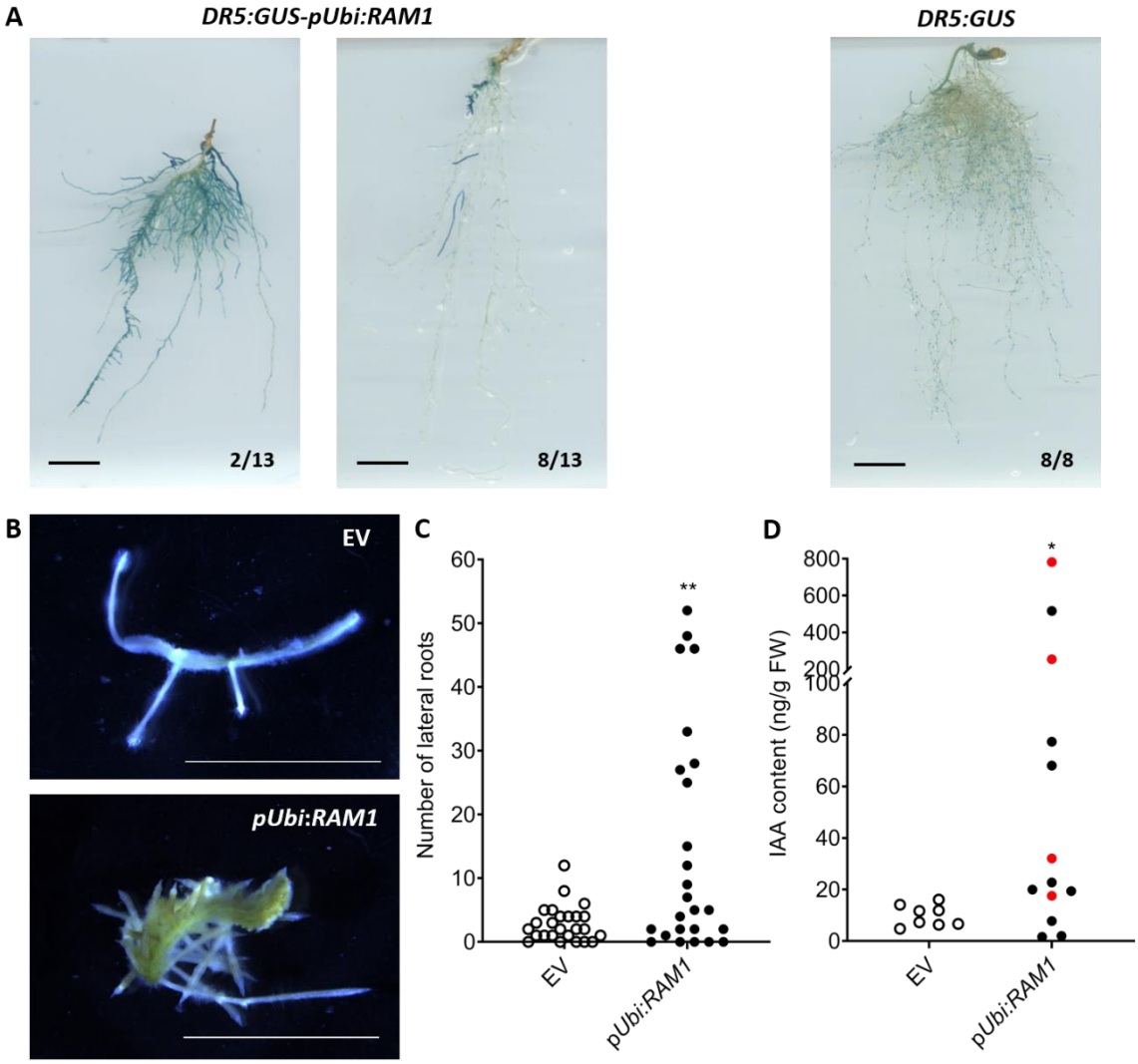

Fig. 7 Hairy roots overexpressing *RAM1* and empty vector (EV) control in the absence of *R. irregularis*. (**A**) GUS stained roots containing the indicated transgene. Numbers indicate root systems with the displayed phenotype per total number of analyzed transgenic root systems. Scale bars represent 1 cm. (**B**) Lateral root explosion and (**C**) number of lateral roots on *in vitro* cultured hairy root pieces overexpressing *RAM1* as compared with EV control. Scale bars in (**B**) represent 1 cm. (**D**) IAA content in hairy roots overexpressing *RAM1* as compared with empty vector control. Red dots indicate the root materials with strongly increased lateral root numbers. Asterisks indicate significant difference compared with empty vector control according to the student's t-test. *, p < 0.05; **, p < 0.01.

Common Name	Scientific Name	Protein models	Group[a]	AMS status[b]	Origin[c]
Lyreleaf rockcress	*Arabidopsis lyrate*	20	Dicot	Non-host	Phytozome13
Mouse ear cress	*Arabidopsis thaliana*	22	Dicot	Non-host	TAIR10
Purple false brome	*Brachyposium distachyon*	28	Monocot	host	Phytozome13
Red shepherd's purse	*Capsella rubella*	19	Dicot	Non-host	Phytozome13
Papaya	*Carica papaya*	13	Dicot	Non-host	Phytozome13
Chickpea	*Cicer arietinum*	27	Dicot	host	Phytozome13
Orange	*Citrus sinensis*	59	Dicot	host	Phytozome13
Salt cress	*Eutrema salsugineum*	21	Dicot	Non-host	Phytozome13
Birdsfoot trifoil	*Lotus japonicus*	32	Dicot	host	Lotus base v3.0
White lupin	*Lupinus album*	43	Dicot	Non-host	White Lupin Genome v1.0
Cassava	*Manihot esculenta*	30	Dicot	host	Phytozome13
Barrel medic	*Medicago truncatula*	41	Dicot	host	JCVI 4.0
4.0	*Oryza sativa*	27	Monocot	host	Phytozome13
Moss	*Physcomitrella patens*	15	Bryophyte	Non-host	Phytozome13
Tomato	*Solanum lycopersicum*	21	Dicot	host	Phytozome13
Potato	*Solanum tuberosum*	21	Dicot	host	Phytozome13
Sorghum	*Sorgum bicolor*	25	Monocot	host	Phytozome13
Greater duckweed	*Spirodela polyrhiza*	16	Monocot	Non-host	Phytozome13
Grape	*Vitis vinifera*	20	Dicot	host	Phytozome13

Table 6 List of 19 species used for phylogenetic analyses. Letters in superscripts **a**, taxonomic group used in the study; **b**, ability to establish AMS, based on published literature (Bravo et al., 2016; Delaux et al., 2014); **c**, origin of genomic data.

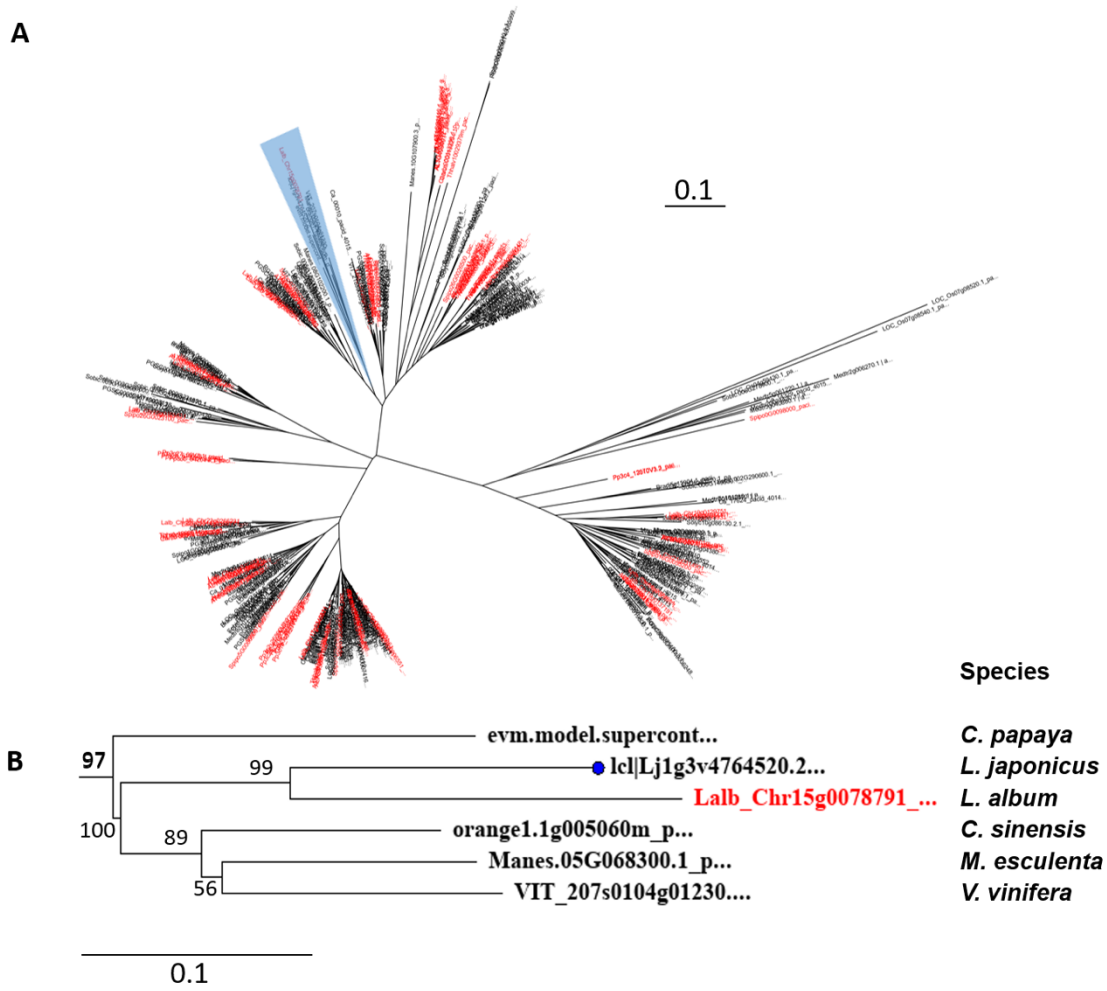

Fig. 8 Phylogenetic tree of putative ARFs in 19 species. (**A**) Phylogenetic relationships were constructed using the blast hits of CDS (e-value < 1e-10 and sequence coverage > 30%) from each database. Each branch in the tree was colored on the basis of the ability of the plant species to establish AMS. Black, AMS host species; red, AMS non-host species. Blue triangle represents clade which includes *LjARF17*. (**B**) Zoom-in of the blue triangle. Blue dot shows where *LjARF17* is. The Scale bars represent amino acid substitutions per site. *C. papaya*, *Carica papaya*; *L. japonicus*, *Lotus japonicus*; *L. album*, *Lupinus album*; *C. sinensis*, *Citrus. sinensis*; *M. esculenta*, *Manihot esculenta*; *V. vinifera*, *Vitis vinifera*.

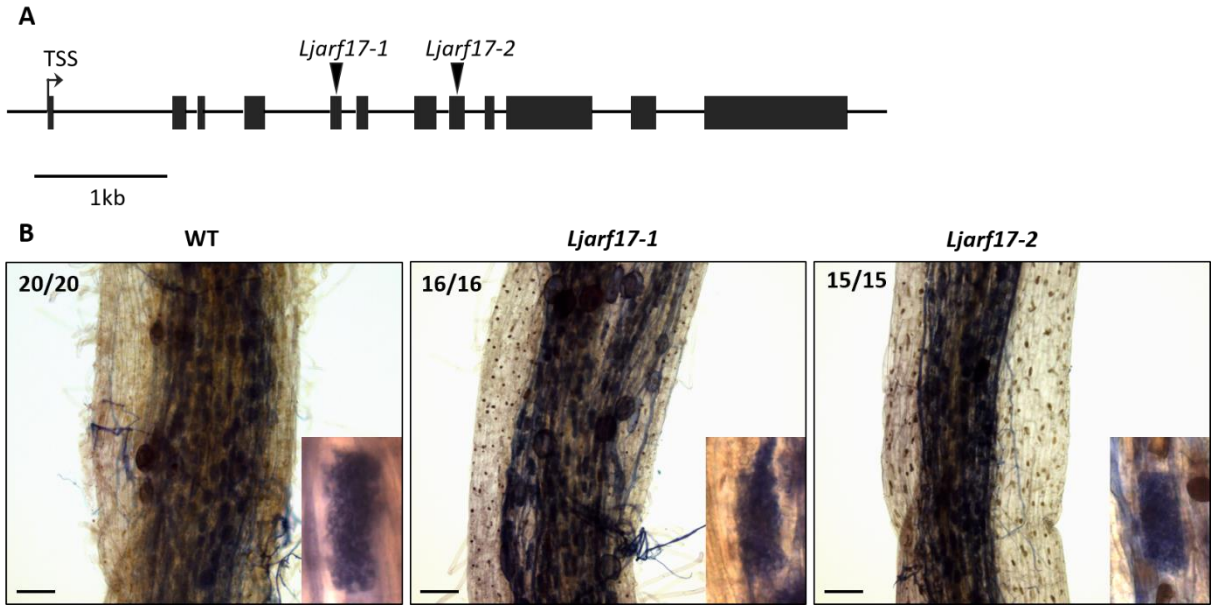

Fig. 9 Identification and phenotyping of *Ljarf17* mutants. (**A**) Gene structure of *LjARF17* with the *LORE1* insertions (triangle), *Ljarf117-1* and *Ljarf17-2*. Black boxes indicate exons separated by introns (thin lines). TSS, transcriptional start site. (**B**) Bright filed microscope images of *L. japonicus* wild-type, *Ljarf17-1 and Ljarf17-2* mutants colonized by *R. irregularis* at 5 wpi. The fungus was stained with ink-acetic acid. Insets show close up of arbuscules; Numbers indicate root systems with the displayed phenotype per total number of analyzed root systems. Scale bar, 100 µm

g) Exogenous auxin treatment does not affect arbuscule morphology

Our previous observations suggested that auxin signaling may act downstream of RAM1. Other evidence showed in other species, that auxin positively affects arbuscule branching (Etemadi et al., 2014) or colonization (Buendia et al., 2019). Based on this, we hypothesized that RAM1 may regulate arbuscule growth *via* auxin signaling. To test this hypothesis, we treated *L. japonicus* roots with the synthetic auxins NAA or 2,4-D. Because high concentrations of NAA and 2,4-D can strongly influence root development and 2,4-D in particular can be lethal to dicotyledons, I first monitored the effect of NAA or 2,4-D concentration on root development by measuring root length in each condition (Fig. S1). NAA application at concentrations of 1 nM to 100 nM did not influence the root length significantly in both wild-type and *ram1-4*. 2,4-D treatment was not lethal to *L. japonicus* and 1 nM 2,4-D even improved the primary root growth in wild-type, which subsequently declined at 10 nM. However, 2,4-D did not influence the root growth of *ram1-4*. Next, I quantified root length colonization after treatment with the two synthetic auxins. Unlike the previous study which showed improvement of arbuscule abundance in response to auxin treatment in tomato, *M.*

truncatula and rice (Etemadi et al., 2014), we did not detect any increase in response to either NAA or 2,4-D in *L. japonicus* wild-type and *ram1-4*. In contrast, 10 nM and 100 nM NAA treatment even reduced the root length colonization in wild-type. It is worth noting that colonization in the *ram1* mutant was already low since *RAM1* deficiency impairs AM colonization, and therefore it was difficult to test whether NAA has an effect on root length colonization of *ram1-4* (Fig. 10A). While *L. japonicus* roots were less sensitive to 2,4-D, no significant difference was detected between treated and non-treated roots in both wild-type and *ram1-4* (Fig. 10B). Overexpression of *miR393* which targets the mRNA of auxin receptors, causes inhibition of arbuscule development (Etemadi et al., 2014). This raised the hypothesis that auxin signaling affects arbuscule development. Therefore, we paid attention to arbuscule growth by auxin treatment. In the first experiment, I observed that the arbuscules were bigger in *ram1-3* treated with 1 nM NAA or 2,4-D as compared with the solvent control while fine branching was not rescued (Fig. S2A). This was also confirmed by the measurement of arbuscule size (Fig. S2B). However, such increase in arbuscule size triggered by auxin treatment in *ram1* mutants could not be reproduced in subsequent experiments. I did not observe the bigger arbuscules in the auxin treated samples again. Instead, no obvious differences were observed in three independent replicates of the same experiment (Fig. 11A and 11B).

h) Genetic manipulation of auxin signaling does not affect arbuscule morphology

Since I observed once that stunted arbuscules in *ram1* became bigger by exogenous auxin treatment (Fig. S2), we hypothesized that auxin plays a role in arbuscule growth. On one hand, we put efforts in repeating the auxin treatment essay to examine if it causes bigger arbuscules. On the other hand, we performed genetic approaches in parallel to verify the observation with an independent method. One approach was to manipulate auxin signaling in *ram1* compared with wild-type using hairy root transgenic line containing *VP16-IAA17mImII* as an auxin signaling activator (Li et al., 2009) driven by the 2-kb promoter fragment (including the 5' UTR) of *RAM1*. *IAA17mImII*, a stabilized and weakened version of auxin signaling repressor *IAA17*, could be converted to an activator by fusing the herpes simplex virus VP16 activation domain to its N-terminus (Li et al., 2009; Tiwari et al., 2004). This construct was expressed specifically in colonized regions of the root (Pimprikar et al., 2016) and was used to avoid significant root morphological changes caused by overexpression of

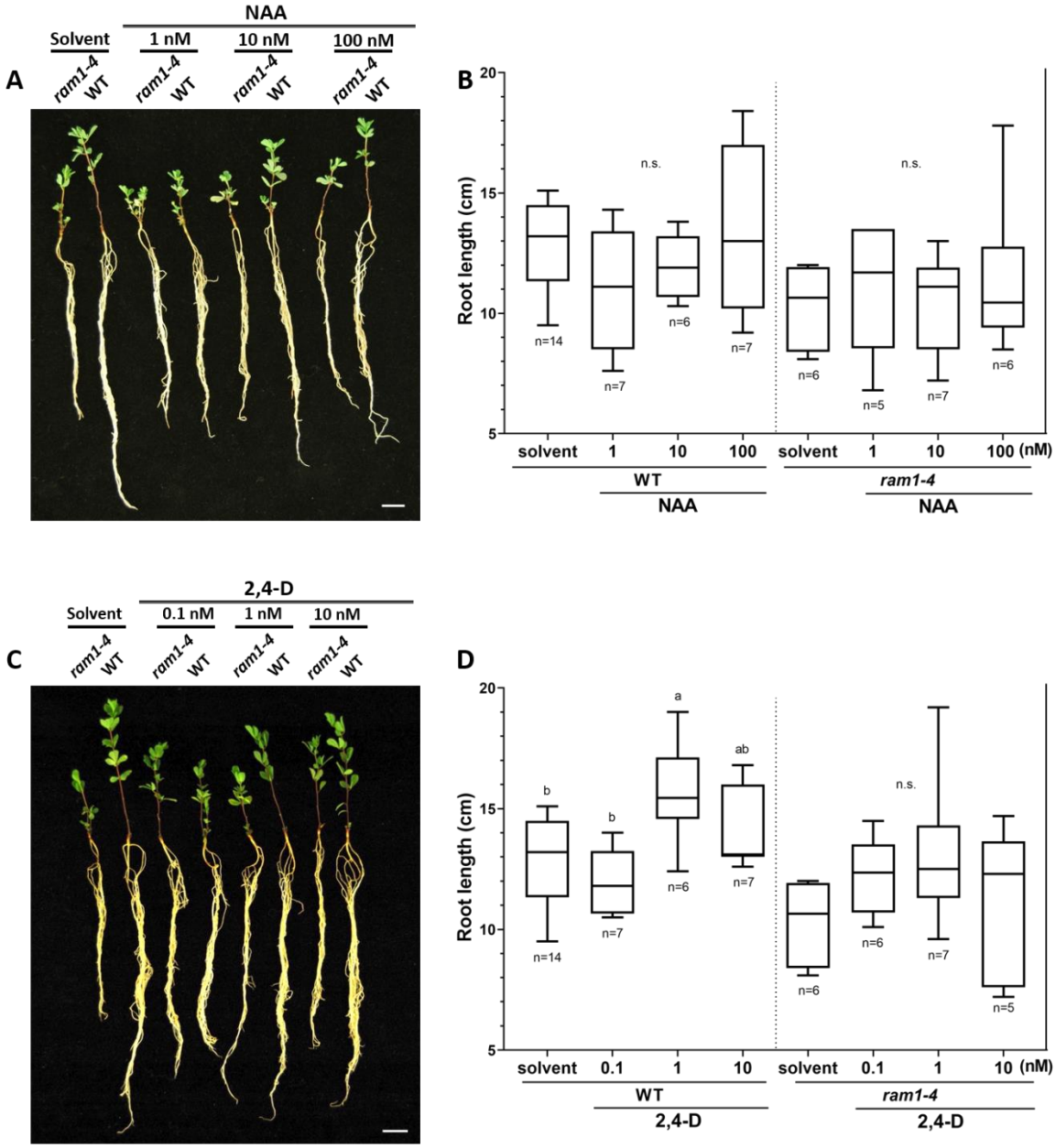

Fig. S1 Effect of auxin treatment on root development of *L. japonicus* wild-type and *ram1-4* colonized with *R. irregularis* at 5 wpi. (**A** and **B**) Effect of different concentration of NAA (1, 10 and 100 nM). (**C** and **D**) Effect of different concentration of 2,4-D (0.1, 1 and 10 nM). Scale bar presents 1 cm (**A** and **C**). Error bars represent standard error of the mean (SEM) (**B** and **D**). Different letters indicate different statistical groups (ordinary one-way ANOVA, Tukey-Kramer test). (**B**) WT: F (3, 30) = 1.489, p-value = 0.2374, n = 34; *ram1-4*: F (3, 20) = 0.2236, p-value = 0.8788, n = 24. (**D**) WT: F (3, 29) = 5.644, p-value = 0.0036, n = 33; *ram1-4*: F (3, 20) = 1.796, p-value = 0.1804, n = 24.

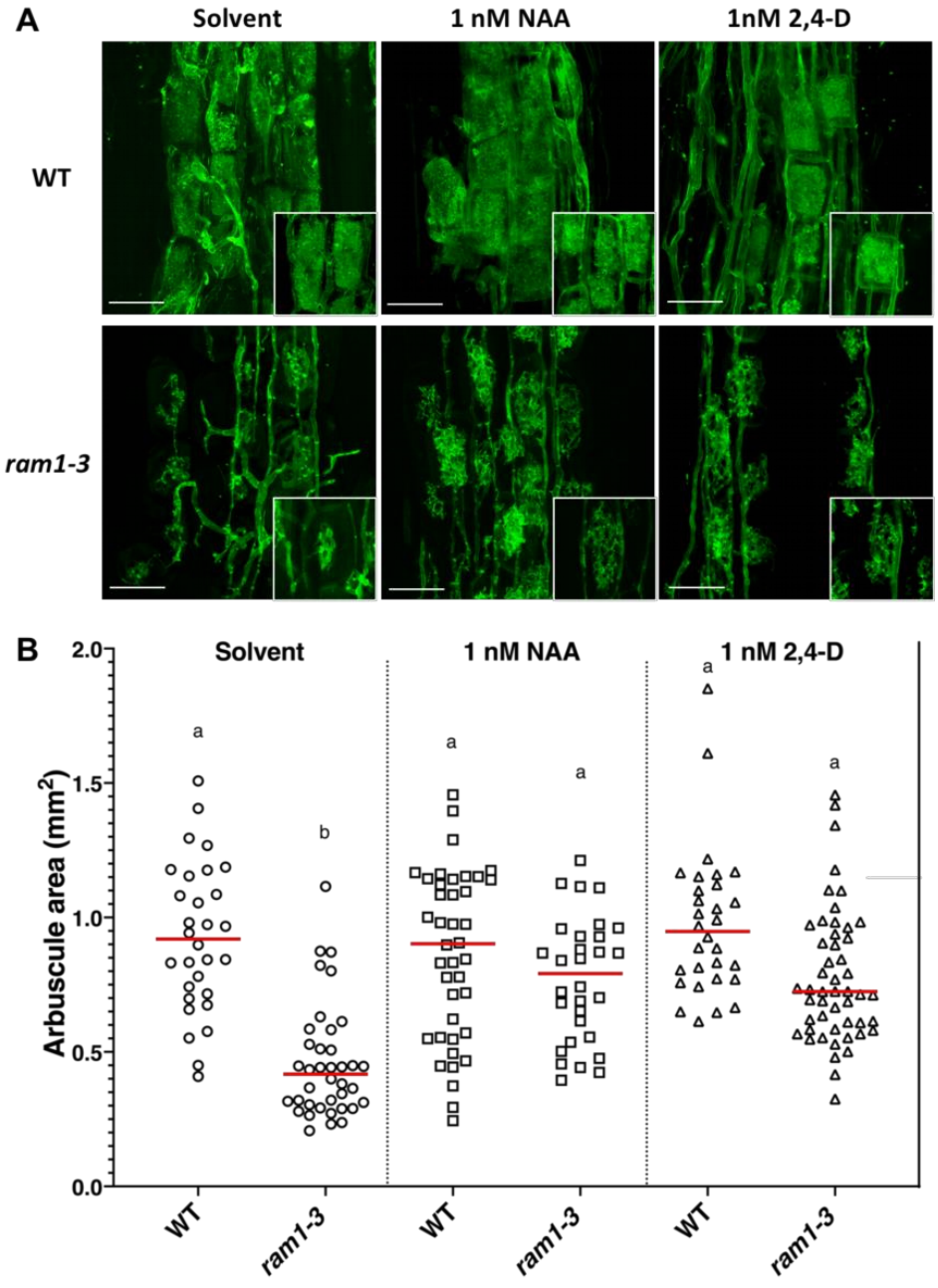

Fig. S2 Auxin treatment affected arbuscule morphology. All the plants were inoculated with *R. irregularis* for 5 weeks. (**A)** Laser scanning confocal images of *L. japonicus* roots of wild-type and *ram1-3* mutant treated with solvent, 1nM NAA and 1nM 2,4-D, respectively. The fungus is stained with WGA-AlexaFluor488. Insets show close up of arbuscules. Scale bar, 50 µm**. (B**) Arbuscule size measurement. Each dot presents the size of an individual arbuscule. Six to ten arbuscules from each of five plants were randomly chosen and the area of each arbuscule was measured. Different letters indicate different statistical groups (ordinary one-way ANOVA, Tukey-Kramer test). F (5, 212) = 17.8, p-value < 0.0001, n = 218.

VP16-IAA17mImII. *DR5*:*GUS* was placed in tandem with *IAA17mImII* in the golden gate plasmid or used alone as an empty vector control as an indicator of the induction of auxin signaling. In addition to root tips and lateral root primordia, *DR5*:*GUS* in the empty vector control was expressed in arbuscule-containing cells in the wild-type, but not in the two allelic *ram1* mutants, consistent with the aforementioned analysis of auxin responses in the wild-type and *ram1* (Fig. 5). In roots expressing *VP16-IAA17mImII*, *DR5*:*GUS* was visualized in the wild-type arbuscule-containing cells as expected. However, no induction was detected in the *ram1* mutants (Fig. 12A). To make sure that *IAA17mImII* was properly expressed, its transcript accumulation was analyzed by RT-qPCR. *IAA17mImII* was expressed in both wild-type and *ram1-3* (Fig. 12B). In addition to expression of *ARF17*, transcripts of *SAUR*s and another auxin-responsive gene *GH3* (Nadzieja et al., 2018) were analyzed. *GH3* genes in tomato were induced in response to auxin treatment and AuxREs were identified in their promoters (Liao et al., 2015; Chen et al., 2017). The qRT-RCR showed that *SAUR*s and *GH3* were induced by *VP16-IAA17mImII* in wild-type, suggesting that auxin signaling was indeed activated. Interestingly, *VP16-IAA17mImII* could not induce auxin response genes in *ram1-3*, which was supported by the observation of no detectable *DR5*:*GUS* induction in the roots (Fig. 12A and 12B). In terms of the arbuscule morphology, neither arbuscule branching nor size in *ram1* mutants were rescued by *VP16-IAA17mImII* (Fig. 12A and 12C). These data taken together suggested an interesting scenario that the activation of auxin signaling by *VP16-IAA17mImII* depends on *RAM1*.

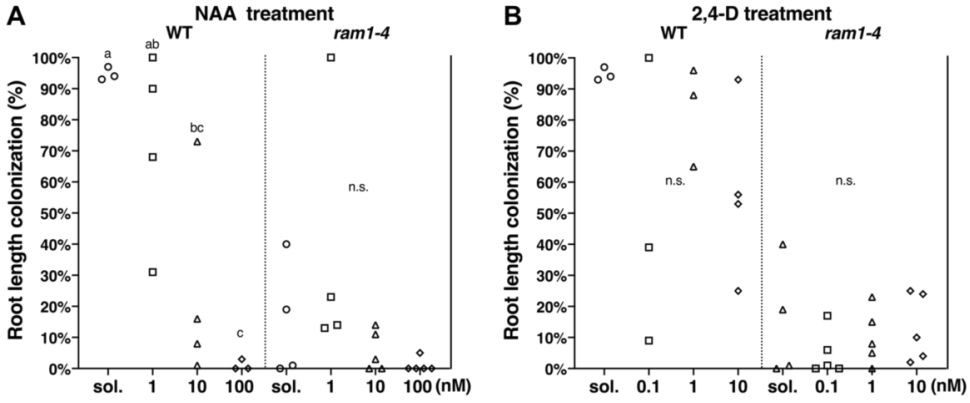

Fig. 10 Response of total root length colonization to auxin treatment. Total root length colonization of *L. japonicus* wild-type and *ram1-4* in response to solvent (sol.) and different concentrations of NAA (1, 10 or 100 nM) (**A**) and 2,4-D (0.1, 1 or 10 nM) (**B**). Different letters indicate different statistical groups (ordinary one-way ANOVA test). (**A**) WT: F (3, 10) = 9.734, p-value = 0.0026, n = 14; *ram1-4*: F (3, 14) = 2.438, p-value = 0.1077, n = 18. (**B**) WT: F (3, 9) = 1.807, p-value = 0.2159, n = 13; *ram1-4*: F (3, 15) = 0.6641, p-value = 0.5869, n = 19.

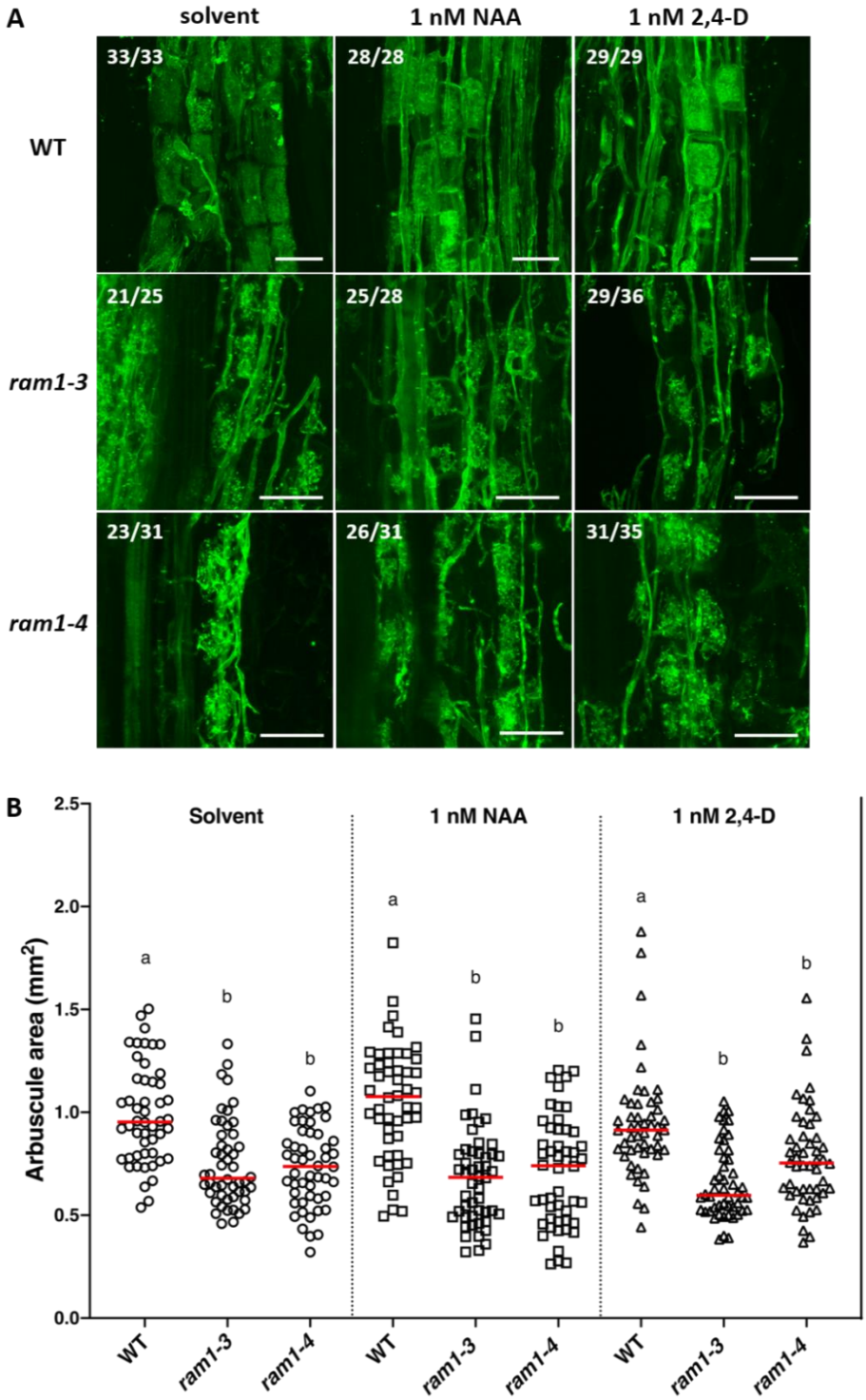

Fig. 11 Auxin treatment did not affect arbuscule morphology and size in *ram1* mutants. (**A**) Laser scanning confocal images of *L. japonicus* roots of wild-type, *ram1-3* and *ram1-4* mutants treated with solvent, 1 nM NAA and 1 nM 2,4-D displayed in the left, middle and right panel, respectively. The fungus was stained with WGA-AlexaFluor488. Numbers indicate root systems with the displayed phenotype per total number of analyzed root systems. Scale bar, 50 µm. (**B**) Arbuscule size measurement. Each dot represents the size of an individual arbuscule. Ten arbuscules from each of five plants were randomly chosen and the area of each arbuscule was measured. Different letters indicate different statistical groups. Ordinary one-way ANOVA; F (8, 441) = 18.4; p-value < 0.0001; n = 450. All plants were inoculated with *R. irregularis* for 5 weeks.

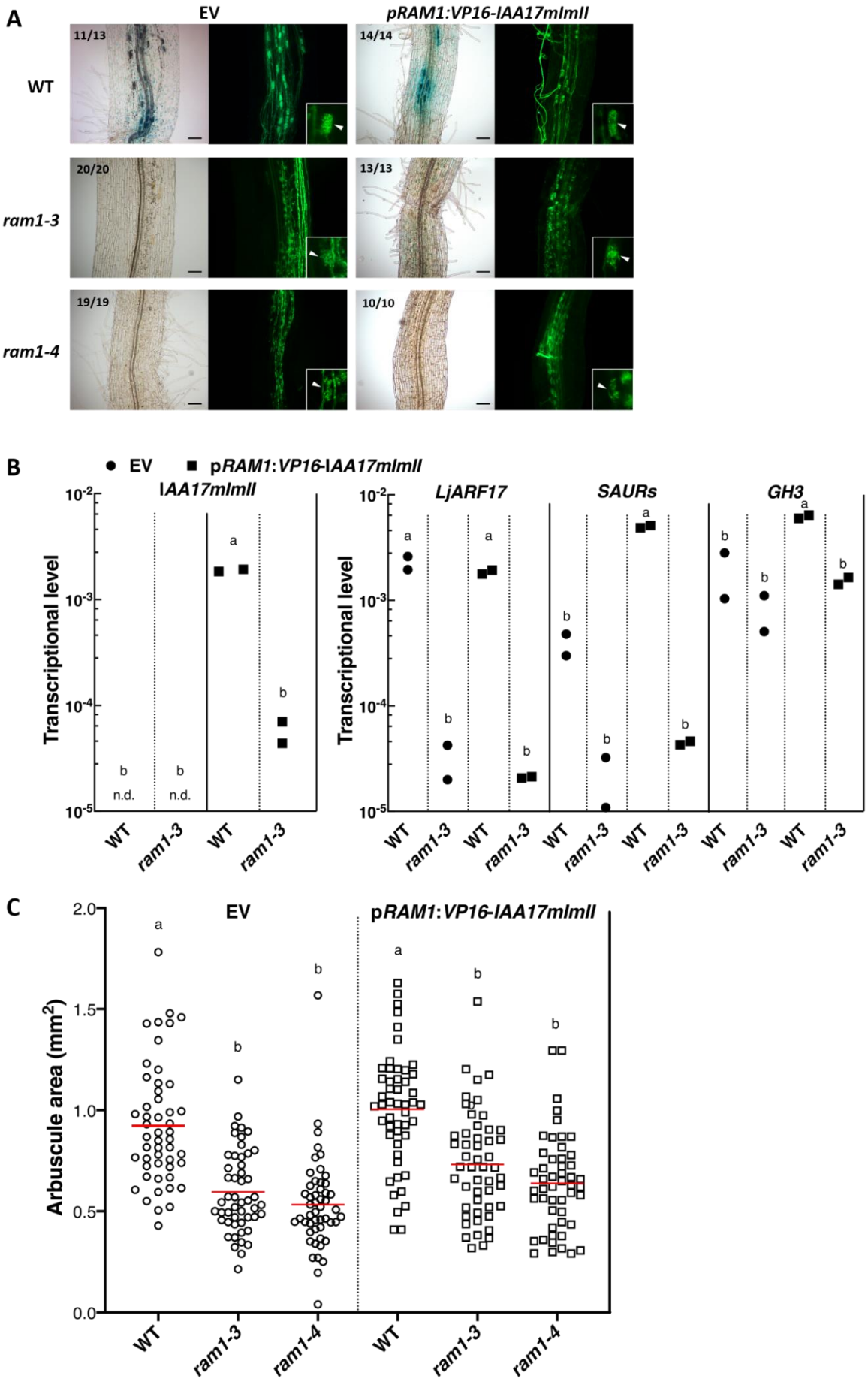
A
EV
pRAM1:VP16-IAA17mImII
WT
ram1-3
ram1-4
11/13
14/14
20/20
13/13
19/19
10/10
B
EV
pRAM1:VP16-IAA17mImII
IAA17mImII
LjARF17
SAURs
GH3
Transcriptional level
n.d.
WT
ram1-3
C
EV
pRAM1:VP16-IAA17mImII
Arbuscule area (mm2)
WT
ram1-3
ram1-4

Fig. 12 Expression of *VP16-IAA17mImII* is not sufficient to trigger arbuscule growth. All the plants were inoculated with *R. irregularis* for 5 weeks. (**A**) Microscopic images of hairy roots of wild-type and *ram1-3* and *ram1-4* transformed with *DR5*:*GUS* (empty vector control, EV) or p*RAM1*:*VP16-IAA17mImII-DR5*:*GUS*. GUS staining is visible in bright field and fungal structure of the same root segment is indicated by green fluorescent WGA-AlexaFluor488 staining. Numbers indicate root systems with the displayed phenotype per total number of analyzed transgenic root systems. Insets show close up of arbuscules. Arrowheads indicate arbuscules. Scale bars represent 100 μm. (**B**) Transcript accumulation of *VP16-IAA17mImII* and auxin response genes (*LjARF17*, *SAUR*s and *GH3*) in root materials from wild-type and *ram1-3*. Transcript accumulation was determined by RT-qPCR and the housekeeping gene *Ubiquitin10* was used for normalization. n.d., transcript was not detected within 40 cycles of RT-qPCR. Different letters indicate different statistical groups (ordinary one-way ANOVA test, Tukey-Kramer test, n=8). *IAA17mImII*: $F_{3, 4} = 1739$, p-value < 0.0001; *LjARF17*: $F_{3, 4} = 50.06$, p-value = 0.0013; *SAURs*: $F_{3, 4} = 941.2$, p-value < 0.0001; *GH3*: $F_{3, 4} = 24.95$, p-value = 0.0047. (**C**) Arbuscule size in roots of the indicated genotypes. Each dot presents the size of an individual arbuscule. Different letters indicate different statistical groups (ordinary one-way ANOVA, Tukey-Kramer test, p-value < 0.0001, n = 150), EV: F (2, 147) = 36.3; p*RAM1*:*VP16-IAA17mImII*: F (2, 147) = 26.4.

i) Overexpression of auxin biosynthesis genes does not affect arbuscule morphology

I also used a second transgenic approach and expressed auxin biosynthesis genes driven by the *RAM1* promoter to overactive the auxin biosynthesis pathway in *ram1* and to test whether arbuscule branching could be restored. In this experiment, I co-expressed the *L. japonicus* homologs of *Arabidopsis thaliana* auxin biosynthesis genes *TRYPTOPHAN AMINOTRANSFERASE OF ARABIDOPSIS 1* (*TAA1*) and *YUCCA6* (*YUC6*) encoding a flavin monooxygenase-like protein in *L. japonicus* roots. Co-overexpression of *AtTAA1* and *AtYUC6* lead to a dramatic increase of lateral roots in *A. thaliana* (Mashiguchi et al., 2011). By RT-qPCR analysis, *TAA1* and *YUC6* transcripts accumulated to higher levels, when they were co-expressed in the wild-type and *ram1-4* than in those expressing empty vector (Fig. 13B). Furthermore, the expression level of the auxin-related genes *ARF17*, *SAUR*s and *GH3* were analyzed, among which *ARF17* and *GH3* were slightly induced. This observation indicated that the ectopically expressed auxin biosynthesis genes likely led to protein products functional in auxin biosynthesis, which successfully triggered auxin signaling (Fig. 13B). We used the promoter of *RAM1* to express *TAA1* and *YUC6* specifically in the colonized regions of the roots (Pimprikar et al., 2016) to avoid significant root morphological changes. Similar to the *VP16-IAA17mImII* experiment, the stunted arbuscules in *ram1* mutants were not rescued by co-expression of *TAA1* and *YUC6* in terms of arbuscule branching and size (Fig. 13A and 13C). No significant increase in root length colonization was observed in co-expression lines

in WT and *ram1* mutants (Fig. 13D). These data supported that induction of auxin signaling in arbuscule cells of *ram1* mutants is not sufficient to trigger arbuscule growth. Thus, RAM1 likely has additional targets.

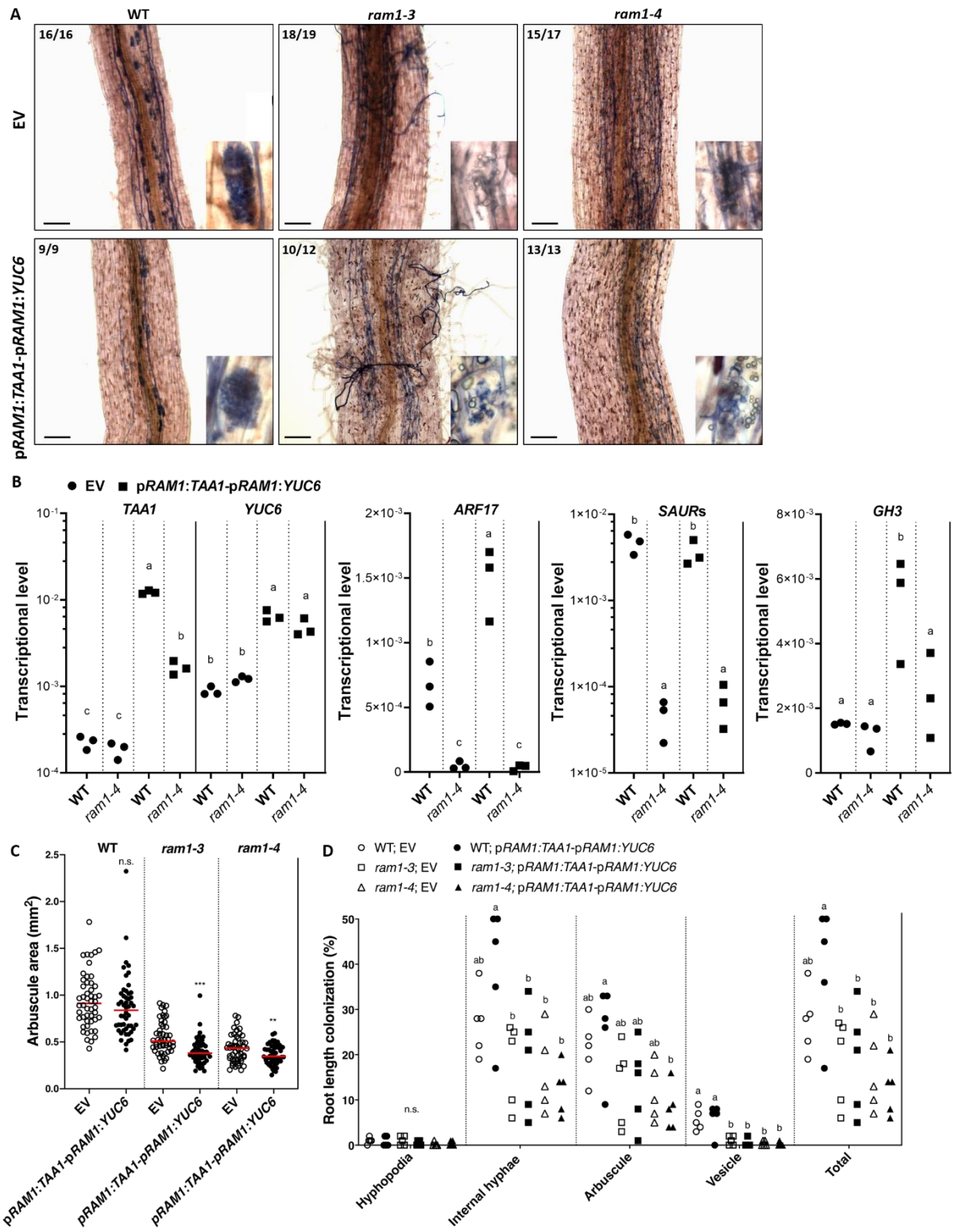

Fig. 13 Over-activation of auxin biosynthesis did not affect arbuscule morphology. All the plants were inoculated with *R. irregularis* for 5 weeks. (**A**) Microscopic images of hairy roots of wild-type, *ram1-3* and *ram1-4* transformed with p*Ubi*:*mCherry* (empty vector control, EV) or p*Ubi*:*mCherry*-p*RAM1*:*TAA1*-p*RAM1:YUC6*. Fungal structures are indicated by ink-acetic acid staining. Numbers indicate root systems with the displayed phenotype per total number of analyzed transgenic root systems. Insets show close-up of arbuscules. Scale bars represent 100 μm. (**B**) Transcript accumulation of *TAA1*, *YUC6*, *ARF17*, *SAUR*s and *GH3* in root materials from wild-type and *ram1-4*. Transcript accumulation was determined by RT-qPCR, and the housekeeping gene *Ubiquitin10* was used for normalization. n.s., not significant. Different letters indicate different statistical groups (ordinary one-way ANOVA test, Tukey-Kramer test, n = 12). *TAA1*: $F_{3, 8}$ = 949.0, p-value < 0.0001; *YUC6*: $F_{3, 8}$ = 38.60, p-value < 0.0001; *ARF17*: $F_{3, 8}$ = 50.25, p-value < 0.0001; *SAUR*s: $F_{3, 8}$ = 22.90, p-value = 0.0003; *GH3*: F $F_{3, 8}$ = 8.862, p-value = 0.0064. (**C**) Arbuscule size of indicated genotypes. Each dot presents the size of an individual arbuscule. Asterisks indicate significant difference compared to EV according to the student's t-test. n.s., not significant; **, p < 0.01; ***, p < 0.001. (**D**) Percent root length colonization of hairy roots of wild-type, *ram1-3* and *ram1-4* transformed with EV or p*Ubi*:*mCherry*-p*RAM1*:*TAA1*-p*RAM1:YUC6*. Different letters indicate different statistical groups (ordinary one-way ANOVA, Tukey-Kramer test, n = 30). Hyphopodia: $F_{5, 24}$ = 0.9143, p-value = 0.4885; Internal hyphae: $F_{5, 24}$ = 4.947, p-value = 0.0030; Arbuscule: $F_{5, 24}$ = 3.498, p-value = 0.0162; Vesicle: $F_{5, 24}$ = 11.60, p-value < 0.0001; Total: $F_{5, 24}$ = 4.875, p-value = 0.0032.

2. Are CCaMK and CYCLOPS travelling between cell layers?

a) Analysis of promoter activity of *CCaMK*

To analyze the spatial activity of the *CCaMK* promoter, *Lotus* wild-type hairy roots were transformed with p*CCaMK*:*NLS*-2x*YFP*, in which the promoter of *CCaMK* was fused to a sequence encoding a nuclear localization signal and two times the yellow fluorescent protein (*NLS*-2x*YFP*). To visualize the arbuscule, a second expression cassette containing the *SbtM1* promoter driving *mCherry* tagged with a secretion signal peptide (p*SbtM1*:*SP-mCherry*) as arbuscule marker, was co-transformed with the p*CCaMK*:*NLS*-2x*YFP* cassette (Fig. 14). After growth with (+AMF) or without (-AMF) *R. irregularis* for five weeks, nuclear YFP signals could be observed in the epidermis and each layer of the cortex in both conditions, which corresponded with GUS activity, when *GUS* expressed was under the control of p*CCaMK* in non-inoculated roots in previous reports (Rival et al., 2012; Hayashi et al., 2014) (Fig. 14). In my study, additional nuclear YFP was not only observed in the endodermis and vascular bundle in non-inoculated roots, but as well as in the endodermis in inoculated roots (Fig. 14). These observations indicate that *CCaMK* is expressed in every root layer in the absence of the fungus, while the expression of *CCaMK* was in epidermis, cortex and endodermis of the root during fungal colonization.

b) Epidermal expression of *CCaMK* restores the AM defect of the *ccamk* mutant

Mutational perturbation of *CCaMK* leads to abolishment of entry of fungal hyphae into roots (*CCaMK* is called *SYM15* in Demchenko et al., 2004; Pimprikar et al., 2016). In contrast to *cyclops* mutants, the AM colonization defect of *ccamk* mutants could not be restored by ectopic expression of *RAM1* (Pimprikar et al., 2016), raising the speculation that *CCaMK* plays an important role in fungal entry into the root epidermal layer. For the establishment of an effective AM symbiosis, it remained unclear whether *CCaMK* is involved in epidermal and/or cortical infection, e.g. hyphal entry into the epidermis, progress of hyphae in the epidermis and cortex, as well as arbuscule formation in the cortex. To analyze the requirement of CCaMK in the symbiotic process, I employed a root epidermis-specific promoter p*Epi308* (p*Epi* will be used hereafter) of *L. japonicus* (Hayashi et al., 2014). Firstly, I confirmed that p*Epi* was specifically active in the root epidermis, and then I tested whether this pattern was changed during fungal colonization. To this end, *Lotus* wild-type hairy roots

were transformed with a fluorescence reporter, p*Epi:NLS*-2x*YFP*, in which the epidermal promoter p*Epi* was fused to *NLS*-2x*YFP*. To visualize the arbuscule, the arbuscule marker p*SbtM1*:*SP-mCherry* as a second expression cassette, was co-transformed with the p*Epi*:*NLS*-2x*YFP* cassette (Keymer et al., 2017) (Fig. 15). After five weeks of growth with (+AMF) or without (-AMF) *R. irregularis*, nuclear YFP signals were observed only in epidermal cells in both conditions, which corresponds with GUS activity under the control of p*Epi* in non-inoculated roots in a previous report (Hayashi et al., 2014). This confirms the specificity of p*Epi* in epidermal induction during inoculation with *R. irregularis* (Fig. 15). Thus, p*Epi* is an ideal epidermal-specific promoter that can be used in this study.

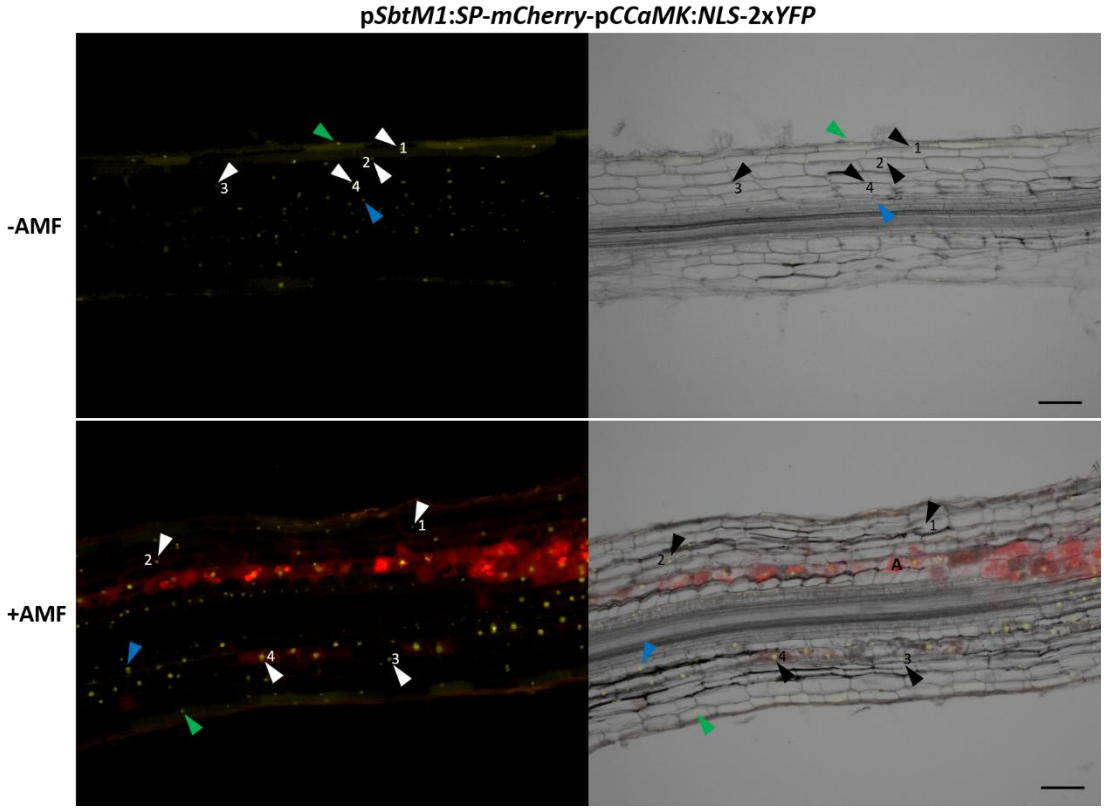

Fig. 14 Analysis of promoter activity of *CCaMK*. Microscopy image of longitudinal root sections containing vascular tissue. Promoter activity indicated by nuclear-localized yellow fluorescence (*NLS*-2x*YFP*) in non-colonized (-AMF) and colonized (+AMF) transgenic *L. japonicus* wild-type roots transformed with a T-DNA containing a 1941 bp promoter fragment starting one base pair 5' of the start codon of *CCaMK* fused to *NLS*-2x*YFP*. Red fluorescence resulting from expression of p*SbtM1*:*SP-mCherry* indicates arbuscules. This arbuscule marker labels the apoplastic space (peri-arbuscular space) surrounding the arbuscule, thereby showing the contour of the arbuscule (Keymer et al., 2017). Arrows with different colors point to the nuclear YFP signals in different root layers, green arrow corresponds to epidermis; white/black to cortex, the numbers 1 to 4 besides the arrows represent the four layers of cortex, the 4th is the inner cortex where arbuscules develop; blue corresponds to endodermis. Scale bar, 100 μm.

To investigate whether epidermis-specific expression of *CCaMK* could restore the lost intraradical colonization in loss of function *ccamk-3* mutants (Fig. 16A), *ccamk-3* was transformed with *CCaMK* under the control of p*Epi*. Interestingly, epidermal expression of *CCaMK* restored intraradical colonization and arbuscule formation without morphological defects. However, restoration of root length colonization was more variable in comparison with a positive control, i. e. *CCaMK* under the control of the *Ubiquitin* promoter (Fig. 16A and 16B). The expression of four AM marker genes, *RAM1*, *SbtM1*, *AMT2.2* and *Vapyrin B* was analyzed as an additional indication of whether the roots were colonized. In non-colonized roots (mock), no inductions of *RAM1*, *SbtM1*, *AMT2.2* and *Vapyrin B* were detected, while in mycorrhizal roots (+AMF), those genes were significantly induced in roots with epidermal expression of *CCaMK* (Fig. 17). These data indicate that intraradical colonization does not require *CCaMK* expression in the cortex and especially in arbuscule-containing cells. Such cell non-autonomous function of *CCaMK* suggests two possibilities, either *CCaMK* regulates intraradical colonization via regulating downstream signal molecules, which travel from the epidermis to the cortex, or CCaMK itself is able to move along with the fungus through the root cell layers.

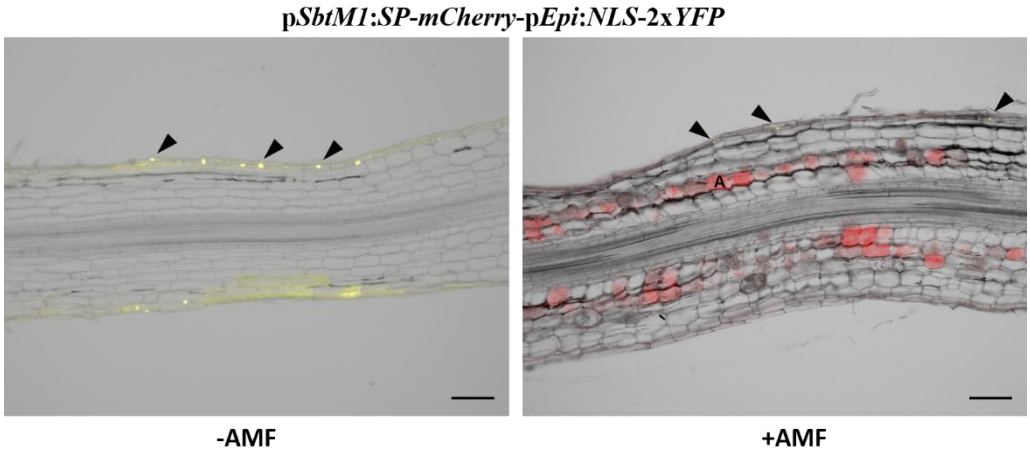

Fig. 15 Analysis of p*Epi* promoter activity. Microscopy images of longitudinal root sections containing vascular tissue. Promoter activity indicated by nuclear-localized yellow fluorescence (*NLS*-2x*YFP*) in non-colonized (-AMF) and colonized (+AMF) transgenic *L. japonicus* wild-type roots transformed with a T-DNA containing a 308 base pair promoter fragment starting one base pair 5' of the start codon of the *Lotus ExpansinA7* (p*Epi*) fused to *NLS*-2x*YFP* (Hayashi et al., 2014). Red fluorescence resulting from expression of p*SbtM1*:*SP-mCherry* indicates arbuscules. This arbuscule marker labels the apoplastic space (peri-arbuscular space) surrounding the arbuscule, thereby evidencing the contour of the arbuscule (Keymer et al., 2017). Arrows point to the nuclear YFP signal in the epidermis. Scale bar, 100 μm.

c) *CCaMK* is possibly capable of travelling

To examine whether CCaMK could move from the epidermis to other root layers, *CCaMK* was C-terminally fused to triple-*GFP*, which was reported to be an useful strategy to block protein movement though plasmodesmata (Brunkard and Zambryski, 2017; Zambryski, 2008). As a control, one-GFP was fused to the C-terminus of CCaMK. Under the control of the *Ubiquitin* promoter (p*Ubi*) and p*Epi*, both p*Ubi*:*CCaMK*-*GFP* and p*Epi*:*CCaMK*-*GFP* restored the defect of intraradical colonization, arbuscule development and colonization level in *ccamk-3* (Fig. 16A and 16C). However, p*Epi*:*CCaMK*-3x*GFP* did not restore colonization, indicating that restriction of CCaMK movement by fusing it to triple-GFP caused its failure to restore colonization in *ccamk-3*. In contrast, p*Ubi*:*CCaMK*-3x*GFP*, which ensures expression of *CCaMK*-3x*GFP* in all tissues restored colonization, indicating that the protein fused with triple-GFP is functional. Taken together these observations indicate that CCaMK can and needs to move from the epidermis into the cortex to restore colonization. The expression of AM marker genes, *RAM1*, *SbtM1*, *AMT2.2* and *Vapyrin B*, were detected as an indication of whether the roots were colonized (Fig. 17). In hairy roots without supply of *R. irregularis* (-AMF), all the plasmids could not activate the expression of the four AM marker genes in *ccamk-3*. In hairy roots of *ccamk-3* grown with *R. irregularis* (+AMF), AM marker genes were induced in roots expressing *CCaMK* fused to *GFP* under control of p*Ubi* and p*Epi*, as well as in roots expressing *CCaMK* fused to triple-*GFP* driven by p*Ubi*. However, induction was not observed when *CCaMK* tagged with triple-*GFP* was driven by p*Epi*. It is worth noting that there are only two replicates for empty vector transformed wild-type without mycorrhization, therefore the statistic difference is not significant although the genes are obviously induced by root colonization with the AM fungus (Fig. 17). The expression pattern of AM marker genes is consistent with the corresponding complementation of colonization (Fig. 16), indicating that CCaMK is able to move from the epidermis to other root layers to regulate AM development.

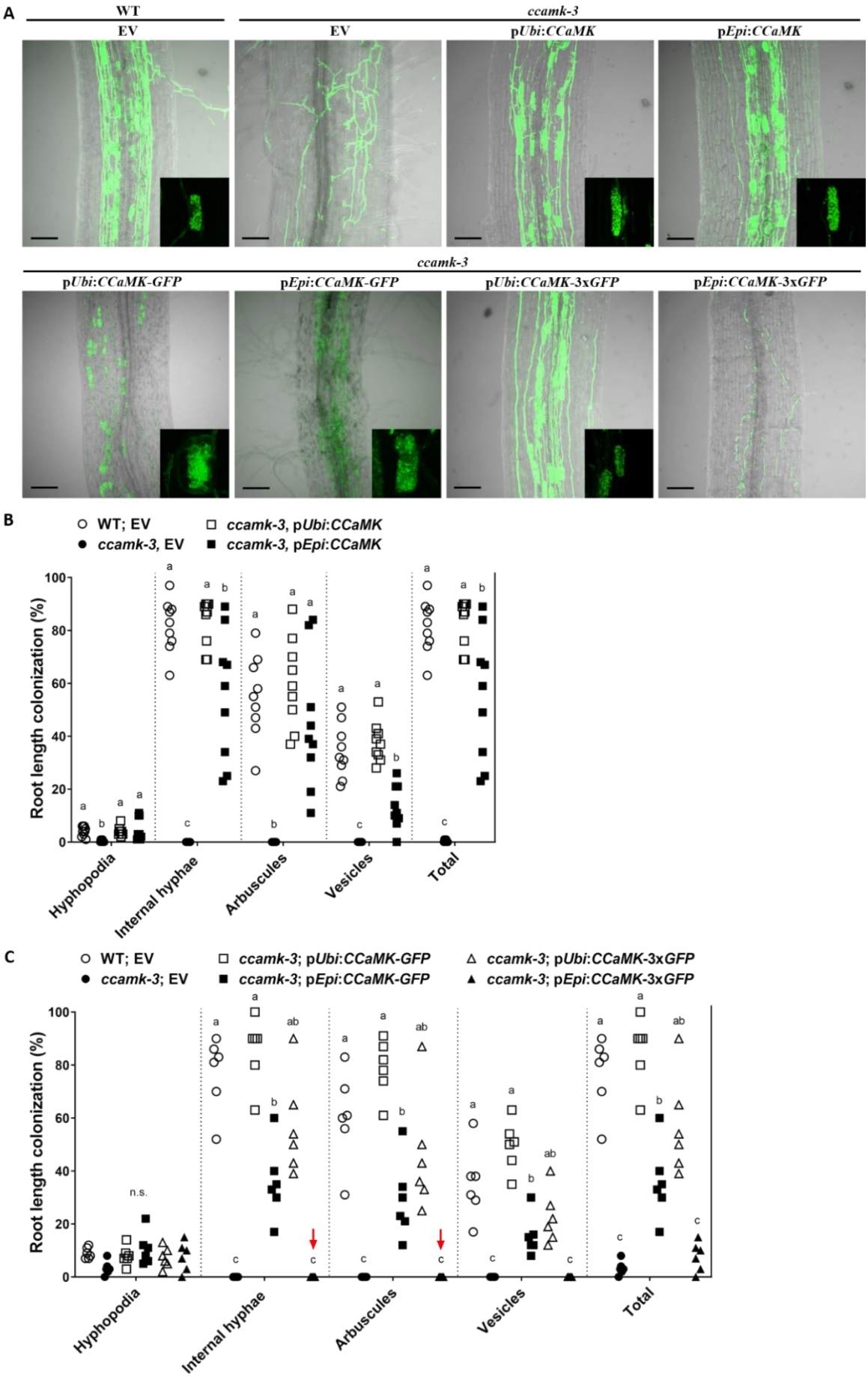
A
WT
EV
ccamk-3
EV
pUbi:CCaMK
pEpi:CCaMK
ccamk-3
pUbi:CCaMK-GFP
pEpi:CCaMK-GFP
pUbi:CCaMK-3xGFP
pEpi:CCaMK-3xGFP
B
WT; EV
ccamk-3, EV
ccamk-3, pUbi:CCaMK
ccamk-3, pEpi:CCaMK
Root length colonization (%)
Hyphopodia
Internal hyphae
Arbuscules
Vesicles
Total
C
WT; EV
ccamk-3; EV
ccamk-3; pUbi:CCaMK-GFP
ccamk-3; pEpi:CCaMK-GFP
ccamk-3; pUbi:CCaMK-3xGFP
ccamk-3; pEpi:CCaMK-3xGFP
Root length colonization (%)
n.s.
Hyphopodia
Internal hyphae
Arbuscules
Vesicles
Total

Fig. 16 Epidermal expression of *CCaMK* can restore AM in *ccamk-3* likely due to movement of the CCaMK. Plants were harvested at 5 wpi with *R. irregularis*. (**A)** Laser scanning confocal images of hairy roots of *L. japonicus* wild-type transformed with an empty vector control (EV) and *ccamk-3* mutant with EV, p*Ubi*:*CCaMK*, p*Epi*:*CCaMK*, p*Ubi*:*CCaMK-GFP*, p*Epi*:*CCaMK-GFP*, p*Ubi*:*CCaMK*-3x*GFP* and p*Epi*:*CCaMK*-3x*GFP*. Insets show close-up of arbuscules. The fungus is stained with WGA-AlexaFluor488. Scale bar, 100 µm. (**B)** and (**C)** Percent root length colonization. Different letters indicate different statistical groups (ordinary one-way ANOVA, Tukey-Kramer test, n = 36). (**B**) hyphopodia: $F_{3, 32} = 5.929$, p-value = 0.0025; internal hyphae: $F_{3, 32} = 70.21$, p-value < 0.0001; arbuscule: $F_{3, 32} = 23.49$, p-value < 0.0001; Vesicle: $F_{3, 32} = 50.01$, p-value < 0.0001; total: $F_{3, 32} = 69.62$, p-value < 0.0001.(**C**) hyphopodia: $F_{5, 30} = 1.988$, p-value = 0.1093; internal hyphae: $F_{5, 30} = 55.05$, p-value < 0.0001; arbuscules: $F_{5, 30} = 33.28$, p-value < 0.0001; vesicles: $F_{5, 30} = 32.01$, p-value < 0.0001; total: $F_{5, 30} = 46.08$, p-value < 0.0001. Red arrow highlights the percentage of internal hyphae and arbuscule in *ccamk-3* with p*Epi*:*CCaMK*-3x*GFP*.

d) CCaMK interacts with CYCLOPS in *L. japonicus* roots

It has been shown that CCaMK interacts with and phosphorylates the transcription factor CYCLOPS in heterologous *N. benthamiana* leaves (Messinese et al., 2007; Yano et al., 2008; Singh et al., 2014; Pimprikar et al., 2016). To examine the interaction of CCaMK and CYCLOPS in *L. japonicus* roots, bimolecular fluorescence complementation (BiFC) was employed using split Citrine as a reporter. The N-terminal 182 amino acids of Citrine were fused to the C-terminus of CCaMK and 74 amino acids from C-terminus of Citrine to the N-terminus of CYCLOPS. Both fused genes were placed under the control of the *Ubiquitin* promoter. The two expression cassettes were combined with another expression cassette p*SbtM1*:*SP-mCherry* as arbuscule marker in one Golden Gate plasmid and transformed into hairy roots of *L. japonicus* wild-type. Five weeks post inoculation with *R. irregularis*, yellow fluorescence was observed in all root cells, suggesting that CCaMK interacts with CYCLOPS in *L. japonicus* (Fig. 18). This led to the hypothesis that CYCLOPS may also move.

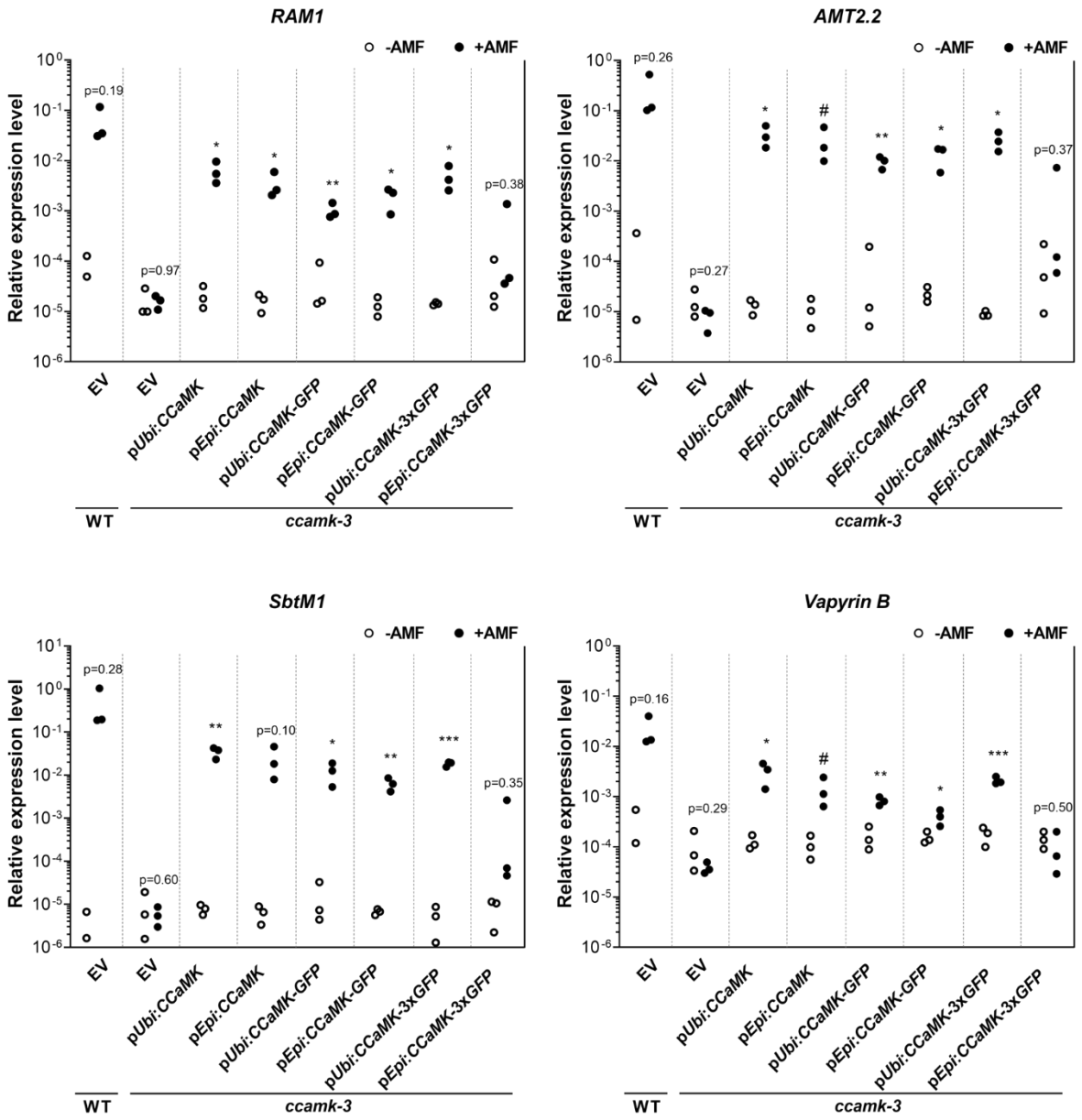

Fig. 17 Transcript accumulation of AM marker genes (*RAM1*, *SbtM1*, *AMT2.2* and *Vapyrin B*) in root material from the experiment shown in Fig. 16 inoculated without (mock) and with *R. irregularis* (+AMF). The transcript level was determined by RT-qPCR, and the housekeeping gene *Ubiquitin10* was used for normalization. Asterisks indicate significant differences compared with mock according to the student's t-test. # < 0.1; *, $p < 0.05$; **, $p < 0.01$; ***, $p < 0.001$.

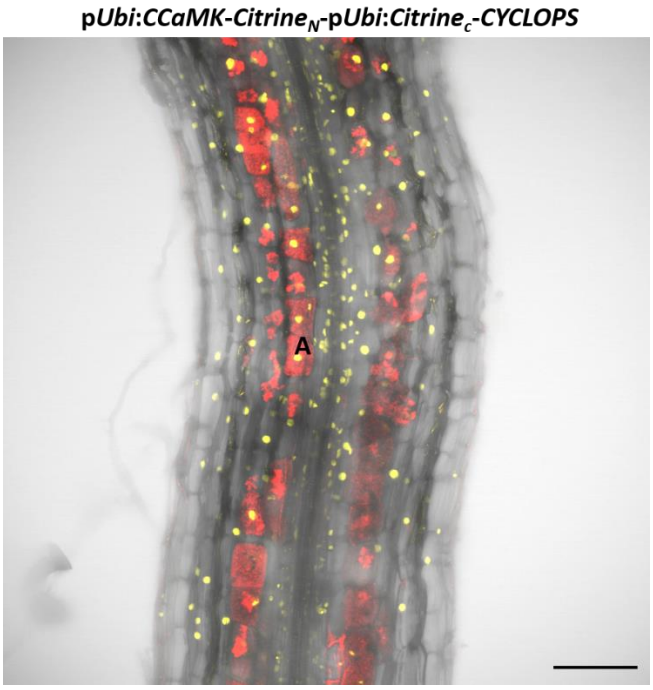

Fig. 18 CCaMK interacts with CYCLOPS in *L. japonicus*. Confocal image of a root segment containing arbuscules. Analysis for interaction of CCaMK and CYCLOPS using BiFC. *L. japonicus* wild-type roots were transformed with tandem p*Ubi*:*CCaMK-Citrine*$_N$ and p*Ubi*:*Citrine*$_C$*-CYCLOPS* and p*SbtM1*:*SP-mCherry*, and inoculated with *R. irregularis* for 5 weeks. *Citrine*$_N$, encoding N-terminal part of Citrine; *Citrine*$_C$, encoding C-terminal part of Citrine. Yellow fluorescence indicates interaction. A, arbuscule, indicated by red florescence. Overlays of fluorescent and bright field images are shown. The size bar represents 100 µm.

e) Epidermal expression of *CYCLOPS* can restore AM in *cyclops-4*

To investigate whether CYCLOPS also moves since its interaction partner CCaMK may move, the colonization phenotype of hairy roots expressing *CYCLOPS* under the control of p*Epi* in the *cyclops-4* mutant background was observed. In AM symbiosis, CYCLOPS is required for arbuscule initiation. Its loss of function mutant *cyclops-4* has only very rare internal hyphae and no arbuscules (Yano et al., 2008; Pimprikar et al., 2016). Epidermal expression of *CYCLOPS* could restore AM development and arbuscule formation without morphological defect in the *cyclops-4* mutant (Fig. 5). This suggests that CYCLOPS acts in a non-cell-autonomous manner and the cortical expression of *CYCLOPS* is not essential for arbuscule formation and development. In contrast to the failure of restoration by p*Epi*:*CCaMK*-3x*GFP*, when CYCLOPS was retained in epidermis and its movement was prevented by fusing triple-GFP, p*Epi*:3x*GFP-CYCLOPS* still complemented the arbuscule phenotype and partially the quantity of colonization (Fig.5), this may imply that CYCLOPS may promote colonization progress via triggering a downstream signal, which moves from the

epidermis to the cortex. Alternatively, the 3xGFP tag is cleaved from CYCLOPS and this needs to be thoroughly investigated in the future.

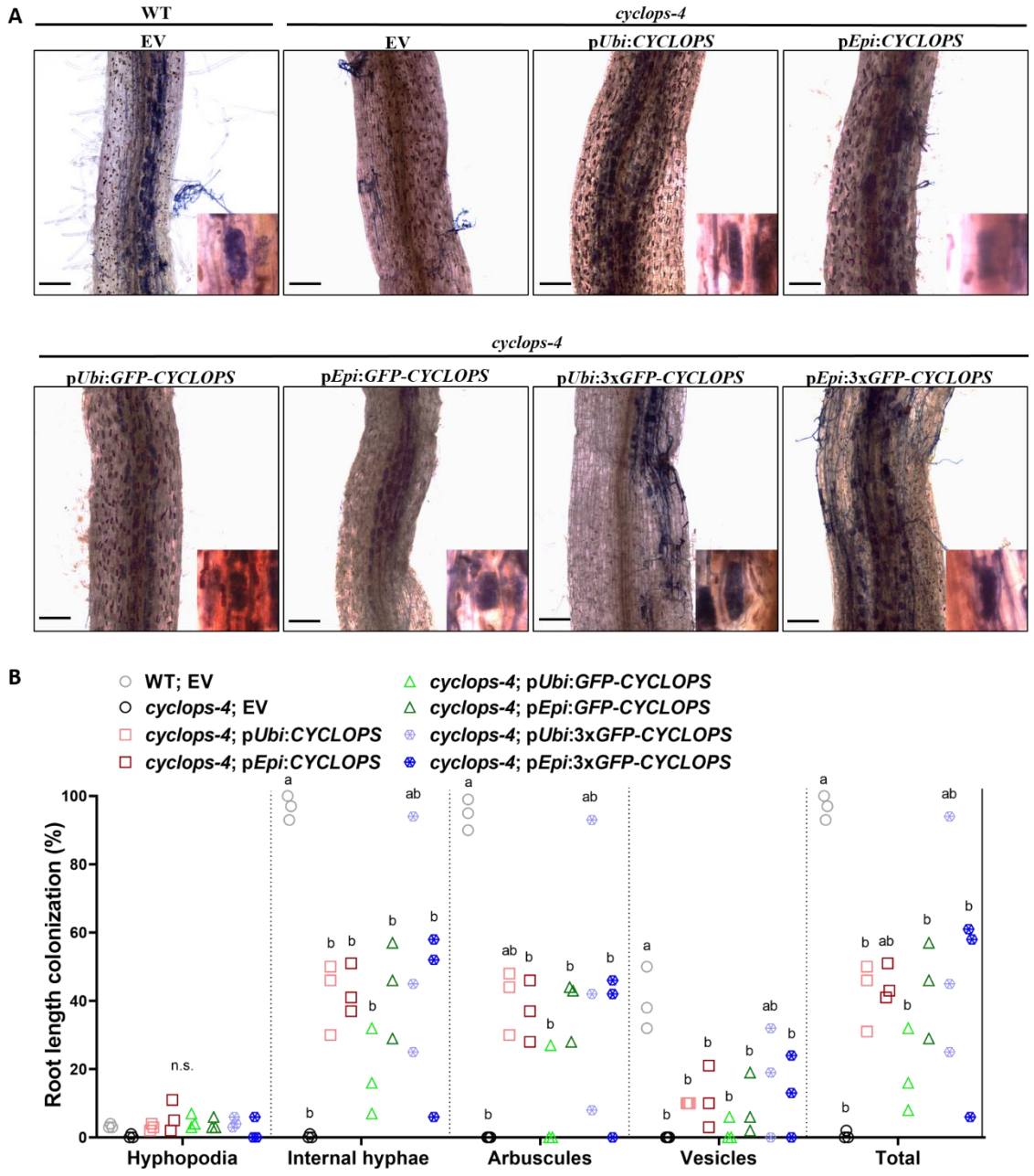

Fig. 19 Epidermal expression of *CYCLOPS* can restore AM in *cyclops-3*. Plants were harvested at 5 wpi with *R. irregularis*. (**A**) Bright field microscope images of hairy roots of *L. japonicus* wild-type transformed with an empty vector control (EV) and *cyclops-4* mutant with the indicated expression cassettes. Insets show close up of arbuscules. The fungus is stained with ink-acetic acid, scale bar, 100 µm. (**B**) Percent root length colonization. Different letters indicate different statistical groups (ordinary one-way ANOVA, Tukey-Kramer test, n = 24). hyphopodia: $F_{7, 16} = 1.632$, p-value = 0.1972, n.s., not significant; internal hyphae: $F_{7, 16} = 7.185$, p-value = 0.0006; arbuscules: $F_{7, 16} = 6.489$, p-value = 0.0010; vesicles: $F_{7, 16} = 5.514$, p-value = 0.0023; total: $F_{7, 16} = 6.849$, p-value = 0.0007.

VII. Discussion

1. Is auxin signaling part of the RAM1-regulated developmental program of arbuscule-containing cells?

The exchange of nutrients is the main benefit for both symbionts involved in arbuscular mycorrhiza symbiosis (AMS) (MacLean et al., 2017). Nutrients are trafficked across the peri-arbuscular membrane (PAM) and the efficiency of nutrient transfer is likely determined by the surface area of the PAM symbiotic interface, which encapsulates every fine arbuscule branch. Therefore, the degree of arbuscule branching is vitally important for this symbiotic association. Auxin signaling has been proposed to play an important role in arbuscule development, especially branching (Etemadi et al., 2014). Other studies showed that some auxin signaling-related mutants exhibit decreased mycorrhizal colonization but without defects in arbuscule morphology. These mutants are the pea mutant *bushy* (*bsh*) with low-IAA level, tomato mutants *diageotropica* (*dgt*) with impaired auxin signaling and *polycotyledon* (*pct*) with hyperactive polar auxin transport (Foo, 2013; Hanlon and Coenen, 2011). Furthermore, promoted auxin biosynthesis leads to increased colonization in *Brachypodium distachyon* (Buendia et al., 2019). To date, the general view is that auxin signaling positively affects arbuscule development as well as the quantity of colonization. However, how auxin is placed in the molecular regulatory network is not understood. Here, I investigated whether auxin signaling acts downstream of RAM1, which is the central regulator of arbuscule development.

a) Auxin signaling can be placed downstream of RAM1 during arbuscule development

Both ABA and auxin were proposed to play a role in arbuscule branching (Herrera-Medina et al., 2007; Etemadi et al., 2014). To examine whether ABA and auxin signaling are regulated by RAM1, I investigated the response of ABA and auxin in *L. japonicus* wild-type and *ram1* mutants by using transgenic reporters. Both ABA and auxin reporters (*RD29b*:*GUS* and *DR5*:*GUS*, respectively) were activated in arbuscule-containing cells (Fig. 4 and 5). Induction of ABA signaling in arbuscule-containing cells seems independent of *RAM1* as *ram1-4* still exhibits the ABA response (Fig. 4). These observations indicate that ABA signaling may act upstream of or in parallel to *RAM1* to

regulate arbuscule development. Crosstalk between ABA and other phytohormones may provide clues for the role of ABA in arbuscule development. For example, ABA was reported to enhance the stabilization of DELLA protein via attenuating bioactive GAs (Achard et al., 2006; Martín-Rodríguez et al., 2016). DELLA is important for arbuscule development (Floss et al., 2013; Pimprikar et al., 2016), and may thus be stabilized through ABA action. In contrast to the independence of arbuscule-containing cell-related ABA signalling of *RAM1*, several pieces of evidence suggest that auxin response in cells harboring arbuscules are dependent on *RAM1* (Summarized in Fig. 20). For example, when *RAM1* was absent, the activation of *DR5*:*GUS* failed in arbuscule containing cells and the induction of auxin response genes in mycorrhizal roots were abolished (Fig. 5 and 6B). Furthermore, constitutive expression of *RAM1* induced strong expression of *DR5*:*GUS* and formation of lateral roots, which is symptomatic of increased auxin signaling (Fig. 7). *LjARF17* is one of the auxin response genes induced by AM fungi and the expression of *LjARF17* is dependent on *RAM1* (Fig. 6B). Several auxin response elements (AuxREs and TGA) and an AM specific cis-regulatory element Myc2 were identified together in the promoter of *LjARF17* (Fig. 6A). Thereby, I speculated that RAM1 may regulate arbuscule development at least in part via auxin signaling (Fig. 20). However, *arf17* mutants exhibited a mature arbuscule phenotype similar to the wild-type control (Fig. 9). It is possible that the *LjARF17* is a transcriptional repressor of auxin signaling, therefore the absence of *ARF17* leads to the promotion of arbuscule growth which is more difficult to distinguish than impaired arbuscule branching in comparison with wild-type (Fig. 9). Another possibility is that the *LjARF17* acts as a transcriptional activator, but functional redundancy may exist, by one of the other 32 predicted *ARF* genes in the *L. japonicus* genome (Table 6). In previous studies, ARFs and the auxin transcriptional repressors AUX/IAAs were suggested to be involved in the AM symbiosis (Huang et al., 2018; Bassa et al., 2012; Bassa et al., 2013; Guillotin et al., 2017). Two auxin transcriptional activators ARF7 and ARF19 were suggested to positively regulate phosphate starvation response in Arabidopsis (Huang et al., 2018) and it is possible that orthologs or homologs also mediate the phosphate-responsive trait arbuscular mycorrhiza. *SlIAA27*, encoding an ARF repressor, has been shown to be down-regulated by exogenous auxin treatment and up-regulated by mycorrhization (Bassa et al., 2012; Bassa et al., 2013). RNAi silencing of *IAA27* causes decreased colonization level and down-regulation of strigolactone biosynthesis genes (Guillotin et al., 2017), suggesting that AM was decreased due to reduced strigolactone

exudation.

In addition to *LjARF17*, the expression of AM-induced *SAUR*s was also dependent on *RAM1* (Fig. 3B). *SAUR*s are well-known auxin-induced genes. *AtSAUR19* was proposed to promote cell expansion (Spartz et al., 2012). Further research into the mechanistic function of *SAURs* pointed out that *AtSAUR19* negatively regulates a PP2C-D subfamily of type 2C protein phosphatases, which inhibit plasma membrane (PM) H^+-ATPase activity. Therefore, *AtSAUR19* can stimulate the activity of (PM) H^+-ATPase (Spartz et al., 2014). The fungus and plant PMs are separated by a common interfacial apoplast (Pumplin and Harrison, 2009; Harrison, 2012). Although the fungus invades and inhabits the inner cortical cell, the PM remains intact but elongates and additionally, the PAM separating the fungus and plant cytoplasm is synthesized (Harrison, 2005; Pumplin and Harrison, 2009; Harrison, 2012). The apoplast surrounding the arbuscule is highly acidic, as shown by staining based on an ion-trap mechanism. The acidity was suggested to be indispensable for nutrient transfer due to a generated electrochemical potential between the symbiotic interface and the cytoplasm of both symbionts (Guttenberger, 2000a, b). HA1, an H^+-ATPase, localizes specifically to the PAM but not to the PM of the corresponding cortical cell (Krajinski et al., 2014). H^+-ATPases were suggested to be involved in the acidification process of the interfacial apoplast, and therefore play an important role in nutrient flow during the AM symbiosis (Gianinazzi-Pearson, 1996, 2000; Harrison, 1998; Krajinski et al., 2014; Wang et al., 2014). Nutrient exchange, as the main benefit of AM symbiosis, is of pivotal importance for arbuscule development (Javot et al., 2007b; Zhang et al., 2010; Jiang et al., 2017; Keymer et al., 2017). Taken together, it is possible that the AM-induced *RAM1*-dependent *SAUR*s regulate the H^+-ATPase in the arbuscular interface and thus affects arbuscule development. However, this still needs to be genetically addressed.

AM symbiosis influences the architecture of the host root, especially lateral root development. Increased root branching is recognized as a common feature of AM fungi-colonized roots. It is considered as a means of increasing sites for colonization, although it could also be a side effect of changes in hormone signaling and nutritional status of the host (Gutjahr and Paszkowski, 2013; Fusconi, 2014). Auxin signaling not only regulates the AM symbiosis, but also influences AM-associated effects on plant growth and architecture (Pozo et al., 2015). In my study, ectopic expression of RAM1 increased the lateral root development (Fig. 4). Auxin signaling is associated with the central regulator of arbuscule

development, RAM1. Thus, my work provides more knowledge towards an understanding of the complexity of AM symbiosis regulation by phytohormones.

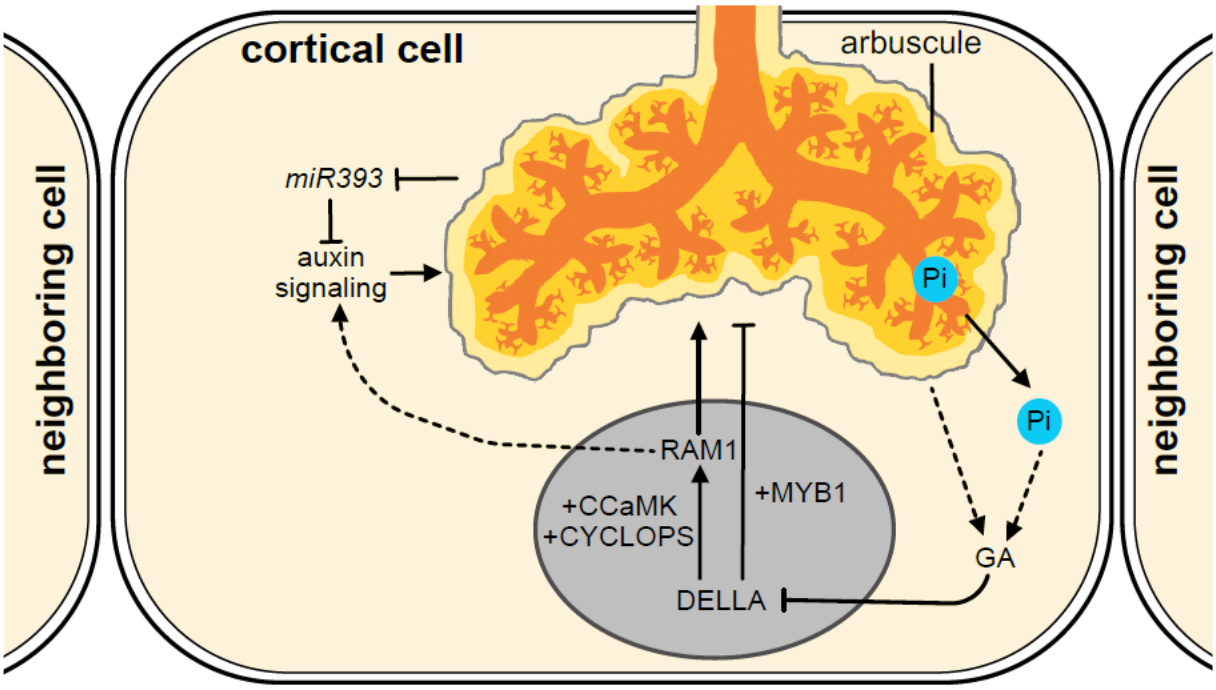

Fig. 20 Phytohormones are involved in regulation of arbuscule development in root cortical cells. Auxin signaling and GA biosynthesis are suggested to be induced in colonized cortical cells (Etemadi et al., 2014; Liao et al., 2015; Floss et al., 2013; Takeda et al., 2015), and GA production is reduced by Pi starvation (Devaiah et al., 2009). GA is well known to induce degradation of DELLA proteins (Alvey and Harberd, 2005; Floss et al., 2013). DELLA, in concert with CCaMK and CYCLOPS activates the expression of *RAM1* and promotes arbuscule development (Pimprikar et al., 2016); whereas in complex with a MYB1 transcription factor, DELLA induces expression of arbuscule degeneration-associated hydrolases, thus leading to arbuscule degeneration (Floss et al., 2017). Mycorrhization also leads to down regulation of the microRNA *miR393* in roots where it negatively regulates arbuscule development via inhibiting the generation of auxin receptors, therefore promoting arbuscule development (Etemadi et al., 2014). The figure is modified from Müller and Harrison, 2019.

b) The effect of exogenous auxin on AM colonization in wild-type and *ram1* of *L. japonicus*

To understand whether auxin acts downstream of *RAM1*, I examined whether the low colonization in *ram1* mutants can be restored by exogenous addition of auxin. In my study, exogenous NAA caused an obvious reduction of colonization level in wild-type and a gentle negative effect on *ram1-4* (Fig. 10A). Etemadi and co-authors reported

that 0.1 nM 2,4-D treatment in wild-type of tomato and *M. truncatula* had positive effects on the amount of root colonization by AM fungi (Etemadi et al., 2014). While in my study with *L. japonicus*, 2,4-D with concentrations from 0.1 to 10 nM did not promote the root length colonization for wild-type and *ram1-4* (Fig. 10B). However, in wild-type roots of *L. japonicus*, 2,4-D treatment led to a reduction of root colonization and the colonization level was very variable among individual plants, therefore, the reduction was not statistically significant (Fig. 10B). In comparison with tomato and *M. truncatula*, the different effects of 2,4-D on *L. japonicus* might be due to species-specific auxin sensitivities. These findings indicate that the absence of *RAM1* may decrease the sensitivity of mycorrhizal colonization to auxin. In addition, AM colonization is sensitive to environmental conditions. For instance, high concentration of phosphate inhibits AM colonization (Javot et al., 2007b). Light conditions, such as low ratio of red/far red light, cause reduced amount of colonization (Nagata et al., 2015). Such conditions or species-specific physiological optima may have caused the difference in responsiveness of AM colonization to auxin in *Lotus* in comparison with tomato and *Medicago* (Etemadi et al., 2014). We also examined whether exogenous auxin could promote arbuscule growth in *ram1*. However, the increased size of arbuscules caused by auxin treatment was observed only once and was not reproducible (Fig. S2 and 11). The auxin triggered arbuscule growth is possibly dependent on a precise environmental condition. Interestingly, *DR5*:*GUS* and commonly auxin-responsive genes such as *SAUR*s and *GH3* were induced by the auxin signaling activator *VP16-IAA17mImII* in wild-type, but not in *ram1* (Fig. 12A and 12B). This demonstrates that the *VP16-IAA17mImII* induced auxin responses are dependent on RAM1. We currently cannot explain this. It is possible that RAM1 directly interacts with IAA17*mImII* thereby promoting its transcriptional activity.

2. Are CCaMK and CYCLOPS travelling between cell layers?

In plants, many micro- and macro-molecules, such as water, ions, RNAs, proteins, metabolites and plant viruses, traffic from cell to cell via plasmodesmata (Zambryski and Crawford, 2000; Maule, 2008; Burch-Smith et al., 2011). Also, proteins, such as some fluorescent proteins and transcription factors were reported to travel from cell to cell (Gaudioso-Pedraza et al., 2018; Nakajima et al., 2001). However, to my knowledge, nuclear-localized kinases have not been presented to move between cells. Therefore, this study, for the first time, suggests that a nuclear-localized kinase may move between cell layers.

a) CCaMK may be capable of moving from epidermis to cortex

The analysis of *CCaMK* promoter activity confirmed that *CCaMK* is expressed in both epidermis and cortex during mycorrhization (Fig. 14). However, I observed that the epidermal expression of *CCaMK* is sufficient for establishing all fungal intraradical structures during AM symbiosis. For example, the loss of intraradical colonization in *ccamk-3*, especially the arbuscule formation and development in the inner cortex, was restored by epidermal-driven *CCaMK* (Fig. 16A and 16B). Furthermore, triple-GFP was fused to CCaMK under the control of p*Epi* to restrict the movement of CCaMK from epidermis to cortex in *ccamk-3*. In contrast to the restoration of fungal development in *ccamk-3* roots by the expression of p*Epi*:*CCaMK-GFP*, p*Epi*:*CCaMK*-3x*GFP* failed to restore it (Fig. 16A and 16C). This indicates that CCaMK itself may move from the epidermis to the cortex. The p*Epi* promoter (Hayashi et al., 2014) employed in this study was analyzed and confirmed to be specific for epidermal expression of the *L. japonicus* roots in response to fungal colonization (Fig. 15). The main fungal structures, the arbuscules, develop in non-adjacent inner cortical layers, which cannot be affected by the p*Epi* promoter. Taking all these data together, I suggest that CCaMK is possibly capable of traveling from epidermis to cortex, although this movement does not appear to be necessary for AM formation, as the endogenous *CCaMK* promoter is active in all cell layers. However, one could speculate that CCaMK movement may increase the speed of colonization and possibly enable additional expression of the CCaMK promoter in cells that are going to be colonized.

b) Epidermal expression of *CYCLOPS* can restore AM development in *cyclops* mutant

CYCLOPS is a direct phosphorylation target of CCaMK and the physical

interaction between CCaMK and CYCLOPS in heterologous systems such as yeast and *Nicotiana benthamiana* leaves have been reported in several studies (Messinese et al., 2007; Yano et al., 2008; Singh et al., 2014; Pimprikar et al., 2016). This study presents for the first time that CCaMK interacts with CYCLOPS in legume roots by BiFC assay (Fig. 18). This raises the speculation that CYCLOPS may also travel along with CCaMK.

Epidermis expression of *CYCLOPS* complemented the arbuscule development in the root cortex of *cyclops-4*, which, without complementation, displays only very rare internal hyphae and no formation of arbuscules (Fig. 19). In contrast to CCaMK fused to triple-GFP under the control of p*Epi*, which failed to restore the intraradical colonization in *ccamk-3*, CYCLOPS fused to triple-GFP driven by p*Epi* restored arbuscule formation and development in *cyclops-4* (Fig. 19). This result seems to suggest that CYCLOPS does not move but can act from the epidermis in a non-cell-autonomous manner. For example, CYCLOPS in the epidermis could trigger a downstream signal, such as RAM1 via transcriptional regulation, which moves from the epidermis to the cortex. In addition, the triple-GFP might be cleaved from a certain amount of CYCLOPS-3xGFP fusion proteins, thereby allowing CYCLOPS to diffuse through plasmodesmata into the cortex. Whatever the case, it is highly surprising that AM colonization does not require cortical expression of *CYCLOPS*.

There are conflicting reports on the expression pattern of *CYCLOPS* in the literature. In the absence of fungus, Messinese and co-authors showed that the promoter of the *CYCLOPS* ortholog *IPD3* in *M. truncatula* is active in vascular bundles using the promoter:*GUS* assay (Messinese et al., 2007). However, a recent study suggested that the functionally redundant *IPD3* and *IPD3L* were both expressed in all the root layers (Jin et al., 2018). The expression pattern of *CYCLOPS* in colonized roots still remains elusive and needs to be addressed in further studies. It is possible that if *CCaMK* is artificially only in the epidermis, as in this study, it may move to the cortex and phosphorylate CYCLOPS, if CYCLOPS would be expressed there. If *CYCLOPS* would be expressed only in the epidermis, CCaMK and CYCLOPS together could act in a non-cell-autonomous manner and induce other molecular signals, for example RAM1, which may travel to the cortex to trigger cortex cell rearrangement for arbuscule formation. Overexpression of RAM1 restores colonization of *cyclops* mutants but not of *ccamk-13*, leading to the hypothesis that CCaMK has more targets than just CYCLOPS (Pimprikar et al., 2016). This could be an explanation for the scenario that epidermal restricted CCaMK cannot restore AM development, while epidermal restricted CYCLOPS can. CCaMK may need to be in the cortex to phosphorylate

additional targets in this cell type. Alternatively, there could be an experimental problem, CCaMK accumulation, when the gene is expressed under the control of p*Epi*, is too low to set off the non-cell autonomous signal, while for CYCLOPS, the triple-GFP may be cleaved, thereby allowing CYCLOPS to travel.

VIII. Conclusion

Auxin signaling has been reported to positively affect arbuscule development as well as the quantity of root colonization by arbuscular mycorrhiza fungi (Hanlon and Coenen, 2011; Foo, 2013; Etemadi et al., 2014; Buendia et al., 2019). Based on these previous studies, one aim of this thesis was to address how auxin signaling is placed relative to the central regulator of arbuscule development, RAM1, in a signaling network. RAM1 has been shown to promote arbuscule development (Park et al., 2015; Xue et al., 2015; Rich et al., 2015; Pimprikar et al., 2016; Pimprikar and Gutjahr, 2018). This thesis reports that the induction of ABA signaling reporter *RD29b*:*GUS* is activated in arbuscule-containing cells but does not depend on *RAM1*, while auxin signaling reporter *DR5*:*GUS* in arbuscule-containing cells is dependent on *RAM1*, suggesting that ABA signaling may act upstream of or in parallel to *RAM1*, while auxin signaling can be placed downstream of *RAM1* to regulate arbuscule development. The dependence of the auxin response on *RAM1* is also supported by the RT-qPCR data showing that the AM-induced auxin-responsive genes, *LjARF17* and *SAUR*s, are not induced in the *ram1* mutants. Taking together these results with the observation that ectopic expression of *RAM1* activates *DR5*:*GUS* and the formation of lateral roots in absence of the fungus, I conclude that RAM1 may directly or indirectly induce auxin signaling or biosynthesis in arbuscule containing cells. *LjARF17* was found by phylogenetic analysis to be specifically present in genomes of AM-competent plants and an AM-specific cis-regulatory element Myc2 was identified in its promoter together with three auxin response elements. However, *Ljarf17* mutants are not affected in arbuscule morphology, indicating that LjARF17 is not required for arbuscule branching. Furthermore, the first application of exogenous auxin promoted arbuscule growth in *ram1* but this was not reproducible in further independent experiments. Based on the result of the first auxin treatment assay, the auxin signaling activator *VP16-IAA17mImII* and the auxin biosynthesis *YUC6* and *TAA1* were transgenically expressed in *ram1* under the control of the *RAM1* promoter. Arbuscule growth was affected in none of the transgenic plants, indicating that induction of auxin signaling in arbuscule-containing cells of *ram1* mutants did not work, or is insufficient to trigger arbuscule growth. This implies that other RAM1-dependent mechanisms are required. *VP16-IAA17mImII* could interestingly neither induce *DR5*:*GUS* nor auxin-responsive genes in *ram1-3*, demonstrating that RAM1 is required for the *VP16-IAA17mImII*

induced auxin response and suggesting that RAM1 may directly interact with the target ARF of IAA17*mImII*.

The establishment of successful AM symbiosis involves symbiotic rearrangement of cells in both the root epidermis and the cortex. Besides, a coordinated regulation between the two root layers is indispensable. Therefore, the other aim of this thesis was to investigate the requirement of two symbiotic genes encoding a nuclear-localized kinase CCaMK and its target, a transcription factor CYCLOPS, during the AM symbiosis. *CCaMK* and *CYCLOPS* act upstream of *RAM1* in the AM symbiotic pathway, mutants of *CCaMK* or *CYCLOPS* exhibit more severe phenotypes than stunted arbuscule in *ram1*, *ccamk* fails to allow formation of intracellular hyphae and arbuscules; while *cyclops* displays severely impaired formation of intracellular hyphae and no arbuscules. We found that expression of *CCaMK* using an epidermis-specific promoter could restore intraradical colonization in *ccamk-3* mutant roots including intraradical hyphae and arbuscules in the cortex. When *CCaMK* was fused with 3xGFP, there was no restoration of intraradical colonization and arbuscule development, suggesting that CCaMK is capable of moving from the epidermis to the cortex. I confirmed that CCaMK and CYCLOPS interact in legume roots by BiFC assay, raising the hypothesis that CYCLOPS may also travel along with CCaMK. Epidermis expression of *CYCLOPS* could also rescue the arbuscule formation in *cyclops-4*. However, this also occurred with *CYCLOPS-3xGFP*, suggesting that CYCLOPS itself may not move but induce (a) mobile molecular signal(s).

IX. References

Achard, P., Cheng, H., De Grauwe, L., Decat, J., Schoutteten, H., Moritz, T., Van Der Straeten, D., Peng, J., and Harberd, N.P. (2006). Integration of plant responses to environmentally activated phytohormonal signals. Science *311*, 91-94.

Adolfsson, L., Nziengui, H., Abreu, I.N., Šimura, J., Beebo, A., Herdean, A., Aboalizadeh, J., Široká, J., Moritz, T., Novák, O., *et al.* (2017). Enhanced Secondary- and Hormone Metabolism in Leaves of Arbuscular Mycorrhizal Medicago truncatula. Plant Physiology *175*, 392-411.

Akiyama, K., Matsuzaki, K.-i., and Hayashi, H. (2005). Plant sesquiterpenes induce hyphal branching in arbuscular mycorrhizal fungi. Nature *435*, 824-827.

Alvey, L., and Harberd, N.P. (2005). DELLA proteins: integrators of multiple plant growth regulatory inputs? Physiologia Plantarum *123*, 153-160.

Augé, R.M., Toler, H.D., and Saxton, A.M. (2015). Arbuscular mycorrhizal symbiosis alters stomatal conductance of host plants more under drought than under amply watered conditions: a meta-analysis. Mycorrhiza *25*, 13-24.

Bago, B., Pfeffer, P.E., and Shachar-Hill, Y. (2000). Carbon metabolism and transport in arbuscular mycorrhizas. Plant physiology *124*, 949-958.

Bassa, C., Etemadi, M., Combier, J.-P., Bouzayen, M., and Audran-Delalande, C. (2013). Sl-IAA27 gene expression is induced during arbuscular mycorrhizal symbiosis in tomato and in Medicago truncatula. Plant signaling & behavior *8*, e25637.

Bassa, C., Mila, I., Bouzayen, M., and Audran-Delalande, C. (2012). Phenotypes associated with down-regulation of Sl-IAA27 support functional diversity among Aux/IAA family members in tomato. Plant and Cell Physiology *53*, 1583-1595.

Besserer, A., Bécard, G., Jauneau, A., Roux, C., and Séjalon-Delmas, N. (2008). GR24, a synthetic analog of strigolactones, stimulates the mitosis and growth of the arbuscular mycorrhizal fungus Gigaspora rosea by boosting its energy metabolism. Plant Physiology *148*, 402-413.

Besserer, A., Puech-Pagès, V., Kiefer, P., Gomez-Roldan, V., Jauneau, A., Roy, S., Portais, J.-C., Roux, C., Bécard, G., and Séjalon-Delmas, N. (2006). Strigolactones stimulate arbuscular mycorrhizal fungi by activating mitochondria. PLoS Biol *4*, e226.

Binder, A., Lambert, J., Morbitzer, R., Popp, C., Ott, T., Lahaye, T., and Parniske, M. (2014). A modular plasmid assembly kit for multigene expression, gene silencing and silencing rescue in plants. PLoS One *9*, e88218.

Bonfante, P., and Anca, I.-A. (2009). Plants, mycorrhizal fungi, and bacteria: a network of interactions. Annual review of microbiology *63*, 363-383.

Bonfante, P., and Genre, A. (2008). Plants and arbuscular mycorrhizal fungi: an evolutionary-developmental perspective. Trends in plant science *13*, 492-498.

Bravo, A., York, T., Pumplin, N., Mueller, L.A., and Harrison, M.J. (2016). Genes conserved for arbuscular

mycorrhizal symbiosis identified through phylogenomics. Nature Plants *2*, 1-6.

Brunkard, J.O., and Zambryski, P.C. (2017). Plasmodesmata enable multicellularity: new insights into their evolution, biogenesis, and functions in development and immunity. Current Opinion in Plant Biology *35*, 76-83.

Buee, M., Rossignol, M., Jauneau, A., Ranjeva, R., and Bécard, G. (2000). The pre-symbiotic growth of arbuscular mycorrhizal fungi is induced by a branching factor partially purified from plant root exudates. Molecular Plant-Microbe Interactions *13*, 693-698.

Buendia, L., Ribeyre, C., Bensmihen, S., and Lefebvre, B. (2019). Brachypodium distachyon tar2lhypo mutant shows reduced root developmental response to symbiotic signal but increased arbuscular mycorrhiza. Plant Signaling & Behavior *14*, e1651608.

Burch-Smith, T.M., Stonebloom, S., Xu, M., and Zambryski, P.C. (2011). Plasmodesmata during development: re-examination of the importance of primary, secondary, and branched plasmodesmata structure versus function. Protoplasma *248*, 61-74.

Campanella, J.J., Smith, S.M., Leibu, D., Wexler, S., and Ludwig-Müller, J. (2007). The Auxin Conjugate Hydrolase Family of Medicago truncatula and Their Expression During the Interaction with Two Symbionts. Journal of Plant Growth Regulation *27*, 26-38.

Carbonnel, S., and Gutjahr, C. (2014). Control of arbuscular mycorrhiza development by nutrient signals. Frontiers in Plant Science *5*, 462.

Chabaud, M., Genre, A., Sieberer, B.J., Faccio, A., Fournier, J., Novero, M., Barker, D.G., and Bonfante, P. (2011). Arbuscular mycorrhizal hyphopodia and germinated spore exudates trigger Ca2+ spiking in the legume and nonlegume root epidermis. New Phytologist *189*, 347-355.

Charpentier, M., Sun, J., Wen, J., Mysore, K.S., and Oldroyd, G.E.D. (2014). Abscisic Acid Promotion of Arbuscular Mycorrhizal Colonization Requires a Component of the PROTEIN PHOSPHATASE 2A Complex. Plant Physiology *166*, 2077-2090.

Chen, X., Liao, D., Yang, X., Ji, M., Wang, S., Gu, M., Chen, A., and Xu, G. (2017). Three cis-regulatory motifs, AuxRE, MYCRS1 and MYCRS2, are required for modulating the auxin-and mycorrhiza-responsive expression of a tomato GH3 gene. Plant and Cell Physiology *58*, 770-778.

Cook, C., Whichard, L.P., Turner, B., Wall, M.E., and Egley, G.H. (1966). Germination of witchweed (Striga lutea Lour.): isolation and properties of a potent stimulant. Science *154*, 1189-1190.

Czechowski, T., Bari, R. P., Stitt, M., Scheible, W. R., and Udvardi, M. K. (2004). Real-time RT-PCR profiling of over 1400 Arabidopsis transcription factors: unprecedented sensitivity reveals novel root-and shoot-specific genes. The Plant Journal *38*, 366-379.

Danneberg, G., Latus, C., Zimmer, W., Hundeshagen, B., and Bothe, H. (1993). Influence of vesicular-arbuscular mycorrhiza on phytohormone balances in maize (Zea mays L.). Journal of Plant Physiology *141*, 33-39.

Das, D., and Gutjahr, C. (2019). Role of phytohormones in arbuscular mycorrhiza development. The model legume Medicago truncatula, 485-500.

Declerck, S., Strullu, D.G., and Plenchette, C. (1998). Monoxenic culture of the intraradical forms of Glomus sp. isolated from a tropical ecosystem: a proposed methodology for germplasm collection. Mycologia *90*, 579-585.

Delaux, P.-M., Varala, K., Edger, P.P., Coruzzi, G.M., Pires, J.C., and Ané, J.-M. (2014). Comparative phylogenomics uncovers the impact of symbiotic associations on host genome evolution. PLoS Genet *10*, e1004487.

Demchenko, K., Winzer, T., Stougaard, J., Parniske, M., and Pawlowski, K. (2004). Distinct roles of Lotus japonicus SYMRK and SYM15 in root colonization and arbuscule formation. New Phytologist *163*, 381-392.

Devaiah, B.N., Madhuvanthi, R., Karthikeyan, A.S., and Raghothama, K.G. (2009). Phosphate starvation responses and gibberellic acid biosynthesis are regulated by the MYB62 transcription factor in Arabidopsis. Molecular plant *2*, 43-58.

Devers, E.A., Teply, J., Reinert, A., Gaude, N., and Krajinski, F. (2013). An endogenous artificial microRNA system for unraveling the function of root endosymbioses related genes in Medicago truncatula. BMC Plant Biology *13*, 82.

Dickson, S. (2004). The Arum-Paris continuum of mycorrhizal symbioses. New Phytologist *163*, 187-200.

Dickson, S., Smith, F.A., and Smith, S.E. (2007). Structural differences in arbuscular mycorrhizal symbioses: more than 100 years after Gallaud, where next? Mycorrhiza *17*, 375-393.

Dubrovsky, J.G., Sauer, M., Napsucialy-Mendivil, S., Ivanchenko, M.G., Friml, J., Shishkova, S., Celenza, J., and Benková, E. (2008). Auxin acts as a local morphogenetic trigger to specify lateral root founder cells. Proceedings of the National Academy of Sciences *105*, 8790-8794.

Edlund, A., Eklof, S., Sundberg, B., Moritz, T., and Sandberg, G. (1995). A microscale technique for gas chromatography-mass spectrometry measurements of picogram amounts of indole-3-acetic acid in plant tissues. Plant physiology *108*, 1043-1047.

Etemadi, M., Gutjahr, C., Couzigou, J.-M., Zouine, M., Lauressergues, D., Timmers, A., Audran, C., Bouzayen, M., Bécard, G., and Combier, J.-P. (2014). Auxin perception is required for arbuscule development in arbuscular mycorrhizal symbiosis. Plant Physiology *166*, 281-292.

Favre, P., Bapaume, L., Bossolini, E., Delorenzi, M., Falquet, L., and Reinhardt, D. (2014). A novel bioinformatics pipeline to discover genes related to arbuscular mycorrhizal symbiosis based on their evolutionary conservation pattern among higher plants. BMC plant biology *14*, 333.

Feddermann, N., Duvvuru Muni, R.R., Zeier, T., Stuurman, J., Ercolin, F., Schorderet, M., and Reinhardt, D. (2010). The PAM1 gene of petunia, required for intracellular accommodation and morphogenesis of arbuscular mycorrhizal fungi, encodes a homologue of VAPYRIN. The Plant Journal *64*, 470-481.

Fester, T., and Hause, B. (2007). Drought and Symbiosis: Why Is Abscisic Acid Necessary for Arbuscular Mycorrhiza? New Phytologist, 383-386.

Fitter, A.H. (2005). Darkness visible: reflections on underground ecology. Journal of Ecology *93*, 231-243.

Fitze, D., Wiepning, A., Kaldorf, M., and Ludwig-Müller, J. (2005). Auxins in the development of an arbuscular mycorrhizal symbiosis in maize. Journal of plant physiology *162*, 1210-1219.

Floss, D.S., Gomez, S.K., Park, H.-J., MacLean, A.M., Müller, L.M., Bhattarai, K.K., Lévesque-Tremblay, V., Maldonado-Mendoza, I.E., and Harrison, M.J. (2017). A transcriptional program for arbuscule degeneration during AM symbiosis is regulated by MYB1. Current Biology *27*, 1206-1212.

Floss, D.S., Lévesque-Tremblay, V., Park, H.-J., and Harrison, M.J. (2016). DELLA proteins regulate expression of a subset of AM symbiosis-induced genes in Medicago truncatula. Plant Signaling & Behavior *11*, e1162369.

Floss, D.S., Levy, J.G., Lévesque-Tremblay, V., Pumplin, N., and Harrison, M.J. (2013). DELLA proteins regulate arbuscule formation in arbuscular mycorrhizal symbiosis. Proceedings of the National Academy of Sciences *110*, E5025-E5034.

Foo, E. (2013). Auxin influences strigolactones in pea mycorrhizal symbiosis. Journal of Plant Physiology *170*, 523-528.

Fukaki, H., and Tasaka, M. (2009). Hormone interactions during lateral root formation. Plant molecular biology *69*, 437.

Fusconi, A. (2014). Regulation of root morphogenesis in arbuscular mycorrhizae: what role do fungal exudates, phosphate, sugars and hormones play in lateral root formation? Annals of Botany *113*, 19-33.

Gaudioso-Pedraza, R., Beck, M., Frances, L., Kirk, P., Ripodas, C., Niebel, A., Oldroyd, G.E., Benitez-Alfonso, Y., and de Carvalho-Niebel, F. (2018). Callose-regulated symplastic communication coordinates symbiotic root nodule development. Current Biology *28*, 3562-3577. e3566.

Genre, A., Chabaud, M., Balzergue, C., Puech-Pagès, V., Novero, M., Rey, T., Fournier, J., Rochange, S., Bécard, G., Bonfante, P., *et al.* (2013). Short-chain chitin oligomers from arbuscular mycorrhizal fungi trigger nuclear Ca2+spiking inMedicago truncatularoots and their production is enhanced by strigolactone. New Phytologist *198*, 190-202.

Genre, A., Chabaud, M., Timmers, T., Bonfante, P., and Barker, D.G. (2005). Arbuscular Mycorrhizal Fungi Elicit a Novel Intracellular Apparatus in Medicago truncatula Root Epidermal Cells before Infection. The Plant Cell *17*, 3489-3499.

Genre, A., Ivanov, S., Fendrych, M., Faccio, A., Žárský, V., Bisseling, T., and Bonfante, P. (2012). Multiple exocytotic markers accumulate at the sites of perifungal membrane biogenesis in arbuscular mycorrhizas. Plant and Cell Physiology *53*, 244-255.

Gianinazzi-Pearson, V. (1996). Plant cell responses to arbuscular mycorrhizal fungi: getting to the roots of the symbiosis. The Plant Cell *8*, 1871.

Gianinazzi-Pearson, V., Arnould, C., Oufattole, M., Arango, M., and Gianinazzi, S. (2000). Differential activation of H+-ATPase genes by an arbuscular mycorrhizal fungus in root cells of transgenic tobacco. Planta *211*, 609-613.

Giovannetti, M. (2000). Spore germination and pre-symbiotic mycelial growth. In Arbuscular mycorrhizas: physiology and function (Springer), pp. 47-68.

Giovannetti, M., Sbrana, C., Avio, L., Citernesi, A., and Logi, C. (1993). Differential hyphal morphogenesis in arbuscular mycorrhizal fungi during pre-infection stages. New Phytologist *125*, 587-593.

Girardin, A., Wang, T., Ding, Y., Keller, J., Buendia, L., Gaston, M., Ribeyre, C., Gasciolli, V., Auriac, M.-C., Vernié, T., *et al.* (2019). LCO Receptors Involved in Arbuscular Mycorrhiza Are Functional for Rhizobia Perception in Legumes. Current Biology *29*, 4249-4259.e4245.

Gobbato, E., Wang, E., Higgins, G., Bano, S.A., Henry, C., Schultze, M., and Oldroyd, G.E. (2013). RAM1 and RAM2 function and expression during arbuscular mycorrhizal symbiosis and Aphanomyces euteiches colonization. Plant signaling & behavior *8*, e26049.

Guillotin, B., Etemadi, M., Audran, C., Bouzayen, M., Bécard, G., and Combier, J.P. (2017). Sl-IAA27 regulates strigolactone biosynthesis and mycorrhization in tomato (var. MicroTom). New Phytologist *213*, 1124-1132.

Gutjahr, C. (2014). Phytohormone signaling in arbuscular mycorhiza development. Current Opinion in Plant Biology *20*, 26-34.

Gutjahr, C., Banba, M., Croset, V., An, K., Miyao, A., An, G., Hirochika, H., Imaizumi-Anraku, H., and Paszkowski, U. (2008). Arbuscular Mycorrhiza–Specific Signaling in Rice Transcends the Common Symbiosis Signaling Pathway. The Plant Cell *20*, 2989-3005.

Gutjahr, C., Novero, M., Guether, M., Montanari, O., Udvardi, M., and Bonfante, P. (2009). Presymbiotic factors released by the arbuscular mycorrhizal fungusGigaspora margaritainduce starch accumulation inLotus japonicusroots. New Phytologist *183*, 53-61.

Gutjahr, C., and Parniske, M. (2013). Cell and developmental biology of arbuscular mycorrhiza symbiosis. Annual review of cell and developmental biology *29*, 593-617.

Guttenberger, M. (2000a). Arbuscules of vesicular-arbuscular mycorrhizal fungi inhabit an acidic compartment within plant roots. Planta *211*, 299-304.

Guttenberger, M. (2000b). A rapid staining procedure for arbuscules of living arbuscular mycorrhizas using neutral red as acidotropic dye. Plant and soil *226*, 211.

Hanlon, M.T., and Coenen, C. (2011). Genetic evidence for auxin involvement in arbuscular mycorrhiza initiation. New Phytologist *189*, 701-709.

Harrison, M.J. (1998). Development of the arbuscular mycorrhizal symbiosis. Current opinion in plant biology *1*, 360-365.

Harrison, M.J. (2005). Signaling in the arbuscular mycorrhizal symbiosis. Annu Rev Microbiol *59*, 19-42.

Harrison, M.J. (2012). Cellular programs for arbuscular mycorrhizal symbiosis. Current Opinion in Plant Biology *15*, 691-698.

Harrison, M.J., Dewbre, G.R., and Liu, J. (2002). A Phosphate Transporter from Medicago truncatula Involved in the Acquisition of Phosphate Released by Arbuscular Mycorrhizal Fungi. The Plant Cell *14*, 2413-2429.

Hayashi, T., Banba, M., Shimoda, Y., Kouchi, H., Hayashi, M., and Imaizumi-Anraku, H. (2010). A dominant function of CCaMK in intracellular accommodation of bacterial and fungal

endosymbionts. The Plant Journal *63*, 141-154.

Hayashi, T., Shimoda, Y., Sato, S., Tabata, S., Imaizumi-Anraku, H., and Hayashi, M. (2014). Rhizobial infection does not require cortical expression of upstream common symbiosis genes responsible for the induction of C a2+ spiking. The Plant Journal *77*, 146-159.

Heck, C., Kuhn, H., Heidt, S., Walter, S., Rieger, N., and Requena, N. (2016). Symbiotic fungi control plant root cortex development through the novel GRAS transcription factor MIG1. Current Biology *26*, 2770-2778.

Herrera-Medina, M.J., Steinkellner, S., Vierheilig, H., Ocampo Bote, J.A., and García Garrido, J.M. (2007). Abscisic acid determines arbuscule development and functionality in the tomato arbuscular mycorrhiza. New Phytologist *175*, 554-564.

Hijikata, N., Murase, M., Tani, C., Ohtomo, R., Osaki, M., and Ezawa, T. (2010). Polyphosphate has a central role in the rapid and massive accumulation of phosphorus in extraradical mycelium of an arbuscular mycorrhizal fungus. The New phytologist *186*, 285-289.

Ho, I., and Trappe, J. (1973). Translocation of 14 C from Festuca plants to their endomycorrhizal fungi. Nature New Biology *244*, 30-31.

Holford, I. (1997). Soil phosphorus: its measurement, and its uptake by plants. Soil Research *35*, 227-240.

Hong, J.J., Park, Y.-S., Bravo, A., Bhattarai, K.K., Daniels, D.A., and Harrison, M.J. (2012). Diversity of morphology and function in arbuscular mycorrhizal symbioses in Brachypodium distachyon. Planta *236*, 851-865.

Horváth, B., Yeun, L.H., Domonkos, Á., Halász, G., Gobbato, E., Ayaydin, F., Miró, K., Hirsch, S., Sun, J., and Tadege, M. (2011). Medicago truncatula IPD3 is a member of the common symbiotic signaling pathway required for rhizobial and mycorrhizal symbioses. Molecular plant-microbe interactions *24*, 1345-1358.

Huang, K.-L., Ma, G.-J., Zhang, M.-L., Xiong, H., Wu, H., Zhao, C.-Z., Liu, C.-S., Jia, H.-X., Chen, L., Kjorven, J.O., *et al.* (2018). The ARF7 and ARF19 Transcription Factors Positively Regulate PHOSPHATE STARVATION RESPONSE1 in Arabidopsis Roots. Plant Physiology *178*, 413-427.

Huisman, R., Hontelez, J., Mysore, K.S., Wen, J., Bisseling, T., and Limpens, E. (2016). A symbiosis-dedicated SYNTAXIN OF PLANTS 13II isoform controls the formation of a stable host–microbe interface in symbiosis. New Phytologist *211*, 1338-1351.

Ivanov, S., Fedorova, E.E., Limpens, E., De Mita, S., Genre, A., Bonfante, P., and Bisseling, T. (2012). Rhizobium–legume symbiosis shares an exocytotic pathway required for arbuscule formation. Proceedings of the National Academy of Sciences *109*, 8316-8321.

Javot, H., Penmetsa, R.V., Terzaghi, N., Cook, D.R., and Harrison, M.J. (2007a). A Medicago truncatula phosphate transporter indispensable for the arbuscular mycorrhizal symbiosis. Proceedings of the National Academy of Sciences *104*, 1720-1725.

Javot, H., Pumplin, N., and Harrison, M.J. (2007b). Phosphate in the arbuscular mycorrhizal symbiosis: transport properties and regulatory roles. Plant, Cell & Environment *30*, 310-322.

Jentschel, K., Thiel, D., Rehn, F., and Ludwig-Müller, J. (2007). Arbuscular mycorrhiza enhances auxin levels and alters auxin biosynthesis in Tropaeolum majus during early stages of colonization. Physiologia plantarum *129*, 320-333.

Jiang, Y., Wang, W., Xie, Q., Liu, N., Liu, L., Wang, D., Zhang, X., Yang, C., Chen, X., and Tang, D. (2017). Plants transfer lipids to sustain colonization by mutualistic mycorrhizal and parasitic fungi. Science *356*, 1172-1175.

Jin, Y., Chen, Z., Yang, J., Mysore, K.S., Wen, J., Huang, J., Yu, N., and Wang, E. (2018). IPD3 and IPD3L function redundantly in rhizobial and mycorrhizal symbioses. Frontiers in Plant Science *9*, 267.

Jin, Y., Liu, H., Luo, D., Yu, N., Dong, W., Wang, C., Zhang, X., Dai, H., Yang, J., and Wang, E. (2016). DELLA proteins are common components of symbiotic rhizobial and mycorrhizal signalling pathways. Nature Communications *7*.

Keymer, A., Pimprikar, P., Wewer, V., Huber, C., Brands, M., Bucerius, S.L., Delaux, P.-M., Klingl, V., von Röpenack-Lahaye, E., and Wang, T.L. (2017). Lipid transfer from plants to arbuscular mycorrhiza fungi. elife *6*, e29107.

Khalvati, M., Hu, Y., Mozafar, A., and Schmidhalter, U. (2005). Quantification of water uptake by arbuscular mycorrhizal hyphae and its significance for leaf growth, water relations, and gas exchange of barley subjected to drought stress. Plant Biology *7*, 706-712.

Krajinski, F., Courty, P.-E., Sieh, D., Franken, P., Zhang, H., Bucher, M., Gerlach, N., Kryvoruchko, I., Zoeller, D., and Udvardi, M. (2014). The H+-ATPase HA1 of Medicago truncatula is essential for phosphate transport and plant growth during arbuscular mycorrhizal symbiosis. The Plant Cell *26*, 1808-1817.

Kretzschmar, T., Kohlen, W., Sasse, J., Borghi, L., Schlegel, M., Bachelier, J.B., Reinhardt, D., Bours, R., Bouwmeester, H.J., and Martinoia, E. (2012). A petunia ABC protein controls strigolactone-dependent symbiotic signalling and branching. Nature *483*, 341-344.

Leung, J., and Giraudat, J. (1998). Abscisic acid signal transduction. Annual review of plant biology *49*, 199-222.

Lévy, J., Bres, C., Geurts, R., Chalhoub, B., Kulikova, O., Duc, G., Journet, E.-P., Ané, J.-M., Lauber, E., and Bisseling, T. (2004). A putative Ca2+ and calmodulin-dependent protein kinase required for bacterial and fungal symbioses. Science *303*, 1361-1364.

Li, H., Cheng, Y., Murphy, A., Hagen, G., and Guilfoyle, T.J. (2009). Constitutive repression and activation of auxin signaling in Arabidopsis. Plant physiology *149*, 1277-1288.

Liao, D., Chen, X., Chen, A., Wang, H., Liu, J., Liu, J., Gu, M., Sun, S., and Xu, G. (2015). The characterization of six auxin-induced tomato GH3 genes uncovers a member, SlGH3. 4, strongly responsive to arbuscular mycorrhizal symbiosis. Plant and Cell Physiology *56*, 674-687.

Liao, D., Wang, S., Cui, M., Liu, J., Chen, A., and Xu, G. (2018). Phytohormones regulate the development of arbuscular mycorrhizal symbiosis. International journal of molecular sciences *19*, 3146.

Lindsay, P.L., Williams, B.N., MacLean, A., and Harrison, M.J. (2019). A Phosphate-Dependent Requirement for Transcription Factors IPD3 and IPD3L During Arbuscular Mycorrhizal

Symbiosis in Medicago truncatula. Molecular Plant-Microbe Interactions® *32*, 1277-1290.

López-Ráez, J.A., Verhage, A., Fernández, I., García, J.M., Azcón-Aguilar, C., Flors, V., and Pozo, M.J. (2010). Hormonal and transcriptional profiles highlight common and differential host responses to arbuscular mycorrhizal fungi and the regulation of the oxylipin pathway. Journal of Experimental Botany *61*, 2589-2601.

Lota, F., Wegmüller, S., Buer, B., Sato, S., Bräutigam, A., Hanf, B., and Bucher, M. (2013). The cis-acting CTTC–P1 BS module is indicative for gene function of L j VTI 12, a Q b-SNARE protein gene that is required for arbuscule formation in L otus japonicus. The Plant Journal *74*, 280-293.

Luginbuehl, L.H., Menard, G.N., Kurup, S., Van Erp, H., Radhakrishnan, G.V., Breakspear, A., Oldroyd, G.E., and Eastmond, P.J. (2017). Fatty acids in arbuscular mycorrhizal fungi are synthesized by the host plant. Science *356*, 1175-1178.

Luginbuehl, L.H., and Oldroyd, G.E.D. (2017). Understanding the Arbuscule at the Heart of Endomycorrhizal Symbioses in Plants. Current Biology *27*, R952-R963.

MacLean, A.M., Bravo, A., and Harrison, M.J. (2017). Plant signaling and metabolic pathways enabling arbuscular mycorrhizal symbiosis. The Plant Cell *29*, 2319-2335.

Maillet, F., Poinsot, V., André, O., Puech-Pagès, V., Haouy, A., Gueunier, M., Cromer, L., Giraudet, D., Formey, D., Niebel, A., *et al.* (2011). Fungal lipochitooligosaccharide symbiotic signals in arbuscular mycorrhiza. Nature *469*, 58-63.

Martín-Rodríguez, J.A., Huertas, R., Ho-Plágaro, T., Ocampo, J.A., Turečková, V., Tarkowská, D., Ludwig-Müller, J., and García-Garrido, J.M. (2016). Gibberellin–abscisic acid balances during arbuscular mycorrhiza formation in tomato. Frontiers in plant science *7*, 1273.

Mashiguchi, K., Tanaka, K., Sakai, T., Sugawara, S., Kawaide, H., Natsume, M., Hanada, A., Yaeno, T., Shirasu, K., and Yao, H. (2011). The main auxin biosynthesis pathway in Arabidopsis. Proceedings of the National Academy of Sciences *108*, 18512-18517.

Maule, A.J. (2008). Plasmodesmata: structure, function and biogenesis. Current opinion in plant biology *11*, 680-686.

McGonigle, T., Miller, M., Evans, D., Fairchild, G., and Swan, J. (1990). A new method which gives an objective measure of colonization of roots by vesicular—arbuscular mycorrhizal fungi. New phytologist *115*, 495-501.

Meixner, C., Ludwig-Müller, J., Miersch, O., Gresshoff, P., Staehelin, C., and Vierheilig, H. (2005). Lack of mycorrhizal autoregulation and phytohormonal changes in the supernodulating soybean mutant nts1007. Planta *222*, 709-715.

Messinese, E., Mun, J.-H., Yeun, L.H., Jayaraman, D., Rougé, P., Barre, A., Lougnon, G., Schornack, S., Bono, J.-J., and Cook, D.R. (2007). A novel nuclear protein interacts with the symbiotic DMI3 calcium-and calmodulin-dependent protein kinase of Medicago truncatula. Molecular plant-microbe interactions *20*, 912-921.

Miller, J.B., Pratap, A., Miyahara, A., Zhou, L., Bornemann, S., Morris, R.J., and Oldroyd, G.E. (2013). Calcium/Calmodulin-dependent protein kinase is negatively and positively regulated by calcium,

providing a mechanism for decoding calcium responses during symbiosis signaling. The Plant Cell *25*, 5053-5066.

Mukherjee, A., and Ané, J.-M. (2011). Germinating spore exudates from arbuscular mycorrhizal fungi: molecular and developmental responses in plants and their regulation by ethylene. Molecular Plant-Microbe Interactions *24*, 260-270.

Muller, J. (1999). Mycorrhizal fungal structures are stimulated in wildtype peas and in isogenic mycorrhiza-resistant mutants by tri-iodo-benzoic acid (TIBA), an auxin-transport-inhibitor. Symbiosis.

Müller, L.M., and Harrison, M.J. (2019). Phytohormones, miRNAs, and peptide signals integrate plant phosphorus status with arbuscular mycorrhizal symbiosis. Current opinion in plant biology *50*, 132-139.

Nadzieja, M., Kelly, S., Stougaard, J., and Reid, D. (2018). Epidermal auxin biosynthesis facilitates rhizobial infection in Lotus japonicus. The Plant Journal *95*, 101-111.

Nagata, M., Yamamoto, N., Shigeyama, T., Terasawa, Y., Anai, T., Sakai, T., Inada, S., Arima, S., Hashiguchi, M., and Akashi, R. (2015). Red/far red light controls arbuscular mycorrhizal colonization via jasmonic acid and strigolactone signaling. Plant and Cell Physiology *56*, 2100-2109.

Nakajima, K., Sena, G., Nawy, T., and Benfey, P.N. (2001). Intercellular movement of the putative transcription factor SHR in root patterning. Nature *413*, 307-311.

Novero, M., Faccio, A., Genre, A., Stougaard, J., Webb, K.J., Mulder, L., Parniske, M., and Bonfante, P. (2002). Dual requirement of the LjSym4 gene for mycorrhizal development in epidermal and cortical cells of Lotus japonicus roots. New phytologist, 741-749.

Oláh, B., Brière, C., Bécard, G., Dénarié, J., and Gough, C. (2005). Nod factors and a diffusible factor from arbuscular mycorrhizal fungi stimulate lateral root formation in Medicago truncatula via the DMI1/DMI2 signalling pathway. The Plant Journal *44*, 195-207.

Pan, H., Oztas, O., Zhang, X., Wu, X., Stonoha, C., Wang, E., Wang, B., and Wang, D. (2016). A symbiotic SNARE protein generated by alternative termination of transcription. Nature Plants *2*, 1-5.

Paque, S., and Weijers, D. (2016). Q&A: Auxin: the plant molecule that influences almost anything. BMC Biology *14*.

Park, H.-J., Floss, D.S., Levesque-Tremblay, V., Bravo, A., and Harrison, M.J. (2015). Hyphal branching during arbuscule development requires Reduced Arbuscular Mycorrhiza1. Plant Physiology *169*, 2774-2788.

Parniske, M. (2008). Arbuscular mycorrhiza: the mother of plant root endosymbioses. Nature Reviews Microbiology *6*, 763-775.

Paszkowski, U., and Gutjahr, C. (2013). Multiple control levels of root system remodeling in arbuscular mycorrhizal symbiosis. Frontiers in plant science *4*, 204.

Peer, W.A. (2013). From perception to attenuation: auxin signalling and responses. Current Opinion in Plant Biology *16*, 561-568.

Pérez-Torres, C.-A., López-Bucio, J., Cruz-Ramírez, A., Ibarra-Laclette, E., Dharmasiri, S., Estelle, M., and Herrera-Estrella, L. (2008). Phosphate availability alters lateral root development in Arabidopsis by modulating auxin sensitivity via a mechanism involving the TIR1 auxin receptor. The Plant Cell *20*, 3258-3272.

Pimprikar, P., Carbonnel, S., Paries, M., Katzer, K., Klingl, V., Bohmer, M.J., Karl, L., Floss, D.S., Harrison, M.J., and Parniske, M. (2016). A CCaMK-CYCLOPS-DELLA complex activates transcription of RAM1 to regulate arbuscule branching. Current Biology *26*, 987-998.

Pimprikar, P., and Gutjahr, C. (2018). Transcriptional regulation of arbuscular mycorrhiza development. Plant and Cell Physiology *59*, 678-695.

Pozo, M.J., López-Ráez, J.A., Azcón-Aguilar, C., and García-Garrido, J.M. (2015). Phytohormones as integrators of environmental signals in the regulation of mycorrhizal symbioses. New Phytologist *205*, 1431-1436.

Pumplin, N., and Harrison, M.J. (2009). Live-Cell Imaging Reveals Periarbuscular Membrane Domains and Organelle Location in Medicago truncatula Roots during Arbuscular Mycorrhizal Symbiosis. Plant Physiology *151*, 809-819.

Pumplin, N., Mondo, S.J., Topp, S., Starker, C.G., Gantt, J.S., and Harrison, M.J. (2010). Medicago truncatula Vapyrin is a novel protein required for arbuscular mycorrhizal symbiosis. The Plant Journal *61*, 482-494.

Reddy D. M. R, S., Schorderet, M., Feller, U., and Reinhardt, D. (2007). A petunia mutant affected in intracellular accommodation and morphogenesis of arbuscular mycorrhizal fungi. The Plant Journal *51*, 739-750.

Remy, W., Taylor, T.N., Hass, H., and Kerp, H. (1994). Four hundred-million-year-old vesicular arbuscular mycorrhizae. Proceedings of the National Academy of Sciences *91*, 11841-11843.

Rich, M.K., Courty, P.-E., Roux, C., and Reinhardt, D. (2017). Role of the GRAS transcription factor ATA/RAM1 in the transcriptional reprogramming of arbuscular mycorrhiza in Petunia hybrida. BMC Genomics *18*.

Rich, M.K., Schorderet, M., Bapaume, L., Falquet, L., Morel, P., Vandenbussche, M., and Reinhardt, D. (2015). The Petunia GRAS Transcription Factor ATA/RAM1 Regulates Symbiotic Gene Expression and Fungal Morphogenesis in Arbuscular Mycorrhiza. Plant Physiology *168*, 788-797.

Rival, P., de Billy, F., Bono, J.J., Gough, C., Rosenberg, C., and Bensmihen, S. (2012). Epidermal and cortical roles of NFP and DMI3 in coordinating early steps of nodulation in Medicago truncatula. Development *139*, 3383-3391.

Rodriguez, J.Á.M., Morcillo, R.L., Vierheilig, H., Ocampo, J.A., Ludwig-Müller, J., and Garrido, J.M.G. (2010). Mycorrhization of the notabilis and sitiens tomato mutants in relation to abscisic acid and ethylene contents. Journal of Plant Physiology *167*, 606-613.

Routray, P., Miller, J.B., Du, L., Oldroyd, G., and Poovaiah, B. (2013). Phosphorylation of S344 in the calmodulin-binding domain negatively affects CCaMK function during bacterial and fungal symbioses. The Plant Journal *76*, 287-296.

Ruyter-Spira, C., Al-Babili, S., van der Krol, S., and Bouwmeester, H. (2013). The biology of strigolactones. Trends in Plant Science *18*, 72-83.

Sabatini, S., Beis, D., Wolkenfelt, H., Murfett, J., Guilfoyle, T., Malamy, J., Benfey, P., Leyser, O., Bechtold, N., and Weisbeek, P. (1999). An auxin-dependent distal organizer of pattern and polarity in the Arabidopsis root. Cell *99*, 463-472.

Schachtman, D.P., Reid, R.J., and Ayling, S.M. (1998). Phosphorus uptake by plants: from soil to cell. Plant physiology *116*, 447-453.

Shaul-Keinan, O., Gadkar, V., Ginzberg, I., Grünzweig, J.M., Chet, I., Elad, Y., Wininger, S., Belausov, E., Eshed, Y., and Atzmon, N. (2002). Hormone concentrations in tobacco roots change during arbuscular mycorrhizal colonization with Glomus intraradices. New Phytologist *154*, 501-507.

Sieberer, B.J., Chabaud, M., Fournier, J., Timmers, A.C., and Barker, D.G. (2012). A switch in Ca2+ spiking signature is concomitant with endosymbiotic microbe entry into cortical root cells of Medicago truncatula. The Plant Journal *69*, 822-830.

Singh, S., Katzer, K., Lambert, J., Cerri, M., and Parniske, M. (2014). CYCLOPS, A DNA-Binding Transcriptional Activator, Orchestrates Symbiotic Root Nodule Development. Cell Host & Microbe *15*, 139-152.

Smith, S.E., and Smith, F.A. (2011). Roles of Arbuscular Mycorrhizas in Plant Nutrition and Growth: New Paradigms from Cellular to Ecosystem Scales. Annual Review of Plant Biology *62*, 227-250.

Smith, S.E., Smith, F.A., and Jakobsen, I. (2003). Mycorrhizal Fungi Can Dominate Phosphate Supply to Plants Irrespective of Growth Responses. Plant Physiology *133*, 16-20.

Spartz, A.K., Lee, S.H., Wenger, J.P., Gonzalez, N., Itoh, H., Inzé, D., Peer, W.A., Murphy, A.S., Overvoorde, P.J., and Gray, W.M. (2012). The SAUR19 subfamily of SMALL AUXIN UP RNA genes promote cell expansion. The Plant Journal *70*, 978-990.

Spartz, A.K., Ren, H., Park, M.Y., Grandt, K.N., Lee, S.H., Murphy, A.S., Sussman, M.R., Overvoorde, P.J., and Gray, W.M. (2014). SAUR inhibition of PP2C-D phosphatases activates plasma membrane H+-ATPases to promote cell expansion in Arabidopsis. The Plant Cell *26*, 2129-2142.

Spatafora, J.W., Chang, Y., Benny, G.L., Lazarus, K., Smith, M.E., Berbee, M.L., Bonito, G., Corradi, N., Grigoriev, I., and Gryganskyi, A. (2016). A phylum-level phylogenetic classification of zygomycete fungi based on genome-scale data. Mycologia *108*, 1028-1046.

St-Arnaud, M., Hamel, C., Vimard, B., Caron, M., and Fortin, J.A. (1996). Enhanced hyphal growth and spore production of the arbuscular mycorrhizal fungus Glomus intraradices in an in vitro system in the absence of host roots. Mycological Research *100*, 328-332.

Subramanian, K., Charest, C., Dwyer, L., and Hamilton, R. (1995). Arbuscular mycorrhizas and water relations in maize under drought stress at tasselling. New Phytologist *129*, 643-650.

Sun, J., Miller, J.B., Granqvist, E., Wiley-Kalil, A., Gobbato, E., Maillet, F., Cottaz, S., Samain, E., Venkateshwaran, M., Fort, S., *et al.* (2015). Activation of Symbiosis Signaling by Arbuscular Mycorrhizal Fungi in Legumes and Rice. The Plant Cell *27*, 823-838.

Takeda, N., Haage, K., Sato, S., Tabata, S., and Parniske, M. (2011). Activation of a Lotus japonicus subtilase gene during arbuscular mycorrhiza is dependent on the common symbiosis genes and two cis-active promoter regions. Molecular plant-microbe interactions *24*, 662-670.

Takeda, N., Handa, Y., Tsuzuki, S., Kojima, M., Sakakibara, H., and Kawaguchi, M. (2015). Gibberellins interfere with symbiosis signaling and gene expression and alter colonization by arbuscular mycorrhizal fungi in Lotus japonicus. Plant physiology *167*, 545-557.

Takeda, N., Maekawa, T., and Hayashi, M. (2012). Nuclear-localized and deregulated calcium-and calmodulin-dependent protein kinase activates rhizobial and mycorrhizal responses in Lotus japonicus. The Plant Cell *24*, 810-822.

Thangavelu, M., and Tamilselvi, V. (2010). Occurrence and morphology of endorhizal fungi in crop species. Tropical and Subtropical Agroecosystems *12*, 593-604.

Tirichine, L., Imaizumi-Anraku, H., Yoshida, S., Murakami, Y., Madsen, L.H., Miwa, H., Nakagawa, T., Sandal, N., Albrektsen, A.S., and Kawaguchi, M. (2006). Deregulation of a Ca 2+/calmodulin-dependent kinase leads to spontaneous nodule development. Nature *441*, 1153-1156.

Tiwari, S.B., Hagen, G., and Guilfoyle, T.J. (2004). Aux/IAA proteins contain a potent transcriptional repression domain. The Plant Cell *16*, 533-543.

Ulmasov, T., Murfett, J., Hagen, G., and Guilfoyle, T.J. (1997). Aux/IAA proteins repress expression of reporter genes containing natural and highly active synthetic auxin response elements. The Plant Cell *9*, 1963-1971.

Ungar, D., and Hughson, F.M. (2003). SNARE Protein Structure and Function. Annual Review of Cell and Developmental Biology *19*, 493-517.

Van Der Heijden, M.G., Klironomos, J.N., Ursic, M., Moutoglis, P., Streitwolf-Engel, R., Boller, T., Wiemken, A., and Sanders, I.R. (1998). Mycorrhizal fungal diversity determines plant biodiversity, ecosystem variability and productivity. Nature *396*, 69-72.

Vanneste, S., and Friml, J. (2009). Auxin: A Trigger for Change in Plant Development. Cell *136*, 1005-1016.

Vanstraelen, M., and Benková, E. (2012). Hormonal Interactions in the Regulation of Plant Development. Annual Review of Cell and Developmental Biology *28*, 463-487.

Vishwakarma, K., Upadhyay, N., Kumar, N., Yadav, G., Singh, J., Mishra, R.K., Kumar, V., Verma, R., Upadhyay, R.G., Pandey, M., *et al.* (2017). Abscisic Acid Signaling and Abiotic Stress Tolerance in Plants: A Review on Current Knowledge and Future Prospects. Frontiers in Plant Science *08*.

Wang, E., Yu, N., Bano, S.A., Liu, C., Miller, A.J., Cousins, D., Zhang, X., Ratet, P., Tadege, M., and Mysore, K.S. (2014). A H+-ATPase that energizes nutrient uptake during mycorrhizal symbioses in rice and Medicago truncatula. The Plant Cell *26*, 1818-1830.

Weijers, D., and Wagner, D. (2016). Transcriptional Responses to the Auxin Hormone. Annual Review of Plant Biology *67*, 539-574.

Xie, X., Yoneyama, K., and Yoneyama, K. (2010). The strigolactone story. Annual review of phytopathology *48*.

Xue, L., Cui, H., Buer, B., Vijayakumar, V., Delaux, P.-M., Junkermann, S., and Bucher, M. (2015). Network of GRAS transcription factors involved in the control of arbuscule development in Lotus japonicus. Plant Physiology *167*, 854-871.

Yamaguchi-Shinozaki, K., and Shinozaki, K. (1994). A novel cis-acting element in an Arabidopsis gene is involved in responsiveness to drought, low-temperature, or high-salt stress. The Plant Cell *6*, 251-264.

Yano, K., Yoshida, S., Muller, J., Singh, S., Banba, M., Vickers, K., Markmann, K., White, C., Schuller, B., Sato, S., *et al.* (2008). CYCLOPS, a mediator of symbiotic intracellular accommodation. Proceedings of the National Academy of Sciences *105*, 20540-20545.

Yoneyama, K., Yoneyama, K., Takeuchi, Y., and Sekimoto, H. (2007). Phosphorus deficiency in red clover promotes exudation of orobanchol, the signal for mycorrhizal symbionts and germination stimulant for root parasites. Planta *225*, 1031-1038.

Yu, N., Luo, D., Zhang, X., Liu, J., Wang, W., Jin, Y., Dong, W., Liu, J., Liu, H., and Yang, W. (2014). A DELLA protein complex controls the arbuscular mycorrhizal symbiosis in plants. Cell research *24*, 130-133.

Zambryski, P. (2008). Plasmodesmata. Current Biology *18*, R324-R325.

Zambryski, P., and Crawford, K. (2000). Plasmodesmata: gatekeepers for cell-to-cell transport of developmental signals in plants. Annual review of cell and developmental biology *16*, 393-421.

Zhang, D.-P. (2014). Abscisic acid: metabolism, transport and signaling (Springer).

Zhang, Q., Blaylock, L.A., and Harrison, M.J. (2010). Two Medicago truncatula Half-ABC Transporters Are Essential for Arbuscule Development in Arbuscular Mycorrhizal Symbiosis. The Plant Cell *22*, 1483-1497.

Zhang, X., Pumplin, N., Ivanov, S., and Harrison, M.J. (2015). EXO70I is required for development of a sub-domain of the periarbuscular membrane during arbuscular mycorrhizal symbiosis. Current Biology *25*, 2189-2195.

X. Lists of Figures

Sumplementary Figures

XI. List of Tables

XII. Acknowledgement

I would like to thank all the people who have supported and helped me over the last four years.

First of all, I must express my profound gratitude to my supervisor Prof. Dr. Caroline Gutjahr, for offering me the opportunity to join her lab, for the excellently scientific guidance, for supporting my whole doctoral study in many aspects. I believe her very nice personality will continue positively influencing me in my future life.

I also would like to say a big thank you to all of the past and present members of Gutjahr lab. Everyone directly or indirectly has helped me and contributed to this work. The relax and friendly atmosphere in the lab has made my Ph.D study less stressful and this has been important to me. Special thanks must go to Dr. Salar Abu Torab Torabi for the lab training at the time when I joined the lab; Dr. Priya Pimpriya, Michael Paries, Dr. Andreas Keymer, José Antonio Villaécija Aguilar, Dr. Karen V. Hobecker and Haifei Zhang for cooperation, sharing cDNA and plasmids, etc.; Dr. Tian Zeng for helping me in phylogenetic tree analysis; our technicians, Verena Klingl, Regina Hüttl, Philipp Chapman and Ottilie Peis, for their excellent technical support.

Moreover, I would like to thank Prof. Dr. Kerin Ljung for cooperation in the measurement of IAA essay; Dr. David Chiasson and Chloé Cathebras for sharing plasmids and helping in lateral root quantification experiment; PD. Dr. Ulrich Hammer for the consultation of my projects and correction of my thesis; Dr. Tian Zeng, Xiaoyun Gong and Dr. Juan Liang for the correction of my thesis. I would like to thank the whole committee of my defense.

In addition, I am grateful for the financial support by my family, China Scholarship Council and Gutjahr lab.

Last but not the least, heartily thanks to my family, my parents and my husband Hai Wei, and all my friends in Munich. With their encouragement, love and unfailing support, I got the chance to be here and to pursue my dream. For me, it has been a big challenge to study in this foreign country, I would have probably never finished this Ph.D without the support of them.

XIII. Copyright Clearance

Fig. 1 Process of AM development. The figure is taken from Gutjahr and Parniske, 2013.

Copyright Clearance Center Marketplace™

Annual Reviews, Inc. - License Terms and Conditions

This is a License Agreement between Fan Du ("You") and Annual Reviews, Inc. ("Publisher") provided by Copyright Clearance Center ("CCC"). The license consists of your order details, the terms and conditions provided by Annual Reviews, Inc., and the CCC terms and conditions.

All payments must be made in full to CCC.

Order Date	26-Jun-2020	Type of Use	Republish in a thesis/dissertation
Order license ID	1044437-1	Publisher	ANNUAL REVIEWS
ISSN	1530-8995	Portion	Image/photo/illustration

LICENSED CONTENT

Publication Title	Annual review of cell and developmental biology	Publication Type	e-Journal
Article Title	Cell and developmental biology of arbuscular mycorrhiza symbiosis.	Start Page	593
Author/Editor	ANNUAL REVIEWS, INC.	End Page	617
Date	01/01/1995	Issue	1
Language	English	Volume	29
Country	United States of America	URL	http://arjournals.annualreviews.org/loi/cellbio
Rightsholder	Annual Reviews, Inc.		

REQUEST DETAILS

Portion Type	Image/photo/illustration	Distribution	Worldwide
Number of images / photos / illustrations	1	Translation	Original language of publication
Format (select all that apply)	Print, Electronic	Copies for the disabled?	No
Who will republish the content?	Academic institution	Minor editing privileges?	Yes
Duration of Use	Life of current edition	Incidental promotional use?	Yes
Lifetime Unit Quantity	Up to 499	Currency	EUR
Rights Requested	Main product		

NEW WORK DETAILS

Title	Auxin signaling downstream of RAM1 and a non-cell autonomous role of CCaMK in Lotus japonicus arbuscular mycorrhiza development	Institution name	Technical University of Munich
		Expected presentation date	2020-06-26
Instructor name	Fan Du		

ADDITIONAL DETAILS

Order reference number	N/A	The requesting person / organization to appear on the license	Fan Du

REUSE CONTENT DETAILS

Title, description or numeric reference of the portion(s)	Figure 2	Title of the article/chapter the portion is from	Cell and developmental biology of arbuscular mycorrhiza symbiosis.
Editor of portion(s)	Gutjahr, Caroline; Parniske, Martin	Author of portion(s)	Gutjahr, Caroline; Parniske, Martin
Volume of serial or monograph	29	Issue, if republishing an article from a serial	1
Page or page range of portion	593-617	Publication date of portion	2013-10-06

Fig. 2 Transcriptional regulation and morphological arbuscule development in root inner cortical cell. The figure is taken from Pimprikar and Gutjahr, 2018.

No permission is required to reuse the figure in this docroral thesis, this is confirmed by Matthew Lane, who is the publisher based at the Oxford University Press office in Tokyo with responsibility for Plant Cell Physiology.

Fig. 3 Role of phytohormones in different stages of AM development. The figure is taken from Das and Gutjahr, 2019.

PLS Clear

PARTIES:

1. **John Wiley & Sons Limited** (Company number – 00641132) (Licensor); and
2. **Fan Du** (Licensee).

Thank you for your recent permission request. Some permission requests for use of material published by the Licensor, such as this one, are now being facilitated by PLSclear.

Set out in this licence cover sheet (the **Licence Cover Sheet**) are the principal terms under which Licensor has agreed to license certain Licensed Material (as defined below) to Licensee. The terms in this Licence Cover Sheet are subject to the attached General Terms and Conditions, which together with this Licence Cover Sheet constitute the licence agreement (the **Licence**) between Licensor and Licensee as regards the Licensed Material. The terms set out in this Licence Cover Sheet take precedence over any conflicting provision in the General Terms and Conditions.

Free Of Charge Licence Terms

Licence Date:	27/06/2020
PLSclear Ref No:	39209

The Licensor

Company name:	John Wiley & Sons Limited
Address:	The Atrium Southern Gate Chichester PO19 8SQ GB

The Licensee

Licensee Contact Name:	Fan Du
Licensee Address:	Plant Genetics, Emil-Ramann-Str. 4 Freising, Munich 85354

Licensed Material

title:	The Model Legume Medicago truncatula
ISBN:	9781119409144
publisher:	John Wiley & Sons Limited
Are you requesting permission to reuse the cover of the publication?	No

Figure number & title	Figure 7.1.2.1 Role of phytohormones in arbuscular mycorrhiza development.
Page numbers	486

For Use In Licensee's Publication(s)

usage type	Book, Journal, Magazine or Academic Paper-Thesis / Dissertation
Will your dissertation be placed in an online repository?	Yes
Author	Fan Du
Language	English
Other Territory	Germany
Title of dissertation/thesis	Auxin signaling downstream of RAM1 and a non-cell autonomous role of CCaMK in Lotus japonicus arbuscular mycorrhiza development
University or institution	Technical University of Munich
Unlimited circulation?	No

Rights Granted

Exclusivity:	Non-Exclusive
Format:	Thesis / Dissertation
Language:	English
Territory:	World
Duration:	Lifetime of Licensee's Edition
Maximum Circulation:	0